MODELLING OF THE EFFECTS OF TEXTILE INDUSTRY WASTEWATERS ON THE PERFORMANCE OF A MUNICIPAL WASTEWATER TREATMENT PLANT

Prelan Gounder

BSc. Eng (Natal)

Submitted in fulfilment of the academic
requirements for the degree of
MSc. Eng
in the
School of Chemical Engineering
University of KwaZulu-Natal, Durban

August 2006

ABSTRACT

Municipal wastewater treatment plants are designed to treat domestic wastewater. Industrial wastewaters are accepted to sewer provided they do not adversely affect the performance of the wastewater treatment plant. Although by-laws have been promulgated to control the discharge of industrial wastes, they do not directly address the potential inhibitory nature of the discharge. The recalcitrant nature of most dyes, together with their toxicity to micro organisms, makes biological treatment difficult.

Municipal authorities have promoted the use of low environmental impact chemicals in the textile industry through a co-regulatory approach by scoring the textile chemicals. The objective of this investigation is to model the effects of textile industry wastewater, made up of dyes of different scores, on the performance of a wastewater treatment works (WWTW). The score system (Laursen et al., 2002) was used to choose a high and low scoring dye to be used in laboratory experiments. Batch respirometry was used as the experiment since it is a robust and sensitive method. The optimal experiment design method (Dochain and Vanrolleghem, 2001) was used in to design the batch respirometric experiment, the optimal batch respirometric experiment design provided rapid and reliable experimental data that was used in parameter estimation. Batch respirometric experiments were performed with dyes as the test substance, sodium acetate and ammonium chloride being the reference substrates, and activated sludge from Umbilo wastewater treatment works aeration basin. Performing batch respirometric experiments with a series of different dye concentrations of the dyes allowed the deduction of the dependence of the kinetic parameters on the dye concentrations. The results from the respirometric experiments performed with both dyes indicated that; the dyes have a greater inhibitory effect on the autotrophic biomass growth process as compared heterotrophic biomass growth process.

A Batch Respirometric Experiment (BRE) Model was created and the model calibration involved the assessment of the relevant bio-kinetic parameters. Biomass growth kinetic parameter estimations were performed using the measured data from the batch respirometric experiments, the BRE model and numerical optimisation algorithms provided in WEST software package. The results from the parameter estimation indicated that both dyes used in this investigation have a mixed inhibition effect on both heterotrophic and autotrophic biomass growth process.

Inhibition kinetics for both dyes were determined using the estimated kinetic parameters, thereafter the resultant inhibition kinetics was inputted into the activated sludge process model of the COST simulation benchmark model (Copp, 2002). The COST simulation benchmark protocol (Copp, 2002) was used to assess the impact of both dyes on the performance of the COST simulation benchmark wastewater treatment works model. The benchmark model has a fully defined protocol which provides an unbiased basis without reference to any particular wastewater treatment works. From the results of the COST benchmark simulations it was concluded that the high scoring dye had a great negative impact on the performance of the wastewater treatment works model as compared to the low scoring dye.

DECLARATION

I declare that this dissertation, unless indicated, is my own work and that it has not been submitted, in whole or in part, for a degree at another University or Institution.

_____

Prelan Gounder

August 2006

ACKNOWLEDGEMENTS

I would like to acknowledge the following people and organisations for their contribution to this study:

Prof C.A. Buckley	Thank you for giving me the opportunity to undertake this study and for trusting me to complete it. Your leadership and patience were critical factors in the completion of this study.
Family	To my parents and brother, thank you for all your support and for never losing faith in me.
Mrs. K. Foxon	Thank you for advice, input and all ways making time when I required assistance for this study.
University of Gent (Department of Applied Mathematics Biometrics and Process Control)	Thank all the people from Biomath, especially Dr. G. Sin and Prof. P.A Vanrolleghem. It was a privilege to have worked with such remarkable people.
Mr. S. Rajkumar	Thank you for your friendship and encouragement when everything seemed impossible.
God	For providing me with motivation and courage through all the adversity.
Water Research Commission (WRC)	Funding this study.
Umbilo Wastewater Treatment Works	The staff for all their assistance during the of this project.

GLOSSARY

Acclimation	The adaptation of a microbial community to degrade a previously recalcitrant compound through prior exposure.
Activated sludge	A mixed association of prokaryotic and eukaryotic micro organisms, which aerobically decompose waste in a activated sludge effluent treatment system.
Adaptation	A change in the microbial community that increases the rate of transformation of a test compound as a result of prior exposure to that test compound.
Aerobic	The condition of living or acting only in the presence of molecular oxygen.
Algae	Organisms that perform oxygenic photosynthesis and possess chloroplasts. May be single or multi cellular organisms.
Azo dyes	Dyes which contain at least one azo group (-N=N-), and can contain up to four azo groups.
Bacteria	Single-cell, prokaryotic micro organisms.
Batch culture	A closed culture environment in which conditions are continuously changing according to the metabolic state of the microbial culture.
Biodegradable	A property which allows the microbial decomposition of an organic compound to inorganic molecules.
Chemical oxygen demand	A measure of the total amount of organic waste stream.
Degrade	Breakdown into simpler substances by bacterial action.

Effluent	A stream flowing from a sewage tank or industrial process.
Inhibition	An impairment of bacterial function.
Kinetics	The explanation of the observed characteristics of chemical reactions.
Pollution	An adverse alteration of the environment.
Reactive dyes	Reactive dyes are coloured componets capable of forming a covalent bond between the dye molecule and the fibre.
Recalcitrant	Resistant to microbial degradation.
Respiration	The oxidative breakdown and release of energy from nutrient molecules by reactions with molecular oxygen.
Seeding	The use of an actively digesting sludge to aid the start-up of a digester by supplying a quantity of the preferred types of organisms. This usually reduces the time taken for a digester to become active.
Sludge	The general term applied to the accumulated solids separated from wastewater. A large portion of the sludge material in a digester consists of bacteria which are responsible for its decomposition.
Suspended solids	Undissolved non-settleable solids present in wastewater.
Toxicity	An adverse effect (not necessarily lethal) on bacterial metabolism.
Wastewater	General term to denote a combination or mixture of domestic sewage and industrial effluents.

LIST OF ABBREVIATIONS AND SYMBOLS

ABBREVIATIONS

Name	Description	Unit
a	Mole hydrogen in 1 mol-C of biomass	
ASM	Activated sludge model	
ASM1	Activated sludge model number 1	
ASM2	Activated sludge model number 2	
ASM2d	Activated sludge model number 2d	
ASM3	Activated sludge model number 3	
ATU	Allylthiourea	
b	Mole oxygen in 1 mol-C of biomass	
BOD	Biological oxygen demand	mg O_2/L
BRE	Batch respirometric experiment	
c	Mole nitrogen in 1 mol-C of biomass	
$CH_aO_bN_c$	Molecular composition of biomass	1 mol-C
COD	Chemical oxygen demand	mg COD/L

COV	Covariance matrix (inverse of FIM)	
DWAF	Department of Water Affairs and Forestry	
EU	European Union	
FIM	Fisher Information Matrix	
K_La	Mass transfer coefficient	
MLVSS	Mixed liquor volatile suspended solids	mg SS/L
NH4-N	Ammonium concentration	mg N/L
NH_3	Ammonia nitrogen	mg NH_3-N/L
NO_2-N	Nitrite nitrogen	mg NO_2-N/L
NO_3-N	Nitrite nitrogen	mg NO_3-N/L
ODE	Ordinary differential equation	
OED	Optimal experimental design	
pH	Negative logarithm of proton concentration	
S_0/X_0	Initial substrate to biomass ratio	
S/X	Substrate to biomass ratio	

TKN	Total kjeldahl nitrogen	mg N/L
WWTW	Wastewater treatment works	

ROMAN SYMBOLS

Symbol	Description	Unit
b_A	Endogenous decay coefficient of autotrophic biomass	1/d
b_H	Endogenous decay coefficient of heterotrophic biomass	1/d
DO	Dissolved oxygen concentration	mg O_2/L
f_P	Inert particulate fraction of the biomass	
I	Inhibitor concentration	mg/L
J	Objective function	
k_h	Hydrolysis rate	1/d
K_{NH}	Ammonium half-saturation constant	mg N/L
K_{NO}	Nitrate half-saturation constant	mg N/L
K_{OA}	Oxygen half-saturation constant for autotrophic biomass	mg O_2/L

K_{OH}	Oxygen half-saturation constant for biomass heterotrophic	mg O_2/L
K_S	Substrate half-saturation constant	mg COD/L
K_X	Particulate COD half-saturation constant	mg COD/L
N	Number of data points	
p	Number of parameters	
OUR	Oxygen uptake rate	mg O_2/L.min
OUR_{end}	Endogenous oxygen uptake rate	mg O_2/L.min
OUR_{exo}	Exogenous oxygen uptake rate	mg O_2/L.min
$OUR_{\max}$	Maximum oxygen uptake rate value	mg O_2/L.min
Q	Measurement error covariance matrix	
S_{ND}	Soluble degradable organic nitrogen	mg N/L
$S_{NH}(0)$	Initial ammonium concentration	mg N/L
S_{NH}	Ammonium concentration	mg N/L
S_{NO}	Nitrate concentration	mg N/L

S_O	Oxygen concentration	mg O_2/L
$S_S(0)$	Initial soluble readily biodegradable COD	mg COD/L
S_S	Soluble readily biodegradable COD	mg COD/L
V	Reactor volume	L
v_0	Maximum settling velocity	
Y_A	Autotrophic yield coefficient	mg COD/mg NH_4-N
Y_H	Heterotrophic yield coefficient	mg COD/mg COD
X_{BA}	Autotrophic biomass concentration	mg COD/L
$X_{BH}(0)$	Initial heterotrophic biomass concentration	mg COD/L
X_{BH}	Heterotrophic biomass concentration	mg COD/L
X_{ND}	Particulate degradable organic nitrogen	mg N/L
X_S	Slowly biodegradable COD	mg COD/L

GREEK SYMBOLS

Symbol	Description	Unit
δ^{msqr}	Parameter sensitivity	
η_g	Anoxic growth reduction factor	
θ	Parameter	
μ_A	Growth rate for autotrophic biomass	1/d
μ_{mA}	Maximum growth rate of autotrophic biomass	1/d
μ_H	Growth rate for heterotrophic biomass	1/d
μ_{mH}	Maximum growth rate of autotrophic biomass	1/d
τ_A	First order time constant in autotrophic activity	min
τ_H	First order time constant in heterotrophic activity	min
σ	Standard deviation	
σ^2	Variance	

CONTENTS

LIST OF TABLES

LIST OF FIGURES

CHAPTER 1
INTRODUCTION

This chapter outlines the scope of this study and the manner in which this dissertation has been organised.

1.1 Project Outline

This project will describe the inhibitory effects of textile dyes on activated sludge processes. More specifically it is investigated whether the score system accurately describes the negative impact of the textile dyes on wastewater treatment works activated sludge processes. Reliable laboratory and modelling methods are required to assess the inhibitory effect of the textile dyes on activated sludge processes. It is envisaged that this combined laboratory-modelling method will aid in the future aims of the Pollution Research Group; of creating a database of eThekwini Municipality wastewater treatment works models and creating a new tariff system for industries which discharge industrial effluent to wastewater treatment works.

Therefore the aims of this project are to:

- use the score system to choose a high and low scoring dye to be used in laboratory experiments.
- design a respirometric experiment that provides rapid and reliable experimental data that can be used for process modelling.
- create or use an existing activated sludge model, along with respirometric experiment data to obtain kinetic data which can represent the inhibition caused by textile dyes.
- create or use existing wastewater treatment works model, along with kinetic data collected from the process modelling to assess whether the high scoring dye has a greater negative impact on the wastewater treatment works activated sludge processes.

The thesis would attempt to provide a:

- methodology to evaluate the impact of toxic substances on wastewater treatment works activated sludge process.
- optimal respirometric experiment design that will provide reliable data to be used in process modelling.
- activated sludge model which can used to determine kinetic data to be used later in wastewater treatment works model.
- protocol to using the COST Simulation Benchmark procedure to evaluate the effect of toxic substances on a wastewater treatment works model.

1.2 Thesis Outline

The thesis consists of five chapters following this one:

- CHAPTER TWO - LITERATURE REVIEW:
  This chapter provides some background information on the theoretical concepts referred to in this thesis. A full description of the inhibitory nature of textile wastewaters, the score system, respirometry, Optimal Experiment Design (OED) (Dochain and Vanrolleghem, 2001) and activated sludge kinetic models is provided. A brief description of mathematical process modelling and the COST simulation benchmark model (Copp, 2002) used in this study is provided in this chapter. Mathematical process modelling theory is discussed in detail in **Chapter 3**. The COST simulation benchmark model is described in detail in **Chapter 6**.

- CHAPTER THREE – MATHEMATICAL MODELLING THEORY:
  This chapter provides the mathematical process modelling theory used in the quantification of the inhibitory nature of textile dye effluent on the activated sludge processes. A Batch Respirometric Experiment (BRE) model was created to obtain the relevant information to quantify the inhibition of textile dyes on the kinetics of biomass respiratory activity. To determine which of the parameters of the model are central in quantifying the inhibition, the kinetic effects of inhibition have been investigated. Subsequently the BRE model was inputted into wastewater treatment modelling

program WEST. A continuity check and the identifiability study were performed of the BRE model. The model theory of parameter estimation and the method used in WEST is also discussed.

- CHAPTER FOUR – BATCH RESPIROMETRIC EXPERIMENT:
  This chapter describes the batch respirometric experimental protocol developed to quantify the inhibitory effects of textile dyes. The respirometric protocol developed provides information rich data which reliable parameter estimation can be performed. Previous unsuccessful experimental designs used during the optimising of the experimental design are discussed. The batch respirometric experimental optimal design along with the results from this experiment design is presented. This experimental data is used in **Chapter 5** for parameter estimation.

- CHAPTER FIVE – BRE MODEL SIMULATION RESULTS AND DISCUSSION
  In this chapter the results from the identifiability study and parameter estimation performed on the BRE model are presented and discussed. The type of inhibition and the resultant inhibition kinetics of both dyes used in this study are presented. These inhibition kinetics are inputted in the COST benchmark simulation model in **Chapter 6**.

- CHAPTER SIX – ASSESSMENT OF WASTEWATER TREATMENT WORKS PERFORMANCE:
  In this chapter the impact of the textile dyes on the wastewater treatment works performance is assessed, the *COST simulation benchmark* was used for this assessment. Background information on COST and the concept of the COST simulation benchmark are discussed. The simulation benchmark model was used in this study to quantify the inhibitory effect of two dyes and determine whether the high scoring dye has a greater negative impact on wastewater treatment works performance than the low scoring dye.

- CHAPTER SEVEN – DISCUSSION:
  In this chapter the broad spectrum impact of the results presented in **Chapter 4**, **Chapter 5** and **Chapter 6** are discussed. The formulation of the conclusion and recommendations stated in **Chapter 8** is presented in this chapter.

- CHAPTER EIGHT – CONCLUSIONS AND RECOMMENDATIONS:
  In this chapter conclusion and recommendations are presented.

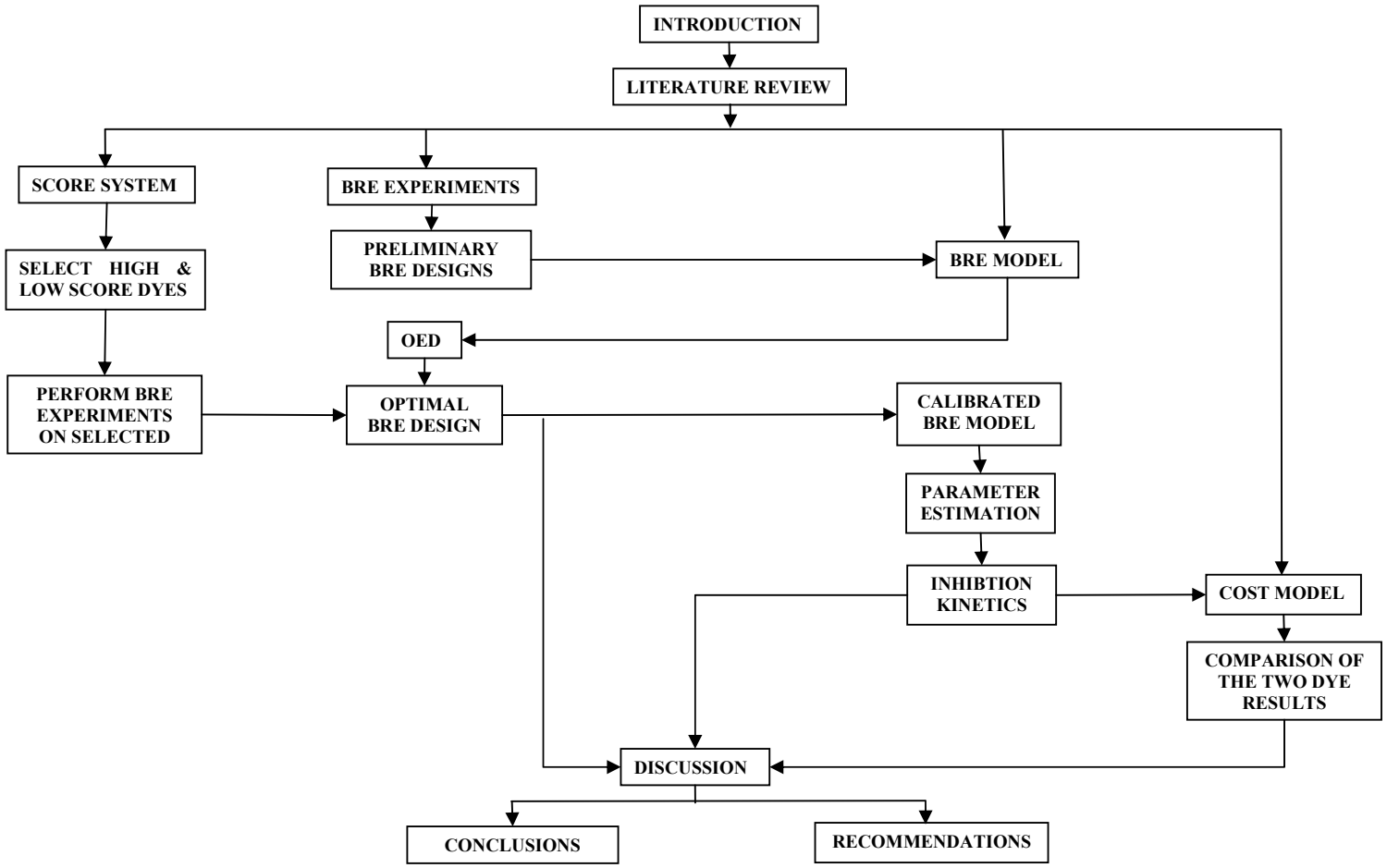

Figure 1-1: Thesis outline. The schematic shows how the thesis has been structured and highlights how different sections are related to each other.

CHAPTER 2
LITERATURE REVIEW

This chapter provides some background information on the theoretical concepts referred to in this thesis. Descriptions of the inhibitory nature of textile wastewaters, the score system, respirometry, activated sludge kinetic models, Optimal Experiment Design (OED), mathematical process modelling and the COST simulation benchmark model used in this study are provided in this chapter. The COST simulation benchmark model, the respirometric experiments and the activated sludge model used in parameter estimation will be discussed in greater detail at a later stage.

2.1 The Toxicity and Inhibitory Nature of Textile Wastewaters

Toxicity is an adverse effect (not necessarily lethal) on the metabolism of bacteria, and inhibition is the impairment of bacteria function (Speece, 1996).

2.1.1 Toxicity of textile wastewaters

Aesthetic environmental impact is a recognised problem associated with textile dye effluents, but the possible toxicity effects on algal growth (Willetts, 1999) has a major impact on the ecosystem as algal photosynthesis is a major source of oxygen in river water. This toxicity is not limited to lower life forms; a toxicity to fish has been documented (Laing, 1991).

2.1.2 Inhibitory nature of textile wastewaters

Textile dyes are designed to be resistant to oxidation, hence textile dye effluent are resistant to oxidative microbial breakdown. Conventional aerobic wastewater treatment is unsuccessful in degrading textile dye effluent. Azo reactive dyes are particularly difficult to treat biologically.

Azo reactive dyes account for about 70% of all the textile dyestuffs produced. They are pigmented components capable of forming a covalent bond between the dye molecule and fibre (Godefroy, 1993). Azo dyes are water-soluble synthetic organic colourants possessing the characteristics azo (-N=N-) bond. Studies have shown that aerobic processes at conventional wastewater treatment works are unable to substantially treat azo dyes, the strong electron withdrawing character of the azo group stabilizes these aromatic pollutants against conversion by bacteria (Razo-Flores, 1997). The treatment of textile dyes by activated sludge has been

researched extensively by many researches (Flege, 1970, Pagga and Brown, 1986), it was found that some dyes are partially degraded but most remain untreated, particularly azo dyes.

Autotrophic biomass responsible for nitrification process is considered to be more sensitive to toxins, than the hetetrophic biomass which is responsible for the carbon oxidation process (Blum and Speece, 1991).

2.2 The Score System

As discussed earlier textile industry wastewaters are difficult to treat through convention activated sludge process, hence resulting in the dyes entering the natural water system. The amount of colourants being discharged has been steadily decreased by cleaner production techniques and pre-treatment of effluent before being discharge into sewer system. Although these counteractive methods have improved the effluent treatment process, a remedy is required to drastically reduce the impact of textile effluents on the environment. A possible remedy is the use of the score system for sorting of chemicals on basis of environmental data and information on consumption (Laursen et al., 2002).

The score system is an administrative method of sorting organic chemicals on the basis of information especially from the chemical supplier's material and data sheets (MSDS). The sorting enables the identification of chemicals and dyestuffs that have a negative impact on the environment and should be subject to closer examination; this is based on the consumption and environmental behaviour of the chemicals and dyestuffs.

The score system is based on four parameters which are important for the characterization of chemicals and dyestuffs which are harmful to the environment. These four parameters are:

- A – Discharged amount of substance to drain over a given period,
- B – Biodegradability
- C – Bioaccumulation and
- D – Toxicity.

Each parameter (i.e. A, B, C or D) is given a score between 1 and 4, with 1 indicating the least environmental impact and 4 indicating the most serious impact. In the case of missing information required to determine the parameter score, the highest score is assigned along with

a remark "4u" ("u" indicating unknown).

2.2.1 A-score (Discharge amount)

The A score is determined from the amount of dye or chemical that is discharged to drain by the facility on site per year. The amount to drain is the total amount of product used from which the quantity of product which adheres to the textile is subtracted.

2.2.2 B-score (Biodegradability)

In most cases the B-score for biological degradability is based on the substance biodegradability in sludge. In some cases it is based on the substance biodegradability in surface water or based on the BOD_5/COD ratio.

2.2.3 C-score (Bioaccumulation)

The C-score can be established on the basis of qualitative information based on solubility. The parameter score can also be obtained from standardised bioaccumulation tests with fish or from examinations based on determination of the distribution of the substance in two-phased mixture of octanol and water (P_{OW} – data). A few products are scored purely on information about the molecular weight.

2.2.4 Exposure score (A x B x C)

The product of A, B and C (i.e. A x B x C) is called the **Exposure score**. The **Exposure score** gives an indication of the potential presence of the substance in the environment. The details of the exposure component scores system is presented in Table 2-1.

Table 2-1: Exposure component parameter scores adapted from (Laursen et al., 2002)

Score Figure → / Parameter ↓	1	2	3	4
A – Discharged amount of substance to drain				
kg/week	< 1	1 – 10	> 10 - 100	> 100
kg/year	< 50	50 - 500	>500 - 5000	> 5000
B – Biodegradability				
Surface water (%)	> 60 (50 – 100)	10 - 60	<10	
Sludge culture (%)		> 70	20 - 70	<20
BOD/COD ratio		>0.5		≤ 0.5
C – Bioaccumulation				
C1 If MW . 1000 g/mol	*			
C2 If 500 ≤ MW ≤1000 g/mol				
P_{OW} - data	< 1000	≥ 1000		
Water solubility g/L	> 10	10 - 2	< 2	
C3 If MW < 500 g/mol				
P_{OW} – data	< 1000			≥ 1000
Water solubility g/L	> 100	100 - 2	> 2 – 0.02	<0.02

The asterisks (*) represents the bioaccumulation score of substance

2.2.5 D-score (Toxicity)

The D-score is based on information about the substance toxicity to fish which is LC_0 or LC_{50}, or on information concerning inhibition resulting from the substance in activated sludge. The method of determining the **Toxicity score** is detailed in Table 2-2.

Table 2-2: Toxicity score adapted from (Laursen et al., 2002)

Score Figure → / Parameter ↓	1	2	3	4
D – Effect concentration divided by effluent concentration	> 1000	1000 - 101	100 - 10	< 10

2.2.6 The score plot

The **Exposure score** is then plotted against the **Toxicity score** to determine whether the substance is a low impact or high impact substance on the environment. A typical plot is presented in Figure 2-1. The substances that fall left of the diagonal line have relatively lower environmental impacts and those which fall to the right of the diagonal line have relatively higher environmental impacts. The high impact substances should be subject to closer examination.

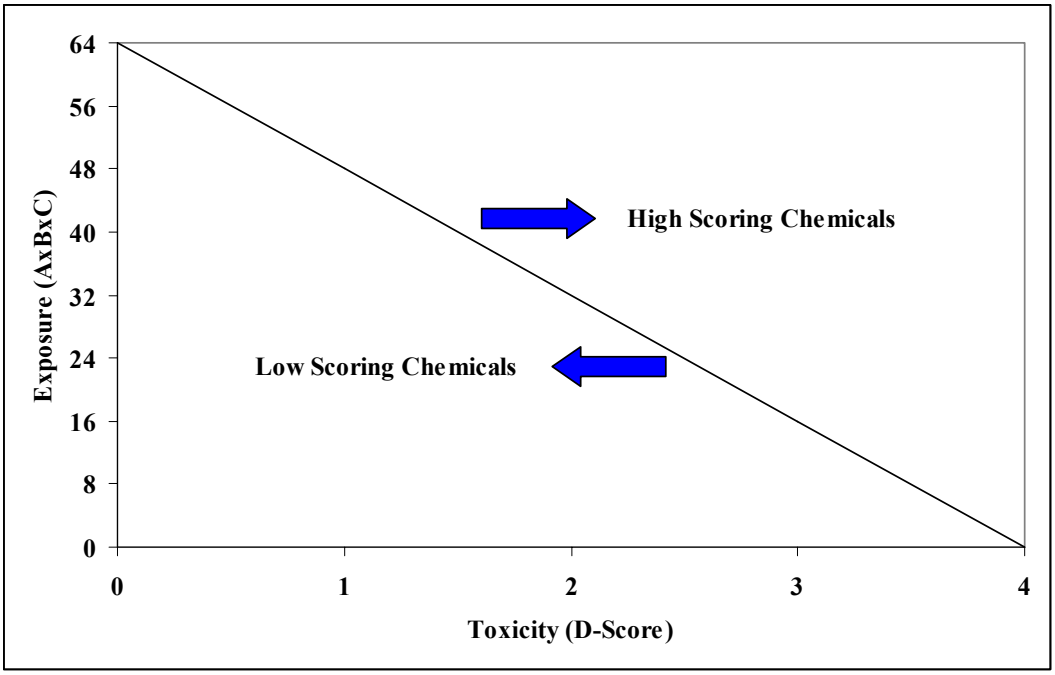

Figure 2-1: Score plot, plot of exposure against toxicity to identify the high impact chemicals

The hypothesis of this is study is that a low score translates to a low toxicity to the activated sludge processes at a municipal wastewater treatment works.

2.3 Respirometry

Respirometry is frequently used in wastewater characterisation and in the determination of activated sludge model kinetics. Respirometry is a measure of the respiration rate of activated sludge biomass and is defined as the amount of oxygen per unit volume and time consumed by the activated sludge biomass. Respirometric data can be used for modelling purposes and in the control of aerobic activated sludge processes (Henze et al., 1987, Vanrolleghem et al., 1999).

Figure 2-2 shows a flow diagram of a respirometer (Spanjers et al., 1998), a respirometer can be classified based on two criteria:

1. The phase in which the oxygen concentration is measure (liquid or gas phase)

2. Batch or continuous flow regime of the gas and liquid phases (flowing or static flow)

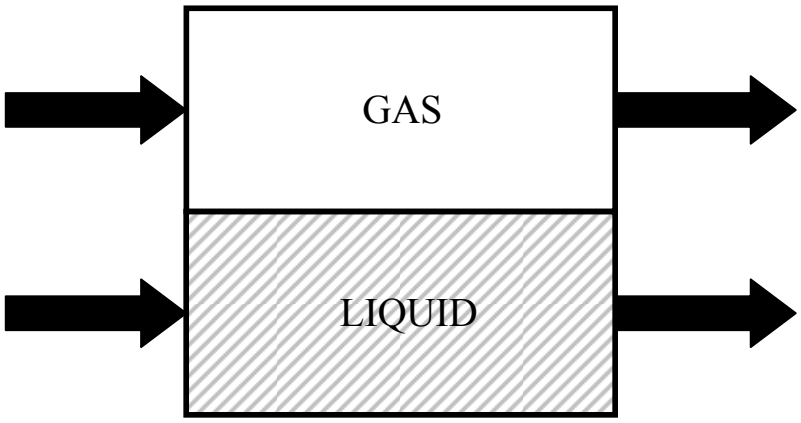

Figure 2-2: Flow diagram of a respirometer (Spanjers et al., 1998)

In general dissolved oxygen concentration is measured in the liquid phase; hence this discussion will be limited to respirometers which measure dissolved oxygen concentration in the liquid phase using dissolved oxygen electrodes. By performing a general mass balance for dissolved oxygen concentration S_O presented in Equation 2-1, the respiration rate can be obtained. The equation consists of a transport term $\frac{Q_{in}}{V}\cdot\left(S_{O,in}-S_O\right)$, aeration term $K_L a\cdot\left(S_O^0-S_O\right)$ and the oxygen uptake rate OUR of the biomass. The transportation term and aeration term may be removed; depends on the configuration of the respirometer.

$$\frac{dS_O}{dt}=\frac{Q_{in}}{V}\cdot\left(S_{O,in}-S_O\right)+K_L a\cdot\left(S_O^0-S_O\right)-OUR \qquad (2\text{-}1)$$

2.3.1 Respirometric Techniques

In the following the sections different respirometric techniques are examined, the advantages and disadvantages of these techniques in the wastewater and kinetic characterisation are

discussed.

2.3.1.1 Static gas – flowing liquid

Static gas – flowing liquid respirometers is a continuous system in which the dissolved oxygen concentration (S_O) is measured at the inlet and outlet of a closed respiration vessel (Spanjers, 1993). Aerated sludge is continuously pumped through the respiration vessel. The OUR is calculated from the dissolved oxygen mass balance over the unaerated respiration vessel, shown in Equation 2-2:

$$\frac{dS_O}{dt} = \frac{Q_{in}}{V} \cdot \left(S_{O,in} - S_O \right) - OUR \qquad (2\text{-}2)$$

Where:

$S_{O,in}$ = inlet dissolved oxygen concentration

S_O = outlet dissolved oxygen concentration

Q_{in}/V = residence time in respiration vessel

For this type of respirometer a closed respiration vessel the aeration term $K_L a \cdot \left(S_O^0 - S_O \right)$ in Equation 2-1 is absent from the dissolved oxygen mass balance, hence complex substrates such as wastewater can be used because the $K_L a$ value determination is not required. Knowledge of the flow rate and reactor volume is required to calculate the residence time Q_{in}/V . The flowrate should be adjusted so as to prevent oxygen limitation condition. When there is a small difference between the two dissolved oxygen probes $\left(S_{O,in} - S_O \right)$ drift in the electrodes may result in erroneous OUR data. To resolve this problem the dissolved oxygen concentration of the inlet and outlet are measured by the same dissolved oxygen probe, this is achieved by switching the direction of flow in the respiration vessel (Spanjers, 1993). This frequent switch in flow direction results in lower measurement frequency of OUR (Vanrolleghem and Spanjers, 1998).

2.3.1.2 Static gas – static liquid

Static gas – static liquid respirometers are typically operated by aerating for short period of time thereafter monitoring the decline of dissolved oxygen concentration with time in a closed

vessel (Cech et al., 1984, Kappler and Gujer, 1992, Kristensen et al., 1992). For this type of respirometer the mass balance of dissolved oxygen shown in Equation 2-1 is simplified to Equation 2-3, since the transportation and aeration terms are removed.

$$\frac{dS_O}{dt} = -OUR \tag{2-3}$$

These respirometers are closed vessels with no head space, since no aeration of the activated sludge sample through surface aeration or bubble in the liquid phase must occur during the experiment. In the case of an open vessel being used the measured data may be influenced by surface aeration, in this case an aeration term may be included in the mass balance equation. Typically the influence of surface aeration is ignored (Randall et al., 1991, Takamatsu et al., 1982). The oxygen transferred through the liquid-air interface can be limited by covering the liquid surface with plastic balls (Wentzel et al., 1995), or by using a vessel that is the diameter of the dissolved oxygen electrode (Gernaey et al., 1997).

The experiments performed with this design are carried out with high substrate concentration and low biomass concentrations (high S_0/X_0 ratio) to prevent oxygen limitation conditions. The danger in performing the respirometric experiment under high S_0/X_0 ratio is that the sludge behaviour may not be representative of the full scale system (Novak et al., 1994). This type of respirometer is limited in the characterisation of wastewater and determination of activated sludge kinetics. Since the experiments are performed under high S_0/X_0 ratio the maximum specific growth rate (μ_{max}) may be determined but the half-saturation constant (K_S) cannot be determined because the substrate concentration may never drop near the value of K_S. Furthermore the problem of oxygen limitation condition associated with this type of respirometer has been resolved by frequent re-aeration of the sample (Suschka and Ferreira, 1986, Watts and Garber, 1993). In addition another solution to the oxygen limitation problem condition has been to over saturate the activated sludge sample with oxygen (Ellis et al., 1996), but the shortcoming of this solution is that the dissolved oxygen concentration will differ from the full-scale operating condition.

Static gas - static liquid respirometers sampling frequency of OUR cycle are rather low, since one OUR value would be obtained per aeration. This low sampling frequency is a disadvantage, because it results in difficulties in determining activated sludge kinetic parameters

(Vanrolleghem and Spanjers, 1998).

2.3.1.3 Flowing gas – static liquid

In flowing gas – static liquid respirometers high concentration of sludge (low S_0/X_0 ratio) can be used because the vessel is continuously aerated, therefore no oxygen limitation does not occur (Blok, 1974, Farkas, 1981, Ros et al., 1988). An advantage of high sludge concentration X_0 is shorter time for experiments. For this type of respirometer the mass balance of dissolved oxygen shown in Equation 2-1 is simplified to Equation 2-4, since the transportation is removed.

$$\frac{dS_O}{dt} = K_L a \cdot \left(S_O^0 - S_O \right) - OUR \tag{2-4}$$

To obtain reliable OUR data an optimal aeration should be determined. If the aeration is too high the OUR data may contain significant amount of measurement noise.

In general, oxygen uptake rate (OUR) can be considered to consist of two components (Spanjers, 1993) as shown in Equation 2-5; the exogenous oxygen uptake rate (OUR_{exo}) which the uptake of the degradable substrate and the endogenous oxygen uptake rate (OUR_{end}).

$$OUR = OUR_{exo} + OUR_{end} \tag{2-5}$$

Under the assumption that OUR_{end} is constant, Equation 2-4 can be changed to Equation 2-6 (Vanrolleghem et al., 1994).

$$\frac{dS_O}{dt} = K_L a \cdot \left(S_{O,eq} - S_O \right) - OUR_{exo} \tag{2-6}$$

When OUR_{exo} is zero, the oxygen concentration in the vessel reaches a steady state value of $S_{O,eq}$ which indicates the equilibrium between the oxygen transfer and endogenous respiration. A flowing gas – static liquid respirometer allows a high frequency measure of OUR data as compared to the static gas – static liquid respirometers (Vanrolleghem et al., 1994). There are

several methods to determine the value of the oxygen transfer coefficient $K_L a$, it can be determined from a separate re-aeration experiment with sludge in the endogenous state (Bandyopadhyay et al., 1967) or from a re-aeration curve obtained after an addition of a known amount of readily biodegradable substrate to the system (Vanrolleghem et al., 1994).

2.4 Optimal Experimental Design (OED)

In this section the concept of optimal experimental design (ODE) (Dochain and Vanrolleghem, 2001) is introduced and a detailed discussion is provided for the concept of OED applied to the design of an experiment in which the data will be used for parameter estimation. The OED methodology was used to obtain the optimal batch respirometric experiment design in this study.

2.4.1 Optimal Experimental Design Concept

Obtaining quality experimental data is a critical task when this data is to be used in model building, model selection and parameter estimation. The experimental design is an important task for modelling, since the experiment design is the critical factor in obtaining good information-rich experiment data. The goals pursed in an experimental design procedure can be categorised in three areas; experiment design for a reliable selection of an adequate mathematical model structure of the process, the design of experiment for precise estimation of model parameters, and the dual problem of structure characterisation and parameter estimation (Dochain and Vanrolleghem, 2001). There are a number of quantitative functions associated with the respective goal of the experimental design. The focus of this study is the design of an experiment for precise estimation of model parameters; therefore the experiment design procedure associated with this goal is discussed in detail. The Optimal Experimental Design (OED) procedure (Dochain and Vanrolleghem, 2001) is summarised in Figure 2-3 (De Pauw, 2005).

Once a preliminary model is created based on previously acquired data, the experiment degrees of freedom and constraints for the experimental design procedure are defined (De Pauw, 2005). The experiment degrees of freedom are subdivided into measurements and manipulations categories (Dochain and Vanrolleghem, 2001). With regard to the measurements in the experiment category several question can be posed: (1) what to measure, (2) where to measure and (3) when to measure (Dochain and Vanrolleghem, 2001). The manipulation category often

is the most important category and relates to the excitation signal that acts on the system to produce highly qualitative information.

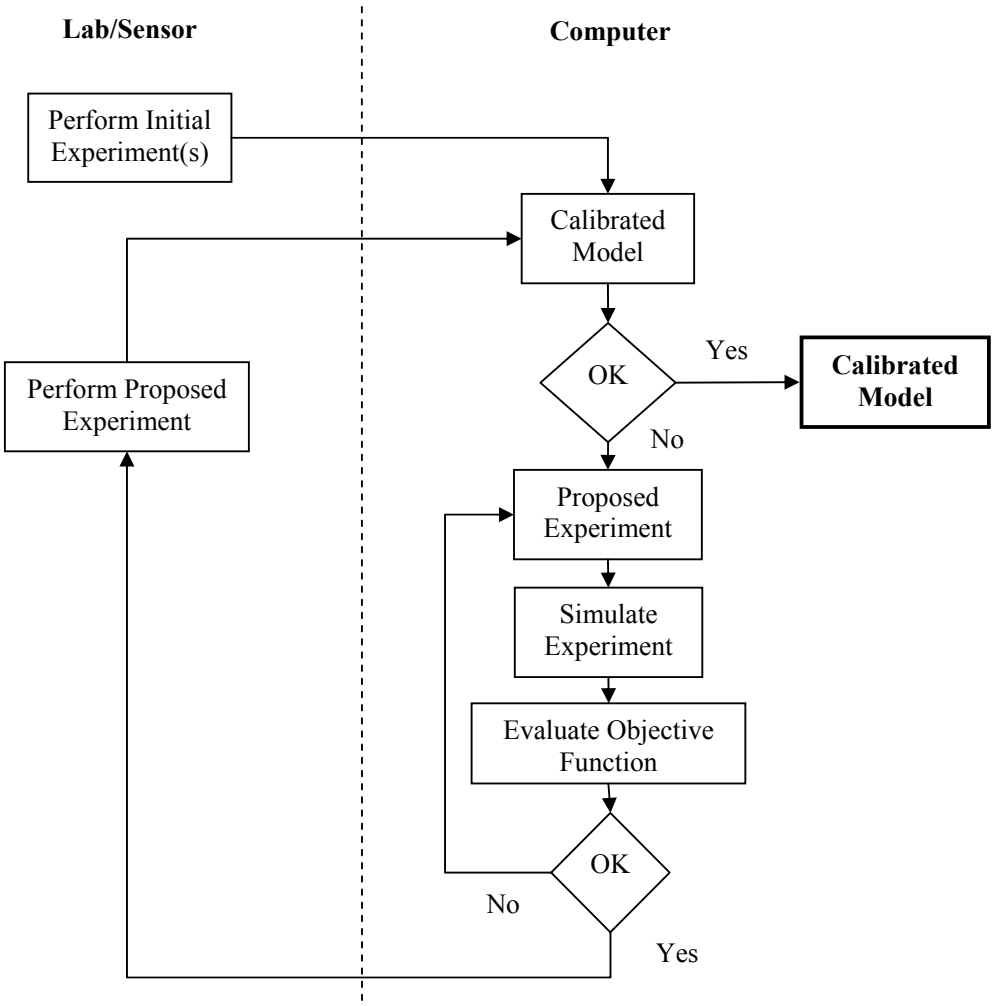

Figure 2-3: Schematic of Optimal Experimental Design (OED) procedure (De Pauw, 2005)

The optimal experiment design procedure for parameter estimation (Dochain and Vanrolleghem, 2001) was applied in the design of this studies batch respirometric experiments. The assessment of the quality of a set of parameter estimates can be based on the way the parameters allow a model to make good predictions of process behaviour. However the most popular method of assessing the quality of parameter estimates is by providing information on

the parameter estimation errors in the form of confidence intervals or by providing the covariance matrix. These concept are related to practical identifiability which and are discussed in detail in **Section 2.7.2** and **Chapter 3, Section 3.5.2.** The objective of the batch respirometric experiment design is to obtain reliable parameter estimate, therefore it is clear that the covariance matrix (V) or similarly the Fischer matrix (F) are central components in this task (refer to **Section 3.5.2** for the respective mathematical expressions of these matrices).

In this study a single variable, oxygen uptake rate (OUR), is measured and fitted. In such a case, a realistic estimate of the parameter estimate confidence can be obtained by evaluating the residual mean square (s^2) (Dochain and Vanrolleghem, 2001).

$$s^2 = \frac{J_{opt}(\theta)}{N - p} \tag{2-7}$$

Where p is the number of parameters in the model, $J_{opt}(\theta)$ is the quadratic objective function which is minimised during parameter estimation (this function is described in detail in **Section 3.5.2**) and N is the number of experimental data points.

If the covariance matrix V is available approximate standard errors ($\sigma(\theta_i)$) for the parameters can be calculated as follows (Dochain and Vanrolleghem, 2001):

$$\sigma(\theta_i) = s\sqrt{V_{ii}} \tag{2-8}$$

2.5 Description of Activated Sludge Kinetic Models

The most common wastewater treatment method is the activated sludge process. In this process bacteria (biomass) remove pollutants; these are in the form of organic carbon, nitrogen and phosphorus. The design of the wastewater treatment works determines which of the pollutants are removed. Dynamic kinetic models of the activated sludge processes have been created as a result of knowledge gained from research into the mechanisms of the different biological degradation processes. This review will focus primarily on Activated Sludge Model No. 1 (ASM1) (Henze et al., 1987), which is the most popular activated sludge model used in the design and operation of wastewater treatment works.

Information of the ASM1 (Henze et al., 1987) and ASM3 (Gujer et al., 1999) activated sludge models are covered. The activated sludge models which include phosphorus removal are not covered in this study, hence ASM2 and ASM2d (Henze et al., 1995, Henze et al., 1999) are not described.

2.5.1 Activated Sludge Model No. 1 (ASM1)

ASM1 is presented in Petersen matrix format in Table 2-4 (Henze et al., 1987). Carbon substrates are defined in terms of Chemical Oxygen Demand (COD) and nitrogen substrates in terms of nitrogen content.

2.5.1.1 Fundamentals of Petersen matrix

The Petersen matrix consists of the components (C_i), parameters (p), and processes (j). The components are state variables and vary with time. Processes are the transformation in which the components take part. The parameters are found in the stoichiometric expressions (α_{ji}) and in the process rate equations (ρ_j), these parameters are constant in respect to independent variables.

Table 2-3: Typical Petersen matrix

Components → **↓ Processes**	**C_1**	**C_2**	**C_i**	**C_n**	**Process Rates**
Process 1	α_{11}	α_{12}	α_{1i}	α_{1n}	ρ_1
Process j	α_{j1}		α_{ji}		ρ_j
Process m				α_{mn}	ρ_m

In the Petersen matrix the mass conservation principle is applied, this is described by Equation 2-9:

$$\sum_{j=1}^{n} \alpha_{ji} = 0 \qquad (2\text{-}9)$$

The dynamics of the i-th component of the Petersen matrix is described by the differential equation, Equation 2-10:

$$\frac{d}{dt}C_i = \sum_{j=1}^{k} \alpha_{ji} \cdot \rho_j \qquad (2\text{-}10)$$

2.5.1.2 ASM1 components

Total COD is subdivided based on solubility, biodegradability, biodegradation and biomass, this partitioning of COD is shown in Figure 2-4. Total COD is divided into biodegradable, non-biodegradable and active mass groups. The biodegradable and non-biodegradable groups are then separated into soluble (S) and particulate (X) components. The non-biodegradable components pass through the system unchanged since they are biologically inert. The soluble inert (S_I) enters and leaves the system at the same concentration. The particulate component X_P is produced through decay of biomass, both particulate components X_P and X_I are removed from the system via sludge wastage. The biodegradable matter consist of readily biodegradable (S_S) and slowly biodegradable (X_S) substrate. Readily biodegradable substrate consists of simple molecules which are utilised by heterotrophic biomass (X_{BH}), and slowly biodegradable substrate consists of complex molecules which are broken down into simple molecules to be consumed by heterotrophic biomass. The active mass is divided into autotrophic biomass (X_{BA}) which consumes ammonia (S_{NH}) and heterotrophic biomass (X_{BH}). The partitioning of total COD is summarised in Equation 2-11.

$$COD_{TOTAL} = S_I + S_S + X_I + X_S + X_{BH} + X_{BA} + X_P \qquad (2\text{-}11)$$

Table 2-4: ASM1 process matrix (Henze et al., 1987)

Component i → / ↓ Process j	1 S_I	2 S_S	3 X_I	4 X_S	5 X_{BH}	6 X_{BA}	7 X_P	8 S_O	9 S_{NO}	10 S_{NH}	11 S_{ND}	12 X_{ND}	13 S_{ALK}	Process rate ρ_j
1 Aerobic growth of heterotrophs		$-\frac{1}{Y_H}$			1			$-\frac{1-Y_H}{Y_H}$		$-i_{XB}$			$-\frac{i_{XB}}{14}$	$\mu_{mH}\left(\frac{S_S}{K_S+S_S}\right)\left(\frac{S_O}{K_{OH}+S_O}\right)X_{BH}$
2 Anoxic growth of heterotrophs		$-\frac{1}{Y_H}$			1				$-\frac{1-Y_H}{2.86Y_H}$	$-i_{XB}$			$\frac{1-Y_H}{14\cdot 2.86Y_H}-i_{XB}/14$	$\mu_{mH}\left(\frac{S_S}{K_S+S_S}\right)\left(\frac{K_{OH}}{K_{OH}+S_O}\right)\times\left(\frac{S_{NO}}{K_{NO}+S_{NO}}\right)\eta_g X_{BH}$
3 Aerobic growth of autotrophs						1		$-\frac{4.57-Y_A}{Y_A}$	$\frac{1}{Y_A}$	$-i_{XB}-\frac{1}{Y_A}$			$\frac{i_{XB}}{14}-\frac{1}{7\cdot Y_A}$	$\mu_{mA}\left(\frac{S_{NH}}{K_{NH}+S_{NH}}\right)\left(\frac{S_O}{K_{OA}+S_O}\right)X_{BA}$
4 Decay of heterotrophs				$1-f_P$	-1		f_P					$i_{XB}-f_P\cdot i_{XP}$		$b_H X_{BH}$
5 Decay of autotrophs				$1-f_P$		-1	f_P					$i_{XB}-f_P\cdot i_{XP}$		$b_A X_{BA}$
6 Ammonification of soluble organic nitrogen										1	-1		$\frac{1}{14}$	$k_a S_{ND} X_{BH}$
7 Hydrolysis of entrapped organics		1		-1										$k_{mh}\frac{X_S/X_{BH}}{K_X+(X_S/X_{BH})}\times\left[\left(\frac{S_O}{K_{OH}+S_O}\right)+\eta_h\left(\frac{K_{OH}}{K_{OH}+S_O}\right)\left(\frac{S_{NO}}{K_{NO}+S_{NO}}\right)\right]X_{BH}$
8 Hydrolysis of entrapped organic nitrogen											1	-1		$\rho_7\left(X_{ND}/X_S\right)$

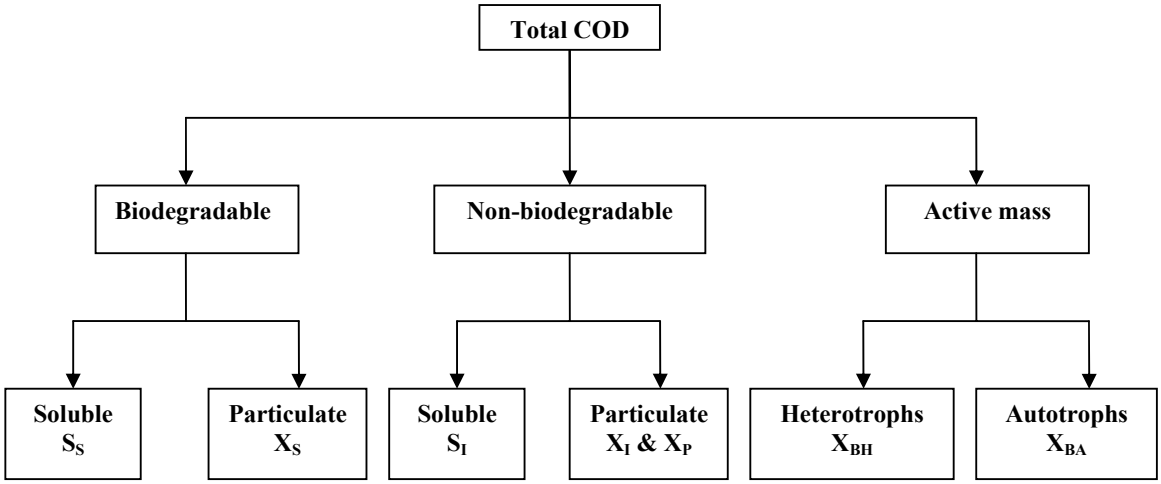

Figure 2-4: COD components of ASM1 adapted from (Petersen, 2000)

Total nitrogen can be subdivided in a similar way as total COD, based on solubility, biodegradability, biodegradation and active mass, this partitioning of nitrogen is displayed in Figure 2-5. Total nitrogen is divided into total kjeldahl nitrogen (TKN) and nitrate/nitrite. Nitrate/nitrite (S_{NO}) is biodegradable nitrogen component; whereas TKN consists of biodegradable, non-biodegradable and active mass nitrogen matter components. The biodegradable and non-biodegradable groups are then separated into soluble (S) and particulate (X) components. The soluble non-biodegradable organic nitrogen (S_{NI}) occurs in negligible amounts so is excluded from the ASM1 model, the particulate non-biodegradable organic nitrogen (X_{NI}) is linked to non-biodegradable particulate components of COD. The biodegradable nitrogen matter consists of ammonia nitrogen (S_{NH}), nitrate/nitrite (S_{NO}), soluble organic nitrogen (S_{ND}) and particulate organic nitrogen (X_{ND}). The particulate organic nitrogen is hydrolysed to soluble organic nitrogen. Soluble organic nitrogen is converted to ammonia nitrogen through the process of ammonification. The ammonia nitrogen is converted in a single step process to nitrate by autotrophic biomass and also serves as the nitrogen source for biomass growth. The fraction of nitrogen content in heterotrophic and autotrophic biomass is indicated by the i_{XB} parameter. The partitioning of total nitrogen is summarised in Equation 2-12.

$$N_{TOTAL} = S_{NH} + S_{ND} + S_{NO} + X_{ND} + X_{NI} + i_{XB} \cdot (X_{BH} + X_{BA}) + i_{XP} \cdot X_P \quad (2\text{-}12)$$

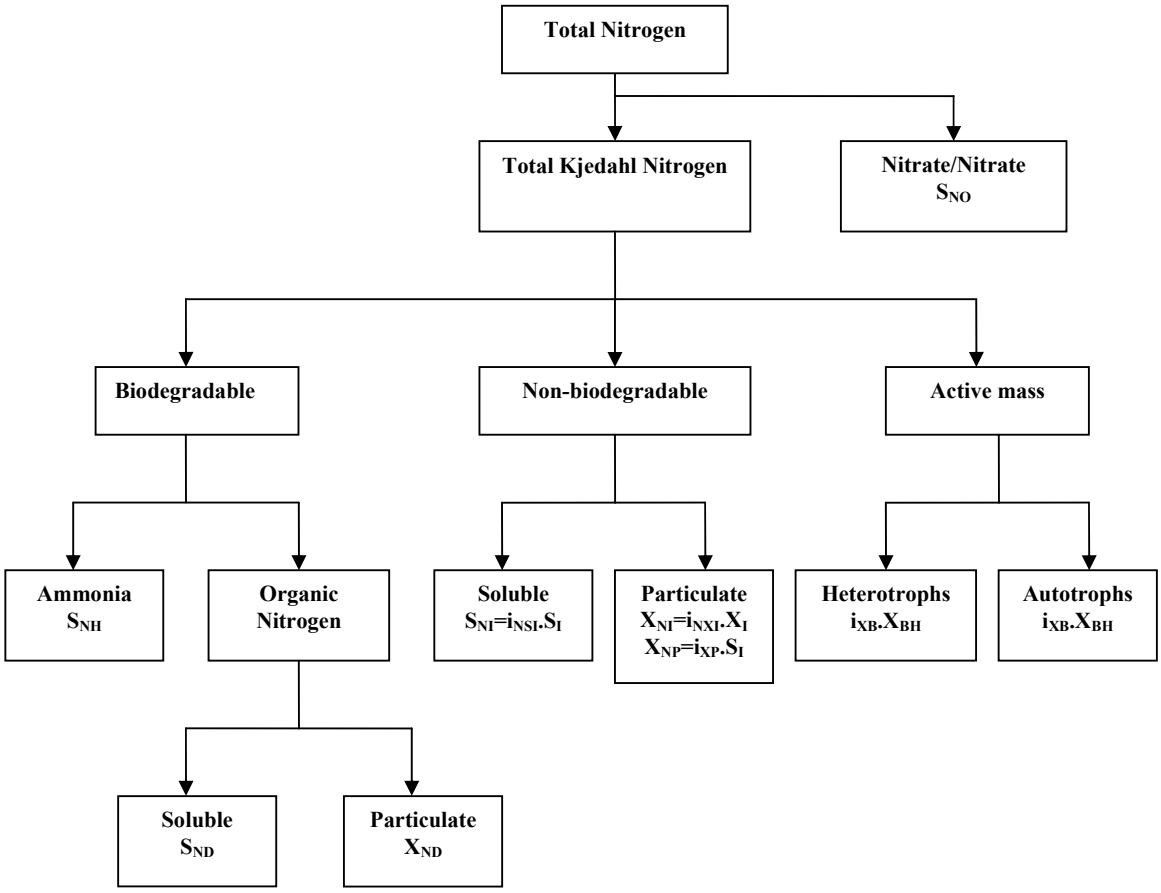

Figure 2-5: Nitrogen components of ASM1 adapted from (Petersen, 2000)

2.5.1.3 ASM1 processes

From Table 2-4 it can be observed that there are four main processes in the ASM1 model (Henze et al., 1987). The growth processes of biomass, that is of hetetrophic (Process 1 and 2) and autotrophic (Process 3) biomass. The decay processes of biomass, once again of hetetrophic (Process 4) and autotrophic (Process 5) biomass. Also the ammonification process (Process 6) of converting organic nitrogen (S_{ND}) to ammonia nitrogen (S_{NH}). Finally the hydrolysis of particulate organic matter processes, which is of slowly biodegradable substrate (X_S) (Process 7) and particulate organic nitrogen (X_{ND}) (Process 8).

Aerobic growth of heterotrophic biomass

The Monod relationship is used to describe aerobic growth of heterotrophs and autotrophs. The growth of heterotrophs occurs by the consumption of readily biodegradable substrate (S_S) and oxygen (S_O), ammonia is incorporated into the biomass.

Anoxic growth of heterotrophic biomass

This is essentially the denitrification process, in which nitrate is used by heterotrophic biomass as a terminal electron acceptor and readily biodegradable substrate (SS) as the substrate. As a result biomass growth occurs and nitrogen gas is formed. The same Monod kinetics as the aerobic process is used, except a correction factor (η_g) is included to account for the anoxic process occurring at slower rate than the aerobic process. In addition a switching function, $K_{OH}/(K_{OH}+S_O)$, is included to describe the inhibition resulting from the presents of oxygen

Aerobic growth of Autotrophic biomass

Aerobic growth of autotrophic biomass is the nitrification process of oxidising ammonia nitrogen (S_{NH}) to nitrate (S_{NO}). This results in the formation of autotrophic biomass and the incorporation of a fraction of S_{NH} into the autotrophic biomass. The nitrification process impacts significantly on alkalinity.

Decay of heterotrophs

The death regeneration concept (Dold, 1980) was used to describe the process reactions which occurs when biomass die. Tradition decay concepts describe the decay process as a fraction of the biomass being broken down to release energy for maintenance. The death regeneration concept has no direct link between the decay of biomass and oxygen represented as COD. The concept describes decay as resulting in the release of slowly biodegradable substrate, which is then broken down into readily biodegradable substrate. This readily biodegradable substrate is used in the growth of more biomass. Hence oxygen utilisation is associated with decay indirectly through the growth of new biomass on released substrate. Simultaneously organic nitrogen is converted to ammonia nitrogen. The magnitude of decay coefficient is greater in this concept than in traditional endogenous respiration concepts. This is as a result of the decay coefficient compensating to obtain the same oxygen utilisation per unit time due to decay.

Therefore the net amount of biomass increases, as a result the biomass growth rate is higher in the death regeneration model than in reality.

Decay of autotrophs

The decay of autotrophs can be explained in a similar way to the decay of heterotrophs.

Ammonification of soluble organic nitrogen

Soluble organic nitrogen (S_{ND}) is converted to ammonia nitrogen (S_{NH}) in a first order process accompanied by alkalinity changes.

Hydrolysis of entrapped organics

Slowly biodegradable substrate (X_S) is broken down into readily biodegradable substrate (S_S). A correction factor (η_h) is included to account for the hydrolysis rate decrease under anoxic conditions.

Hydrolysis of entrapped organics nitrogen

The hydrolysis of entrapped organic nitrogen can be explained in a similar way to the hydrolysis of entrapped organics.

2.5.2 Activated Sludge Model 3 (ASM3)

The ASM3 stoichiometry and process rate equations are presented in matrix form in Table 2-5 and Table 2-6 respectively.

The major difference between ASM1 and ASM3 is that ASM3 accounts for conditions of elevated concentrations of readily biodegradable organic substrate which can lead to storage of polyhydroxy-alkanoates, lipids and glycogen (Petersen, 2000). This process is not included in ASM1; the aerobic storage process is described in ASM3 as the process of readily biodegradable substrate (S_S) being stored in a cell internal component X_{STO}. All readily biodegradable substrate is first stored then used for growth; the energy required for this storage process is obtained from aerobic respiration. Another important difference between ASM1 and ASM3 is the replacement of the death regeneration concept by endogenous respiration. The

death regeneration concept decay coefficient was difficult to determine, while the endogenous respiration process presented in ASM3 is much easier to obtain through batch experiments and is closer to what is experienced in reality (Petersen, 2000).

Table 2-5: Stoichiometric matrix of ASM3 (Gujer et al., 1999)

Component i → / ↓ Process j	1 S_I	2 S_S	3 X_I	4 X_S	5 X_H	6 X_{STO}	7 X_A	8 X_{TSS}	9 S_O	10 S_{NO}	11 S_{NH}	12 S_{N2}	13 S_{ALK}
1 Hydrolysis	f_{S_I}	$1-f_{S_I}$		-1				$-i_{TS,XS}$			$i_{NXS}-i_{NSS}\cdot(1-f_{S_I})$		$\frac{i_{NXS}-i_{NSS}\cdot(1-f_{S_I})}{14}$
2 Aerobic storage of COD		-1				Y_{STO,O_2}		$0.6\cdot Y_{STO,O_2}$	$Y_{STO,O_2}-1$		i_{NSS}		$\frac{i_{NSS}}{14}$
3 Anoxic storage of COD		-1				$Y_{STO,NO}$		$0.6\cdot Y_{STO,NO}$		$-\frac{1-Y_{STO,NO}}{2.86}$	i_{NSS}	$\frac{1-Y_{STO,NO}}{2.86}$	$\frac{i_{NSS}+\frac{1-Y_{STO,NO}}{2.86}}{14}$
4 Aerobic growth					1	$-\frac{1}{Y_{H,O_2}}$		$i_{TS,BM}-\frac{0.6}{Y_{H,O_2}}$	$1-\frac{1}{Y_{H,O_2}}$		$-i_{NBM}$		$-\frac{i_{NBM}}{14}$
5 Anoxic growth					1	$-\frac{1}{Y_{H,NO}}$		$i_{TS,BM}-\frac{0.6}{Y_{H,NO}}$		$\frac{1-1/Y_{STO,NO}}{2.86}$	$-i_{NBM}$	$-\frac{1-1/Y_{H,NO}}{2.86}$	$-\frac{i_{NBM}+\frac{1-1/Y_{STO,NO}}{2.86}}{14}$
6 Aerobic endogenous respiration of heterotrophs			f_{X_I}		-1			$f_{X_I}\cdot i_{TS,X_I}-i_{TS,BM}$	$-(1-f_{X_I})$		$i_{NBM}-f_{X_I}\cdot i_{NXI}$		$\frac{i_{NBM}-f_{X_I}\cdot i_{NXI}}{14}$
7 Anoxic endogenous respiration of heterotrophs			f_{X_I}		-1			$f_{X_I}\cdot i_{TS,X_I}-i_{TS,BM}$		$-\frac{1-f_{X_I}}{2.86}$	$i_{NBM}-f_{X_I}\cdot i_{NXI}$	$\frac{1-f_{X_I}}{2.86}$	$\frac{i_{NBM}-f_{X_I}\cdot i_{NXI}-\frac{f_{X_I}-1}{2.86}}{14}$
8 Aerobic respiration of X_{STO}						-1		–0.6	-1				
9 Anoxic respiration of X_{STO}						-1		–0.6		$-\frac{1}{2.86}$		$\frac{1}{2.86}$	$\frac{1}{14\cdot 2.86}$
10 Nitrification							1	$i_{TS,BM}$	$1-\frac{4.57}{Y_A}$	$\frac{1}{Y_A}$	$-i_{NBM}-\frac{1}{Y_A}$		$\frac{-i_{NBM}-2/Y_A}{14}$
11 Aerobic endogenous respiration of autotrophs			0.2				-1	$f_{X_I}\cdot i_{TS,X_I}-i_{TS,BM}$	$-(1-f_{X_I})$		$i_{NBM}-f_{X_I}\cdot i_{NXI}$		$\frac{i_{NBM}-f_{X_I}\cdot i_{NXI}}{14}$
12 Anoxic endogenous respiration of autotrophs			f_{X_I}				-1	$f_{X_I}\cdot i_{TS,X_I}-i_{TS,BM}$	1	$-\frac{1-f_{X_I}}{2.86}$	$i_{NBM}-f_{X_I}\cdot i_{NXI}$	$\frac{1-f_{X_I}}{2.86}$	$\frac{i_{NBM}-f_{X_I}\cdot i_{NXI}+\frac{1-f_{X_I}}{2.86}}{14}$

Table 2-6: Process rate equations of ASM3 (Gujer et al., 1999)

j	Process	Process rate ρ_j
1	Hydrolysis	$k_h \cdot \frac{X_S/X_H}{K_X + X_S/X_H} \cdot X_H$
2	Aerobic storage of COD	$k_{STO} \cdot \frac{S_O}{K_O + S_O} \cdot \frac{S_S}{K_S + S_S} \cdot X_H$
3	Anoxic storage of COD	$k_{STO} \cdot \eta_{NO} \cdot \frac{K_O}{K_O + S_O} \cdot \frac{S_{NO}}{K_{NO} + S_{NO}} \cdot \frac{S_S}{K_S + S_S} \cdot X_H$
4	Aerobic growth of heterotrophs	$\mu_{mH} \cdot \frac{S_O}{K_O + S_O} \cdot \frac{S_{NH}}{K_{NH} + S_{NH}} \cdot \frac{S_{ALK}}{K_{ALK} + S_{ALK}} \cdot \frac{X_{STO}/X_H}{K_{STO} + X_{STO}/X_H} \cdot X_H$
5	Anoxic growth of heterotrophs	$\mu_{mH} \cdot \eta_{NO} \cdot \frac{K_O}{K_O + S_O} \cdot \frac{S_{NO}}{K_{NO} + S_{NO}} \cdot \frac{S_{NH}}{K_{NH} + S_{NH}} \cdot \frac{S_{ALK}}{K_{ALK} + S_{ALK}} \cdot \frac{X_{STO}/X_H}{K_{STO} + X_{STO}/X_H} \cdot X_H$
6	Aerobic endogenous respiration of heterotrophs	$b_{H,O_2} \cdot \frac{S_O}{K_O + S_O} \cdot X_H$
7	Anoxic endogenous respiration of heterotrophs	$b_{H,NO} \cdot \frac{K_O}{K_O + S_O} \frac{S_{NO}}{K_{NO} + S_{NO}} \cdot X_H$
8	Aerobic respiration of X_{STO}	$b_{STO,O_2} \cdot \frac{S_O}{K_O + S_O} \cdot X_{STO}$
9	Anoxic respiration of X_{STO}	$b_{STO,NO} \cdot \frac{K_O}{K_O + S_O} \frac{S_{NO}}{K_{NO} + S_{NO}} \cdot X_{STO}$
10	Aerobic growth of Autotrophs, Nitrification	$\mu_{mA} \cdot \frac{S_O}{K_{A,O} + S_O} \cdot \frac{S_{NH}}{K_{A,NH} + S_{NH}} \cdot \frac{S_{ALK}}{K_{A,ALK} + S_{ALK}} \cdot X_A$
11	Aerobic endogenous respiration of autotrophs	$b_{A,O_2} \cdot \frac{S_O}{K_{A,O} + S_O} \cdot X_A$
12	Anoxic endogenous respiration of autotrophs	$b_{A,NO} \cdot \frac{K_{A,O}}{K_{A,O} + S_O} \frac{S_{NO}}{K_{A,NO} + S_{NO}} \cdot X_A$

2.5.2.1 ASM3 components

From Figure 2-6 it is observed that ASM3 total COD components are basically defined in the same way as ASM1; except particulate inert produced through decay (X_P) is incorporated into X_I since it is impossible to differentiate between them, and the storage term X_{STO} is introduced. The breakdown of total COD is summarised in Equation 2-13.

$$COD_{TOTAL} = S_I + S_S + X_I + X_S + X_H + X_A + X_{STO} \quad (2\text{-}13)$$

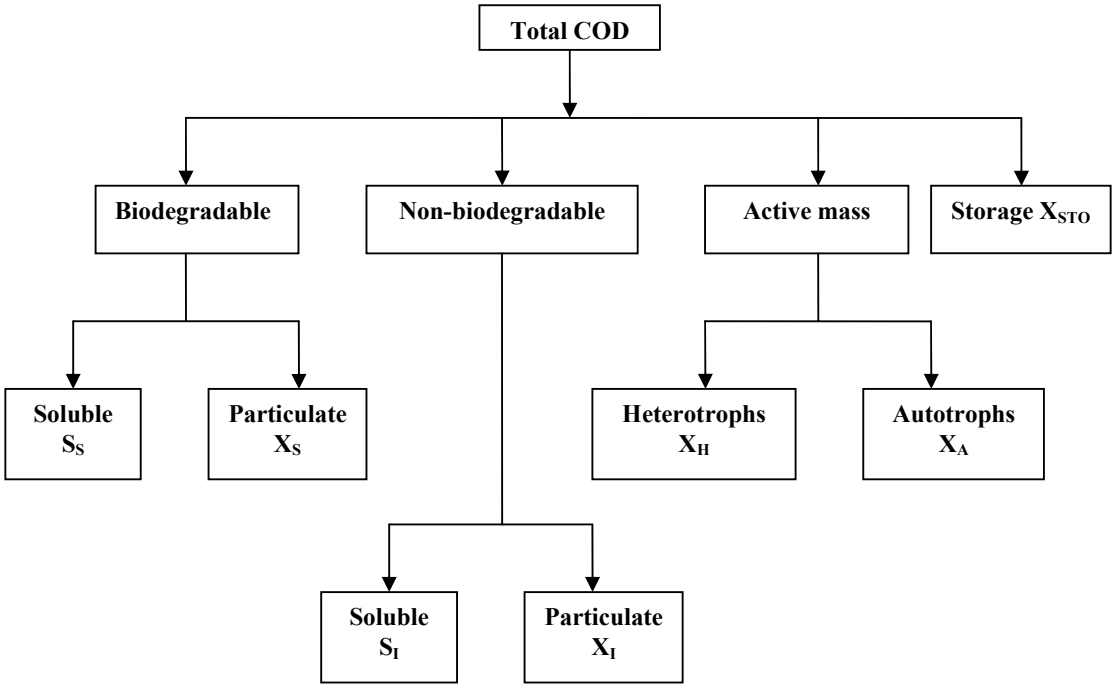

Figure 2-6: COD components of ASM3 adapted from (Petersen, 2000)

A simplified division of total nitrogen is used in ASM3 compared to ASM1; this nitrogen breakdown is presented in Figure 2-7. Soluble and particulate organic nitrogen components are not present in ASM3 since they complicate the model and their concentrations and reaction kinetics cannot be easily determined; these components have been replaced by fractions of nitrogen in components S_I, S_S, X_I, X_S and active biomass. In addition nitrogen gas has been introduced as a component allowing a closed nitrogen balance. The breakdown of nitrogen is summarised in Equation 2-14.

$$N_{TOTAL} = S_{NH} + S_{NO} + S_{N_2} + i_{NSI} \cdot S_I + i_{NSS} \cdot S_S + i_{NXS} \cdot X_S + i_{NBM} \cdot \left(X_H + X_A\right) + i_{NXI} \cdot X_I \quad (2\text{-}14)$$

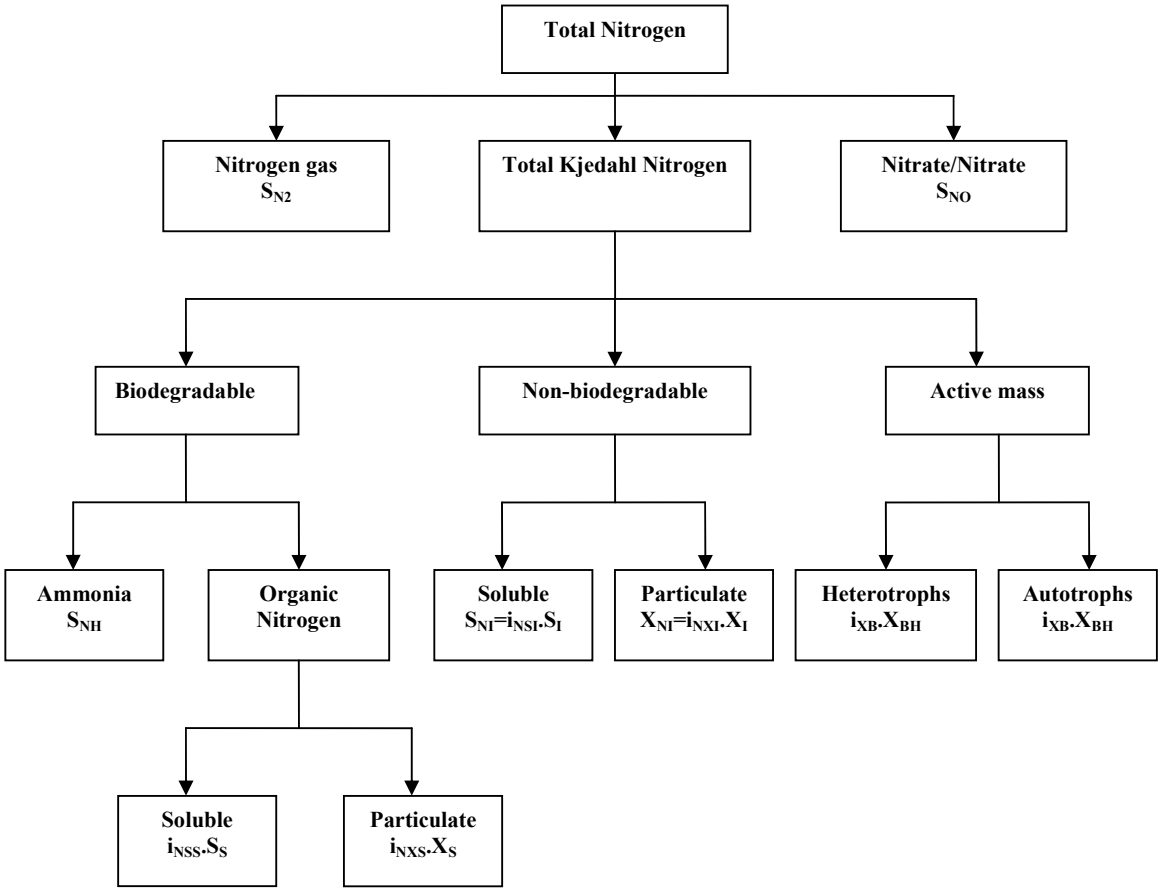

Figure 2-7: Nitrogen components of ASM3 adapted from (Gujer et al., 1999)

2.5.2.2 ASM3 processes

From Table 2-6 it can be observed that there are four main processes in the ASM3 model (Gujer et al., 1999). These processes are storage of readily biodegradable substrate, growth of biomass, decay of biomass and the hydrolysis of particulate organic matter.

Aerobic storage of readily biodegradable substrate

In this process oxygen is consumed through the storage of readily biodegradable in the form of X_{STO}.

Hydrolysis

This process is responsible for the breakdown of slowly biodegradable substrate to readily biodegradable substrate. The process is described in a similar method to the ASM1 hydrolysis process except that this process is now electron donor independent.

Anoxic storage of readily biodegradable substrate

This process is identical to the above process except nitrate is used as a terminal electron acceptor instead of oxygen and a correction factor (η_{NO}) is included to account for that only a fraction of the heterotrophic biomass maybe capable of denitrifying.

Aerobic growth of heterotrophs

X_{STO} and oxygen is consumed during the aerobic process of heterotrophic biomass growth. Nitrogen is also incorporated into the biomass as discussed earlier.

Anoxic growth of heterotrophs

Anoxic growth is similar to aerobic growth, except a correction factor (η_{NO}) is included to describe the reduced growth of biomass observed in anoxic respiration to aerobic respiration.

Aerobic growth of autotrophs

The aerobic growth of autotrophs is similar to the ASM1 process.

Aerobic and Anoxic decay of heterotrophs

The aerobic decay of heterotrophs is independent from the autotrophic biomass decay; this is the main difference from the decay regeneration concept of ASM1. There is a direct link between oxygen COD and the decay of heterotrophic biomass. Anoxic decay of heterotrophs process is described in a same way as aerobic decay.

Aerobic and anoxic decay of autotrophs

The process of aerobic and anoxic decay of autotrophs is the same as the heterotrophic decay processes.

Aerobic and anoxic respiration of storage product

Aerobic and anoxic respiration of storage products processes are the decay processes of the storage product (X_{STO}).

2.6 Mathematical Process Model Building

The modelling methodology for model building described by Dochain and Vanrolleghem (2001) is discussed below; using this methodology the BRE model was created. The model building procedure is summarised in Figure 2-8 (Castensen et al., 1997). After the steps in Figure 2-8 were completed successfully, the created model was used.

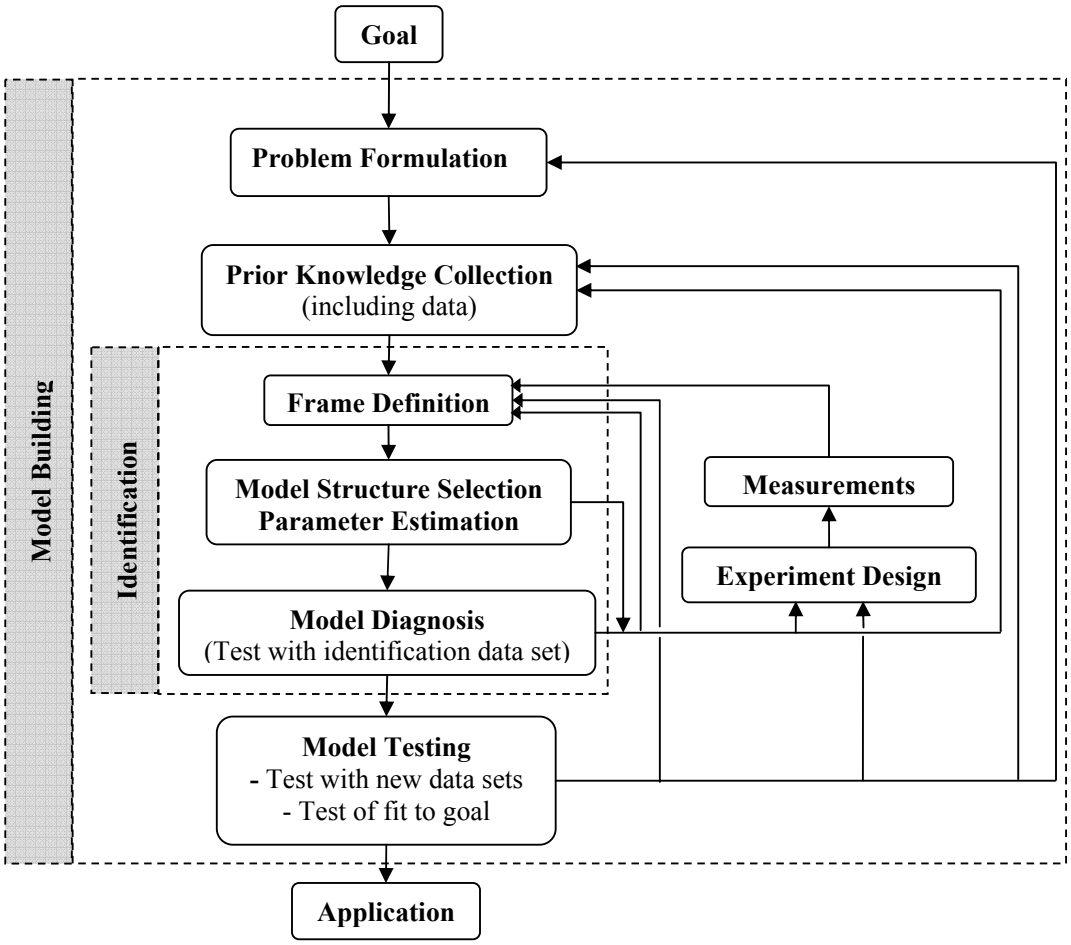

Figure 2-8: The model building procedure (Castensen et al., 1997)

2.6.1 Problem Formulation

The first step in the model building procedure is clearly defining the objective of the model before constructing the model. The overall purpose of the BRE model was to quantify the inhibitory nature of the textile dyes. Therefore the BRE model was constructed with the objective of obtaining reliable estimates of the required parameters to quantify the inhibition, using the form of inhibition kinetics used in COST Benchmark Simulation Model. The method of determining which parameters are required for inhibition quantification is discussed in detail in **Section 3-1**.

2.6.2 Prior Knowledge Collection

This task entails the collection of relevant, available and expert knowledge, from literature or experts in model building. Experiments maybe performed or previous performed experimental data maybe collected and stored. The BRE model is an activated sludge model details of the knowledge obtained for activated sludge models was discussed in detail in **Section 2-5**.

2.6.3 Frame Definition

After performing the first two tasks once, a first iteration of the model building procedure can start. The frame definition task aims to define the conditions under which the model will be used (e.g. temperature, pH, etc), to choose the class of models that seems fit for the task (time series, state-space, distributed parameter, stochastic, etc), to identify the variables that seem important to find a solution to the formulated problem (inputs, outputs, states), the range of time constants that need to be covered by the model, etc.

As soon as the frame is defined, the purposes set and the prior knowledge is collected, one or more possible candidate models are created for the system. The candidate models are created using two types of reasoning (Beck, 1989). The first being the assembling of all prior hypotheses made on the mechanisms and phenomena that govern the behaviour of the system and refuting or confirming these hypotheses on the basis of a set of field data. The second stage determines whether the candidate model approximates reality, this stage involves the evaluation of the model against experimental data and is described as system identification. System identification may be considered as model calibration.

The modelling process is an iterative process in which the experiments play the role of indicating areas of model deficiency and this is tackled in a new hypothesis generating step (Dochain and Vanrolleghem, 2001).

2.6.4 Model Structure Selection

The objective of this task is to select a unique model structure according to the principles of a quality of fit (Dochain and Vanrolleghem, 2001).

2.6.5 Parameter Estimation

Parameter estimation is based on the maximisation or minimisation of a goodness-of-fit

criterion such as Least Squares, Weighted Least Squares, Maximum Likelihood and a number of other methods. The aim of parameter estimation is to provide values for parameters and state variables in the model. The identifiability analysis performed prior to the parameter estimation determines whether for a given set of measured variables, unique parameter values can be obtained. The structural identifiability study evaluates if parameters can be given unique values or not at all, the model or frame definition is then altered to make the model more identifiable. Model reduction can lead to models that require less data, hence improving the models identifiability. The practical identifiability study determines the information content of the dataset intended for parameter estimation. The optimal experimental design (Dochain and Vanrolleghem, 2001) procedure is based on these methods, this design procedure uses the model to calculate experimental conditions such that sufficient information is contained in the data.

2.6.6 Model Diagnosis

After the parameters are estimated, it has to be determined whether the identified model violates the assumptions made in the frame definition. Statistical tests of systematic deviations between model results and measurements, and distributions are frequently used (Dochain and Vanrolleghem, 2001). Furthermore an evaluation whether non-sense parameter values such as; negative affinity constants, initial or boundary values are obtained, this allows the diagnosis of potential violation of the experimental frame (Dochain and Vanrolleghem, 2001).

2.6.7 Model testing

The robustness of the model is evaluated by comparing its performance with data obtained under different conditions than the conditions at the time of the data collection performed for model identification (Dochain and Vanrolleghem, 2001). This process of confronting the model with new data is most often called model validation.

2.7 Identifiability Study for Dynamic Process Models

The identification of a dynamic model is characterised by; activated processes described by the model highly complex with high order non linear systems incorporating a large number of parameters and the scarcity of cheap and reliable on-line sensors (Dochain and Vanrolleghem, 2001). Because of this an identifiability study of the dynamic model prior to any identification is essential. The fundamental objective of the identifiability analysis is to determine whether unique values for the model parameters can be obtained from parameter estimation, given a

certain number of state variables are available for measurement on the basis of the models structural identifiability or on the practical identifiability of the dynamic model from the available data.

2.7.1 Structural Identifiability

Structural identifiability is associated to the possibility of obtaining unique values to each parameter of a dynamic model (Dochain and Vanrolleghem, 2001). The structural identifiability of the dynamic model is determined from the given model structure and assuming model variable data corresponds perfectly to the model. It may be concluded that from the structural identifiability study that combinations of the model parameters and not the individual parameters are identifiable. In this case knowledge of some parameters may be required to achieve identifiability.

2.7.2 Practical Identifiability

Practical identifiability is related to the quality of the data; that is whether the available data are rich enough in information to identify and obtain accurate values for the model parameters (Dochain and Vanrolleghem, 2001). Structural identifiability is performed under the assumption of perfect (i.e. noiseless) data; as a result problems arise when parameter estimations are performed on highly correlated parameters using noise corrupted experimental data. Under these conditions the values of the estimated parameters may not be unique, since a change in one parameter may be compensated by a change in another parameter which could still result in a good fit between the experimental data and the model prediction (Dochain and Vanrolleghem, 2001). The Monod kinetic model has been documented as a biological system model in which parameter estimates may be highly correlated (Boyle and Berthouex, 1974, Holmberg, 1982, Munack, 1989). This problem is frequently encountered in cases in which parameter estimations are performed using insufficient experimental data over a range greater than the experimental data. To solve this problem it has been suggested to use documented parameter values to enforce parameter bounds (Holmberg, 1982) or to increase the sample frequency in a defined period of an experiment to increase the information content of the experimental data.

2.8 Parameter Estimation of Dynamic Models

Parameter estimation is defined as determining the optimum values of the mathematical model parameters with the aid of experimental data assuming the relationships between the variables and the parameters are explicitly known (Dochain and Vanrolleghem, 2001). Certain

parameter values (typically for zero values) result in a part of a model structure being deleted, hence it has been assumed that all parameters do not have these (e.g. zero values) parameter values (Dochain and Vanrolleghem, 2001). In this section concepts and theory of the parameter estimation process which was used in this study are discussed.

2.8.1 Initial Steps in Parameter Estimation

Some preliminary steps need to be performed before the actual parameter estimation is performed. The first step discussed is the selection of parameters that will be estimated and fixed to certain assumed values. The different methods that support this selection are also discussed. In a parameter estimation algorithm, initial parameter estimates need to be given to start the iterative search procedure; hence the choosing of proper initial guesses is essential to obtain successful parameter estimations. The method of choosing initial parameter guesses is discussed.

2.8.1.1 Selection of parameters

The selection of the parameters to be estimated is an important step in the parameter estimation procedure. Parameter are estimated, whereas the variables are calculated by the model or given as time series and constants are assumed to be given from prior knowledge. Initial and boundary conditions of state variables and some inputs can also be formulated with the aid of parameters; hence the set of parameters considered in the parameter estimation problem contains all of these and can be estimated simultaneously (Dochain and Vanrolleghem, 2001). A few of the methods are introduced that are used to select a certain subset of model parameters, these methods are: structural and practical identifiability analysis and sensitivity analysis.

Structural identifiability analysis is a method used to find out the possible identifiable parameters or combinations thereof, provided the data is sufficiently rich in information (refer to **Section 2.7.1** and **Section 3.5.1**). For this reason only the structurally identifiable subset will be contained in the parameter estimation problem. Hence for the identifiable parameter combination of this study presented in **Section 3.5.1,** $\left(1-Y_H\right)/Y_H \cdot \mu_{mH} \cdot X\left(0\right)$ and $\left(1-Y_H\right) \cdot K_S$. One parameter from each combination were chosen to be estimated, μ_{mH} and K_S, and the remainder of parameters were set to values. It should be noted that the parameter estimates obtained are conditioned by the choice of the values of the set parameters.

Practical identifiability problems are encountered because the data are insufficiently informative to reliably estimate all parameters, a sub-selection of this parameter set can be made after an analysis of the parameter estimation error covariance matrix (refer to **Section 2.7.2** and **Section 3.5.2**). By eliminating the parameter that is causing the identifiability problem from the parameter set and giving it an assumed value, the estimation of the other parameters will be highly facilitated. But the estimates obtained will be conditional on the assumed value of the non-identifiable parameters.

A method was developed which used sensitivity analysis as a method to preselect parameter subsets that ensure reliable estimation (Weijers and Vanrolleghem, 1997). This method requires the calculation of sensitivity functions; this becomes tedious when dealing with complex models.

2.8.1.2 Initial Estimates of the Parameters

Except for linear parameter estimation problems in which parameters can be determined readily analytically from the objective function, the minimisation algorithms used for nonlinear parameter estimation need initial guesses for parameter values. The choice of good initial guess determines whether the minimum is successfully obtained and how long it takes to converge towards it. The method to obtain good initial guesses is based on intuition and prior knowledge in selecting initial guesses.

2.9 COST Benchmark Model

The COST Simulation Benchmark Model (Copp, 2002) is an activated sludge wastewater treatment model that was designed to evaluate different control strategies. A fully defined protocol is implemented in the Simulation Benchmark Model, which provides an unbiased basis without reference to any particular wastewater treatment works. This model has also been successful in comparing different wastewater treatment modelling software packages.

The Simulation Benchmark Model configuration is shown in Figure 2-9; it consists of five biological reactors in series, followed by a secondary clarifier. The first two tanks are operated under unaerated and fully mixed conditions; the last three are operated under aerated conditions. The model has two recycles, a nitrate recycle from the fifth tank to back to the first tank and a sludge recycle from the secondary clarifier underflow back to the first tank. There are two

output streams, a sludge waste stream and an effluent stream.

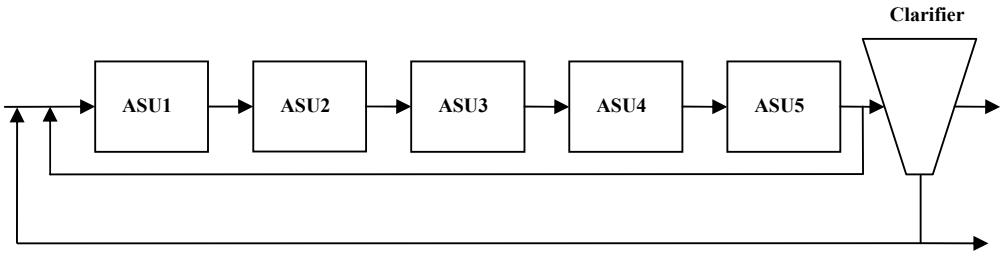

Figure 2-9: Flow diagram of the 'simulation benchmark' configuration showing activated sludge units (ASU) 1 and 2 mixed and unaerated and ASU 3, 4 and 5 aerated

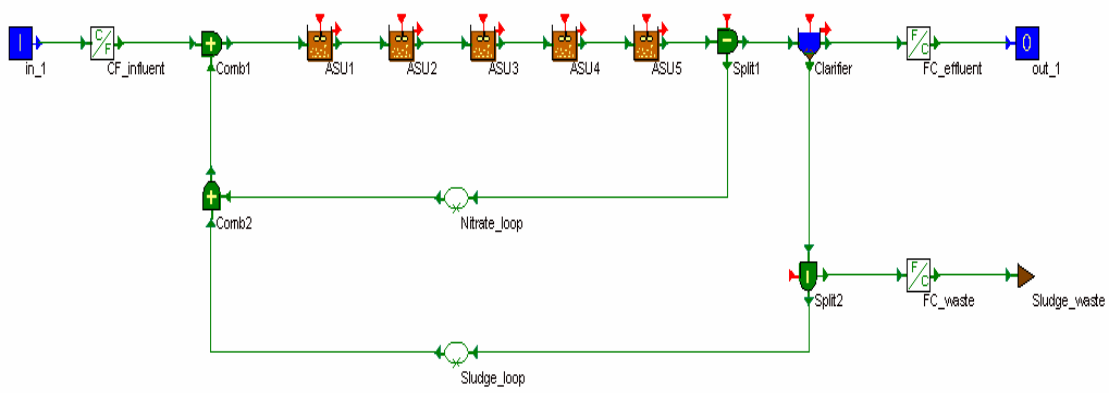

Figure 2-10: COST simulation benchmark model configuration as appears in WEST

The activated sludge reactors (refer to Figure 2-10) are modelled by the Activated Sludge Model No.1 (ASM1) (Henze et al., 1987), which has been described in detail earlier. Kinetic parameter default values expected at 15°C (Henze et al., 1987) are used in the model simulations. The effluent data are obtained from the model after it is simulated for 14 days under dynamic influent conditions. The effluent data along with operational conditions are used to determine the effluent quality index, effluent violations and operational costs. This concept will be discussed further in greater detail in **Chapter 6**.

CHAPTER 3
MATHEMATICAL MODELLING THEORY

This chapter provides the mathematical process modelling theory used in the quantification of the inhibitory nature of textile dye effluent on the activated sludge processes. A Batch Respirometric Experiment (BRE) model was created to obtain the relevant information to quantify the inhibition of textile dyes on the kinetics of biomass respiratory activity. To determine which of the parameters of the model are central in quantifying the inhibition, the kinetic effects of inhibition have been investigated. Subsequently the BRE model was inputted into wastewater treatment modelling program WEST. A continuity check and the identifiability study were performed of the BRE model. Furthermore the model theory of parameter estimation and the method used in WEST is discussed.

3.1 Kinetic Effect of Inhibition

Little is known about the inhibition of textile dyes on activated sludge biomass. Therefore it is particularly difficult to hypothesize mechanistic models from which kinetic effects maybe created. Hence empirical models must be used to aid in understanding how inhibitors are likely to influence the functioning of activated sludge processes. The most basic kinetic approach is to assume that the inhibitor effects the specific substrate removal rate of a biomass in a manner analogous to the way an inhibitor influences enzyme activity (Hartmann and Laubenberger, 1968). The four main types of inhibition (Volskay and Grady, 1988) which occur are; competitive, non-competitive, uncompetitive and mixed. The form of inhibition is dependent on the influence of the inhibitor on the maximum specific growth rate (μ_{max}) of biomass and the half saturation constant (K_m) in a Monod kinetic growth rate expression. The definition of inhibition types is shown qualitatively in Table 3-1.

Table 3-1: Definition of inhibition types (Volskay and Grady, 1988)

Type of Inhibition	Effect on μ_{max}	Effect on K_m
Competitive	None	Increase
Non-competitive	Decrease	None
Uncompetitive	Decrease	Decrease
Mixed	Decrease	Increase

A mathematical way of expressing the effects of different inhibitions types is with simple reversible linear inhibition models (Patterson and Brezonik, 1969). If μ^*_{max} and K^*_m represent the observed values of μ_{max} and K_m in the presence of the inhibitor can be represented by models shown in Table 3-2. The concentration of inhibitor is represented by *I*, while $K_{I,m}$ and $K_{I,S}$ is called the inhibition coefficients of maximum specific growth rate and of half saturation coefficient.

Table 3-2: Quantification of inhibitory effects using simple reversible linear inhibition models adapted from (Volskay and Grady, 1988)

Inhibitor type	Effect on μ_{max}	Effect on K_S
Competitive	$\mu^*_{max} = \mu_{max}$	$K^*_m = K_m \cdot \left(1 + \left(I / K_{I,S}\right)\right)$
Non-competitive	$\mu^*_{max} = \frac{\mu_{max}}{\left(1 + \left(I / K_{I,m}\right)\right)}$	$K^*_m = K_m$
Uncompetitive	$\mu^*_{max} = \frac{\mu_{max}}{\left(1 + \left(I / K_{I,m}\right)\right)}$	$K^*_m = \frac{K_m}{\left(1 + \left(I / K_{I,S}\right)\right)}$
Mixed	$\mu^*_{max} = \frac{\mu_{max}}{\left(1 + \left(I / K_{I,m}\right)\right)}$	$K^*_S = K_S \cdot \left(1 + \left(I / K_{I,S}\right)\right)$

3.2 Description of the Batch Respirometric Experiment (BRE) Model

From the investigation into inhibition above it was concluded that the maximum specific growth rate and half saturation constant were the critical parameters required for the determination of the type of inhibition model.

Hence the Batch Respirometric Experiment (BRE) model was created with the objective of obtaining accurate estimates of maximum specific growth rate and half saturated constant parameters. The batch respirometric experiment model is a combination of ASM1 (Henze et al., 1987) and ASM3 (Gujer et al., 1999) model concepts; it is shown in Table 3-3. Some of the modification to the model was done for mathematical convenience.

Table 3-3: Batch Respirometric Experiment (BRE) kinetic model

Component i → / ↓ Process j	1 S_S	2 X_S	3 X_{BH}	4 X_{BA}	5 X_P	6 S_O	7 S_{NO}	8 S_{NH}	9 S_{ALK}	Process rate ρ_j
1 Aerobic growth of heterotrophs	$-\frac{1}{Y_H}$		1			$-\frac{1-Y_H}{Y_H}$		$-i_{XB}$	$-\frac{i_{XB}}{14}$	$\mu_{mH}\cdot\left(1-e^{-t/\tau_H}\right)\cdot\left(\frac{S_S}{K_S+S_S}\right)\cdot X_{BH}$
2 Aerobic growth of autotrophs				1		$-\frac{4.57-Y_A}{Y_A}$	$\frac{1}{Y_A}$	$-i_{XB}-\frac{1}{Y_A}$	$-\frac{i_{XB}}{14}-\frac{1}{7\cdot Y_A}$	$\mu_{mA}\cdot\left(1-e^{-t/\tau_A}\right)\cdot\left(\frac{S_{NH}}{K_{NH}+S_{NH}}\right)\cdot X_{BA}$
3 Decay of heterotrophs			-1		f_P	$1-f_P$		$i_{XB}-f_P\cdot i_{XP}$		$b_H\cdot X_{BH}$
4 Decay of autotrophs				-1	f_P	$1-f_P$		$i_{XB}-f_P\cdot i_{XP}$		$b_A\cdot X_{BA}$
5 Hydrolysis of entrapped organics	1	-1								$k_h\cdot\frac{X_S/X_{BH}}{K_X+\left(X_S/X_{BH}\right)}\cdot X_{BH}$

3.2.1 BRE Components

The BRE model components are defined in the same way as ASM1 components. Except for the combination of inert particulates X_I and X_P into one inert particulate component X_P, this is same reason that X_P is incorporated into X_I in ASM3 since it is impossible to differentiate between the two inert components; this has been discussed in **Section 2.5.2.1**. Furthermore the BRE model has simplified the division of nitrogen in similar approach to that used in ASM3, discussed in **Section 2.5.2.1**. Soluble (S_{ND}) and inert (X_{ND}) organic nitrogen components are not present in BRE model; these components have been incorporated as fractions of X_P, X_S and active biomass. The soluble inert component (S_I) is absent from the BRE model to simplify the model, since in the ASM1 model it is not involved in any of the processes and the concentration remains unchanged. The breakdown of total COD and total Nitrogen are summarised in Equation 3-1 and Equation 3-2 respectively.

$$COD_{TOTAL} = S_S + X_S + X_{BH} + X_{BA} + X_P \tag{3-1}$$

$$N_{TOTAL} = S_{NH} + S_{NO} + \left(i_{XP} \cdot X_P\right) + i_{XB} \cdot \left(X_{BH} + X_{BA}\right) \tag{3-2}$$

3.2.2 BRE Processes

The BRE model processes are similar to those in ASM1; except the process of anoxic growth of heterotrophs is not present since the experiments are performed under saturated oxygen conditions. Furthermore the hydrolysis of entrapped organic nitrogen has been removed since the inert organic nitrogen component X_{ND} is not present and the ammonification process is absent since this process occurs extremely fast and soluble organic nitrogen S_{ND} has not been included in the model. The BRE model presented in Table 3-3 has three main processes, namely:

- biomass growth
- biomass decay
- hydrolysis of entrapped organic matter

Aerobic Growth of Heterotrophs

The processes of aerobic growth of heterotrophs and autotrophs biomass are described by the same method as ASM1 using the Monod relationship. The growth of heterotrophs occurs by

the consumption of readily biodegradable substrate (S_S) and oxygen (S_O) and ammonia is incorporated into the biomass. An empirical factor was added to the process rate equations (Vanrolleghem et al., 2004); this term serves to represent the fast transient phase observed in respirometric profiles in reaching the maximum OUR value after a substrate pulse. The transient phenomenon is modelled in a simple first order model, in the following way (Vanrolleghem et al., 2004):

$$\mu_{obs} = Trans \cdot \mu \tag{3-3}$$

$$Trans = \left(1 - e^{-t/\tau}\right) \tag{3-4}$$

Where *Trans* is the transient first order term, τ is the first-order time constant (s), *t* is time (s), μ_{obs} is the observed specific growth rate of the biomass (s^{-1}), μ is the maximum specific growth rate (s^{-1}). This first order approach has been successfully used in a number of batch respirometric studies (Gernaey et al., 2002, Sin, 2004).

The batch experiment is operated under saturated oxygen conditions; hence oxygen concentration (S_O) will be much greater than oxygen half saturation coefficient of heterotrophs (K_{OH}) for that reason the switching term ($S_O/K_{OH}+S_O$) is not present in the BRE model.

Aerobic Growth of Autotrophs

Aerobic growth of autotrophic biomass is the nitrification process of oxidising ammonia nitrogen (S_{NH}) to nitrate (S_{NO}). This results in the formation of autotrophic biomass and the incorporation of a fraction of S_{NH} into the autotrophic biomass. This process is described in a similar method to aerobic growth of heterotrophs, except for obvious reasons the ($S_{NH}/K_{NH,N}+S_{NH}$) switching term has been excluded from the process rate expression.

Heterotrophic Decay

The death regeneration concept used in ASM1 was not used to describe the hetetrophic decay process; a modified endogenous respiration process presented in ASM3 was preferred. The death regeneration concept decay coefficient was difficult to determine, while the endogenous respiration process presented in ASM3 is much easier to obtain through batch experiments and is closer to what is experienced in reality. This is explained in **Section 2.5.2**. The ASM1

model decay process has been observed to have an inability in predicting the tail of respirograms where storage effects are emphasized (Sin, 2004), ASM1 does not predict the tails when the substrate pulse contains only readily biodegradable substrate which is the case in this study. To negate this problem the decayed biomass is broken down into fractions of oxygen (S_O), inert particulate (X_P) and ammonia nitrogen (S_{NH}).

Autotrophic Decay

The autotrophic decay process is described the same as the heterotrophic decay process.

Hydrolysis of Entrapped Organics

The hydrolysis of entrapped organics process is described in the same way to the ASM1 process described in **Section 2.5.1.2**, apart from the exclusion of the anoxic term since the experiment is operated under saturated oxygen conditions.

3.3 BRE Model Inputted into WEST Simulation Engine

The BRE model was implemented into the **W**orldwide **E**ngine for **S**imulation, **T**raining and automation (WEST) software package. WEST is a software package designed for environmental engineering simulations. A continuity check and a sensitivity test were performed on BRE model in WEST.

3.3.1 Background of WEST Software Package

WEST was created in the early 1990s by Hemmis in close collaboration with the University of Gent (www.hemmis.com, 2006). It is a powerful tool for dynamic modelling, simulations and optimisations.

3.3.2 WEST Subprograms

WEST consist of a model base which is a collection of text files providing a mathematical description of the processes, a graphical user interface (GUI) and a simulation engine. The model base is written in MSL-USER (Model Specification Language), this is a highly hierarchical structure which represents the dynamics of the system along with symbolic information (Vanhooren et al., 2003). The four subprograms that WEST consists of are:

- WEST Manager
- WEST Model Editor
- WEST Configuration Builder
- WEST Experimental Environment

WEST Manager is a platform in which the user can view created projects and also new projects can be created. All configurations and experiments performed in a project can be viewed and accessed.

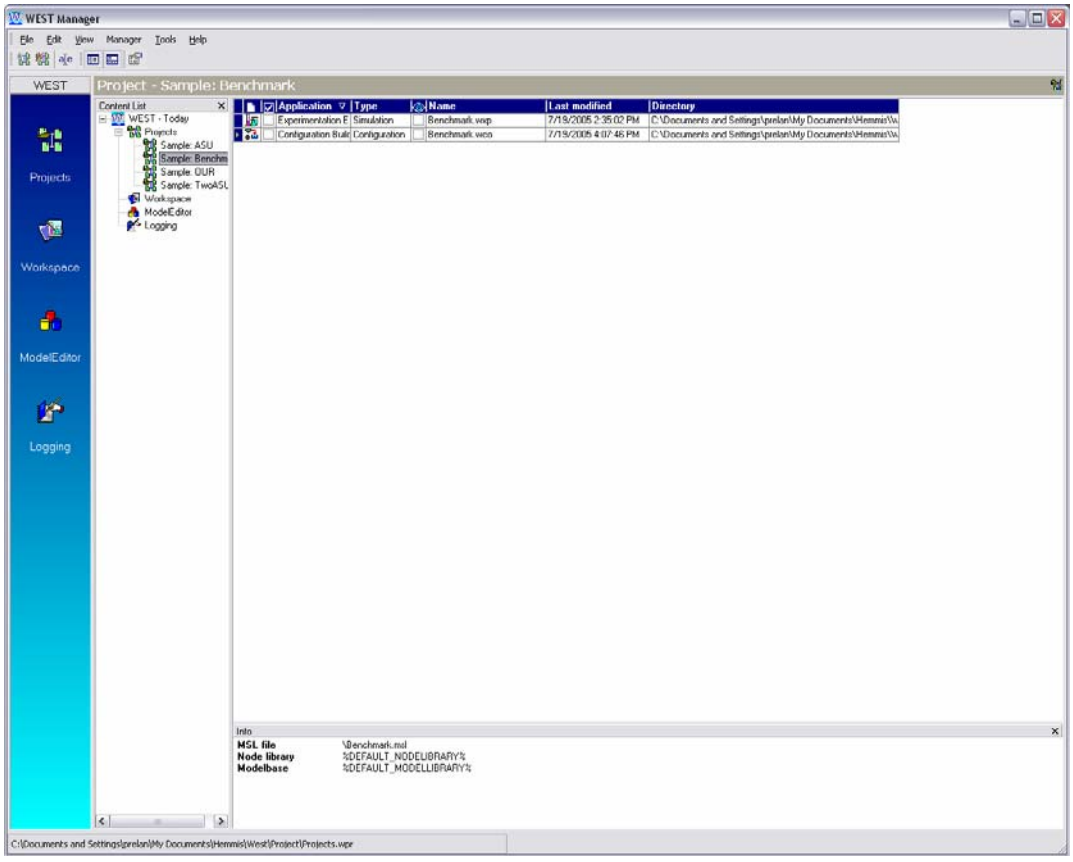

Figure 3-1: Screen shot of WEST sub-program WEST Manager

The *WEST Model Editor* is used to create a new process model or edit an existing process models; this can be performed in the matrix editor or in the MSL text files. Editing any section of the hierarchal structure of WEST can be performed in the *WEST Model Editor* MSL text files. Furthermore stoichiometry continuity check can be performed on newly created models or on edited models.

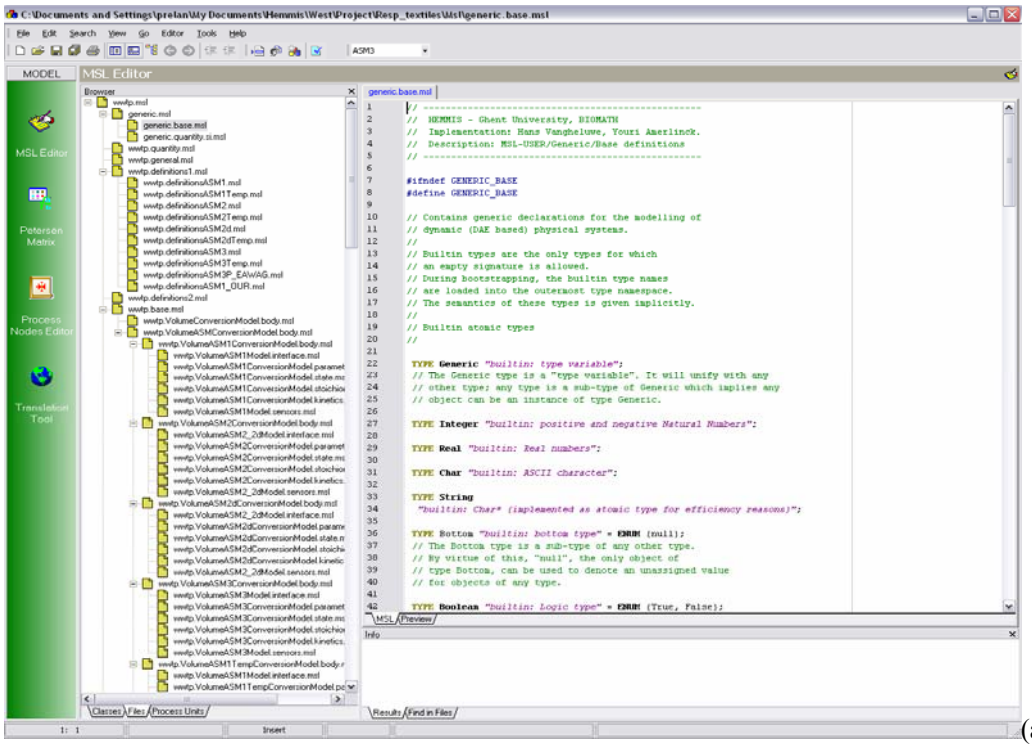

(a)

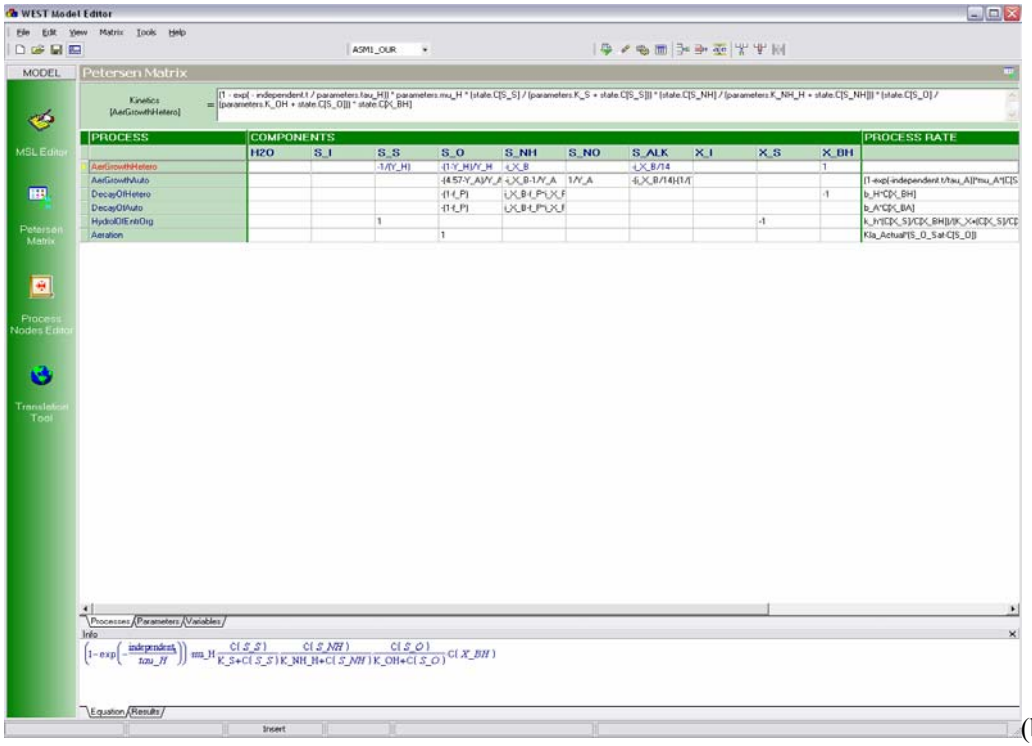

(b)

Figure 3-2: (a) Screen shot of WEST sub-program WEST Model Editor MSL hierarchical structure. (b) Screen shot of WEST sub-program WEST Model Editor Petersen Matrix Editor

WEST Configuration Builder is a subprogram in which the user selects the activated sludge model for the system; thereafter the user creates the desired system configuration by selecting the treatment process units and connecting these process units. The treatment process units are sub-models and the properties of these units can be edited in the *WEST Model Editor*, the process units that are available are activated sludge reactor, primary clarifier, secondary clarifier and many more.

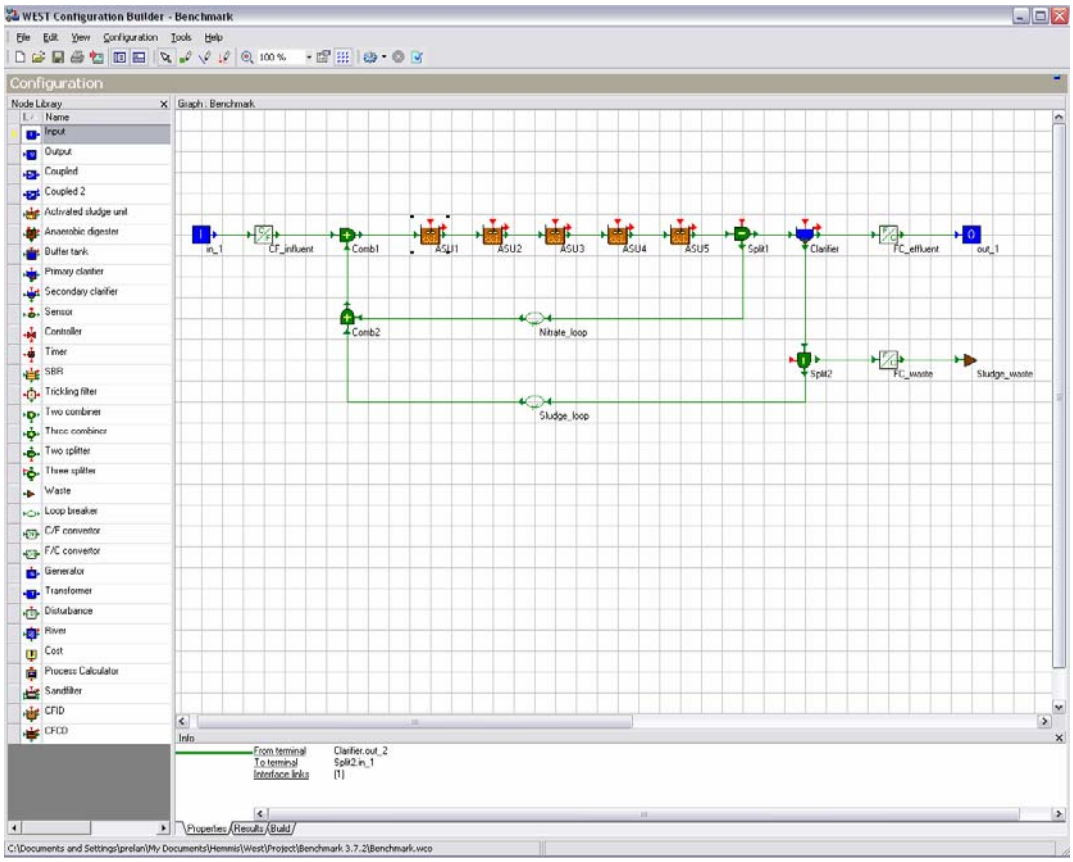

Figure 3-3: Screen shot of WEST sub-program WEST Configuration Builder

WEST Experimental Environment is based on the system model created in *WEST Configuration Builder*. In this subprogram the user sets the values for treatment process unit parameters and variables. The user then has the option of performing a standard simulation, a sensitivity analysis on the system model, optimisation simulations and testing of different scenario.

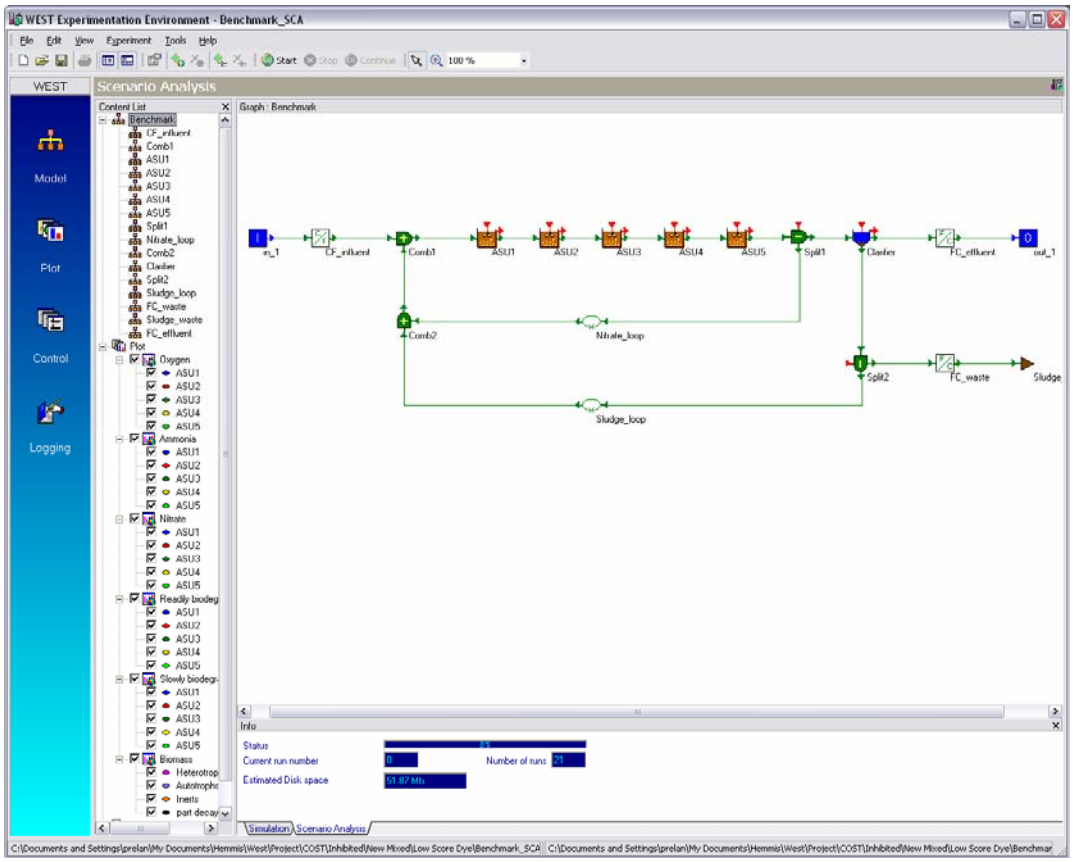

Figure 3-4: Screen shot of WEST sub-program WEST Experimental Environment

3.3.3 Fundamentals of WEST

The sub-models in *WEST Experimental Environment* use fluxes as the reference unit. By applying the mass conservation principle to the fluxes, the following is obtained:

$$\frac{d}{dt}M = 0 \qquad (3\text{-}5)$$

M = vector containing mass (M_i) of each component (i)

The mass balance on a tank with volume (V) with many incoming and outgoing flows (α), can be described as follows:

$$\frac{d}{dt}M_i = \sum_{\alpha}\phi_{i\alpha} + r_i \cdot V \tag{3-6}$$

$$\frac{d}{dt}V = \sum_{i}\left(\frac{1}{\rho_i}\cdot\sum_{\alpha}\phi_{i\alpha}\right) \tag{3-7}$$

Where:

Mi = mass of component i (g)

V = volume of tank (m^3)

$\phi_{i\alpha}$ = net flux in/out of component i in flow a (g/d)

r_i = reaction rate of component i ($g/m^3/d$)

ρ_i = density of component i (g/m^3)

Using the above ordinary differential equations (ODE) of each process unit, WEST sets up algebraic equations for the entire system. In a simulation in WEST these ordinary differential equations are integrated numerically in time and the system algebraic equations are solved simultaneously. The integrator methods in WEST can be divided in three types:

- Fixed step size integrator. This is an integrator that takes a constant step in order to solve the integration of the system of ODEs. The available fixed step integrators in WEST are; AB2, AB3, AB4, Euler, Heun, Midpoint, Milne, Modified Euler and Runge-Kutta 4^{th} order [RK4])

- Adaptive step size integrator. This is an integrator that modifies its step size in order to obtain optimal calculation speed and optimal calculation accuracy. WEST only offers the Runge-Kutta 4^{th} order adaptive step size controller [RK4ASC] as an adaptive step size integrator.

- Stiff solvers. This obtains a high performance gain for stiff systems. A stiff system is a system is a system where there is a large difference between the time constants of the processes (e.g. biological and chemical processes). The two stiff solvers found in WEST are Rosenbrock and CVODE.

The RK4ASC integrator was used in the WEST simulation and optimisation performed in

WEST Experimental Environment for the batch respirometric experiment (BRE) model, since it is fast and accurate. The step size ranged from $6x10^{-4}$ to 6 min for simulations.

The *WEST Experimental Environment* sensitivity analysis, scenario analysis and trajectory optimisation functions were utilized in this study; details of these functions will be discussed later.

3.4 Continuity Check of BRE Model

An important stage in modelling is model verification. Performing the continuity check is a valuable tool for model verification. A continuity check is required to be performed on the model stoichiometry and mass balance.

3.4.1 Stoichiometry Continuity Check

The stoichiometry continuity check is the calculation of a number of continuity equations. Continuity equations are the mathematical equivalent of the principle that in chemical reactions, elements, electrons (or COD) and net electrical charges may neither be formed nor destroyed. In the continuity check it is determined whether the result of the equation is equal to zero or not. The stoichiometry continuity check was performed in WEST and the result of the continuity check was successful.

3.4.2 Mass Balance Continuity Check

A mass balance continuity check was performed on the model to determine whether the model COD and nitrogen components balance. The COD mass balance was determined by performing a simulation in which nitrification was disabled and similarly the nitrogen mass balance was determined by disabling the carbon reduction process. For the COD mass balance the input COD concentration, output COD concentration and Oxygen Uptake Rate (OUR) were used to determine the continuity of the model. The input and output nitrogen concentrations were necessary for the nitrogen balance to determine the continuity of the model.

A detailed calculation of the mass balance continuity check is presented in **Appendix F**. In summary the $Error_{COD}$ is equal to 0 g COD/L and the $Error_{N}$ is 0 g N/L; hence both the COD and Nitrogen mass balance continuity check performed on the model were successful.

3.5 Identifiability Study of Dynamic Models

An identifiability study of the dynamic model prior to any identification is essential for reason discussed in **Section 2.7**. The model theory of structural and practical identifiability is discussed in this section.

3.5.1 Structural Identifiability

The structurally identifiable parameter combinations for heterotrophic growth of ASM1 (Henze et al., 1987) using batch respirometric experiment data is presented in Table 3-4. The same parameter combinations are identifiable for autotrophic growth using batch respirometric experiment data. For a detailed derivation of the identifiable parameter combination presented in Table 3-4 using the Taylor Series Expansion method refer to (Dochain and Vanrolleghem, 2001).

Table 3-4: Identifiable parameter combinations for heterotrophic growth kinetics (Dochain et al., 1995)

No Biomass Growth	Biomass Growth
$\frac{1-Y_H}{Y_H}\cdot\mu_{mH}\cdot X_H(0)$	$\frac{1-Y_H}{Y_H}\cdot X_H(0)$
$(1-Y_H)\cdot S_S(0)$	$(1-Y_H)\cdot S_S(0)$
$(1-Y_H)\cdot K_S$	$(1-Y_H)\cdot K_S$
	μ_{mH}

3.5.2 Practical Identifiability

Practical identifiability is related to whether the available data are rich enough in information to estimate and obtain accurate values for the model parameters. The accuracy of a parameter estimation performed using the available experimental data can be expressed by the value of the minimised quadratic objective functional presented below (Munack, 1991):

$$J(\theta) = \sum_{i=1}^{N} \left(y_i(\hat{\theta}) - y_i \right)^T \cdot Q_i \cdot \left(y_i(\hat{\theta}) - y_i \right) \tag{3-8}$$

Where:

θ = vector of optimised parameters

y_i = experimental data vector of N measurement values

$y_i(\hat{\theta})$ = model predictions at times t_i (i = 1 to N)

Q_i = square matrix of user supplied weighted coefficients

The expected value of the objective functional for a parameter set slightly different from the optimal on is given by (Munack, 1989):

$$E\left[J(\theta + \delta\theta) \right] \cong \delta\theta^T \left[\sum_{i=1}^{N} \left(\frac{\partial y}{\partial \theta}(t_i) \right)^T \cdot Q_i \cdot \left(\frac{\partial y}{\partial \theta}(t_i) \right) \right] \cdot \delta\theta + \sum_{i=1}^{N} tr\left(C_i \cdot Q_i \right) \tag{3-9}$$

The term C_i represents the measurement error covariance matrix, the Q_i matrix is typically chosen as C_i^{-1} to reduce the second term to a scalar. To optimise the practical identifiability; the term between brackets [.] in Equation 3-9 has to be maximised. As a result a maximum difference between $J(\theta + \delta\theta)$ and $J(\theta)$ is obtained, which implies that a fit obtained from a slightly different parameter set is significantly worse (Dochain and Vanrolleghem, 2001). Hence obtaining a unique optimal parameter set. This term between brackets [.] in Equation 3-9 is called the Fischer Information Matrix and describes the information content of the experimental data (Ljung, 1999):

$$F = \sum_{i=1}^{N} \left(\frac{\partial y}{\partial \theta}(t_i) \right)^T \cdot Q_i \cdot \left(\frac{\partial y}{\partial \theta}(t_i) \right) \tag{3-10}$$

This matrix is the inverse of the parameter estimation error covariance matrix of the best linear unbiased estimator(Godfrey and Di Stefano III, 1985):

$$V = F^{-1} = \left[\sum_{i=1}^{N} \left(\frac{\partial y}{\partial \theta}(t_i) \right)^T \cdot Q_i \cdot \left(\frac{\partial y}{\partial \theta}(t_i) \right) \right]^{-1} \tag{3-11}$$

Confidence Region of the Parameter Estimates:

A critical result of a practical identifiability study is to determine the parameter estimation error. The parameter variance of the estimated parameters indicates the level of confidence that can be entrusted in the estimated parameters. In the Fischer Matrix calculation performed earlier the matrix Q_i was defined as the inverse of the measurement error covariance matrix C_i^{-1}, hence by using the covariance matrix V approximate standard errors for the parameters can be calculated as follows:

$$\sigma(\theta_i) = \sqrt{V_{ii}} \tag{3-12}$$

Furthermore confidence intervals for the parameters can be obtained as follows:

$$\theta \pm t_{\alpha ; N - p^{\sigma(\theta_i)}} \tag{3-13}$$

Where the confidence level is specified as 100(1-α) and t-values are obtained from the Student-t distribution.

Sensitivity Functions:

The output sensitivity $\partial y / \partial \theta$ equations play an important role in evaluating the practical identifiability, since this term is a component in both the Fisher Information Matrix and parameter estimation error covariance matrix (Dochain and Vanrolleghem, 2001). Furthermore if the sensitivity equations are proportional the covariance matrix becomes singular and the model is not practically identifiable (Robinson, 1985). In particular in biological models the

sensitivity equations are nearly proportional, resulting in parameter estimates that are highly correlated. This phenomenon can be described by the error functional *J* which looks like a valley, hence several combinations of parameters may describe the same data equally well (Dochain and Vanrolleghem, 2001). Consequently by plotting the sensitivity equations the practical identifiability can be easily evaluated.

The sensitivity equations can be determined in many different methods; the most popular is the analytical derivation and a numerical approximation of the sensitivity. The analytical derivation of the sensitivity equations is the most accurate, but with complex models software programs are necessary to derive the equation to prevent derivation errors.

A numerical approximation basically requires additional evaluations of the model with parameter values that are slightly different from the nominal values used. A parameter θ_i is perturbed at a time with a perturbation factor $\triangle\theta_i$, the sensitivity of output variable y_i to parameter θ_i is then calculated as follows:

$$\frac{\partial y_i}{\partial \theta_i} = \frac{y_i(\theta_i) - y_i(\theta_i + \Delta\theta_i)}{\Delta\theta_i} \tag{3-14}$$

Sensitivity Measure:

Sensitivity measure is another form of sensitivity analysis that is used to rank the influence of parameters on the output variables. The sensitivity measure is defined as (Brun et al., 2002):

$$\delta_j^{msqr} = \sqrt{\frac{1}{n}\sum_{i=1}^{n} s_{ij}^2} \tag{3-15}$$

$$s_{ij} = \frac{\triangle\theta_j}{sc_i} \cdot \frac{\partial y_i}{\partial \theta_j} \tag{3-16}$$

The sensitivity measure, measures the mean sensitivity of the model output to change in the parameter θ_j (in the mean square sense). A high δ_j^{msqr} means that the value of the parameter θ_j has an important influence on the output variable y_i, and a value of zero indicates the output

variable does not depend on the parameter.

3.6 Parameter Estimation of BRE Model

In this section the methodology of parameter estimation is discussed and the WEST parameter estimation method is described.

3.6.1 Objectives in Parameter Estimation: Estimators

The subjective approach of guessing parameter values by a visual inspection of model prediction and data is commonly practiced. A better approach is to objectify the estimation of parameters in the form of functions that represent the goal to fit a model to the data. These functions are typically minimisation functions for which the model parameters are adjusted to achieve a minimum in these functions. This minimisation process is in many dimensions, the number of dimension is the number of parameters to be estimated.

These functions have many names; loss, merit, cost or objective functions. The best known objective function for parameter estimation is the sum of squared errors function. This objective function is presented in Equation 3-17; it is the cost function of the WEST trajectory optimiser which was used in this study parameter estimations.

$$J(\theta) = \sum_{i=1}^{N} \left(y_i - \hat{y}_i(\theta) \right)^2 \qquad (3\text{-}17)$$

Where:

y_i = the observations (a total of N observation)

$\hat{y}_i(\theta)$ = the model prediction for a given parameter set θ

The objective function J is representative of all the information contained in the observations that is not explained by fitting the model to the data (Robinson, 1985). All classic objective functions originate from maximum likelihood (ML) estimators.

3.6.2 Minimisation Approach

As stated in the previous section determining the best parameter estimates typically involves minimising the deviation of the model predictions from the data points using an objective function (J) (Dochain and Vanrolleghem, 2001). The minimisation solution methods for

linear and nonlinear parameters are quiet different. For linear parameters in a one step calculation give best estimates, while for nonlinear parameters numerical methods that search the parameter space in a systematic way is the best estimation method. This study requires nonlinear parameter estimates to be performed, hence nonlinear parameter estimation only is discussed.

Nonlinear parameter estimation problems can not be solved as easily as parameters which appear linearly in the model. In some cases nonlinear parameters can be determined analytically by solving the nonlinear equations. However the problems very quickly turns mathematically inflexible, also the minimum of a nonlinear objective function is required. The purpose is to find, as efficiently as possible values, of parameters (θ) that make $J(\theta)$ minimal. Nonlinear function minimum can either be global (the lowest function value in the whole parameter space) or local (the lowest function value in a finite neighbourhood). No perfect minimisation algorithm exists, therefore a global minimum for nonlinear problems cannot be guaranteed (Dochain and Vanrolleghem, 2001). As a result an important characteristic of a minimisation algorithm will clearly be sensitivity to local minima. The overall procedure of nonlinear parameter estimation is schematised Figure 3-5. Initially, the selection of the parameter to be estimated and the experimental data need to be specified. The algorithm is started by giving first guesses of the parameters. The minimisation algorithm will then request for model predictions corresponding to this first parameter set. These model predictions are obtained by solving the set of model equations and are passed on to the routine where the objective function is calculated by confronting the predictions with the data. On the basis of rules that are different for each minimisation algorithm either a new proposal for parameters is made and sent to the model solver or, if certain criteria are met, the parameter values are passed on to the user as best estimates. Stopping criteria may be that the maximum number of iterations is reached or that no improvement in objective function is found in recent iterations.

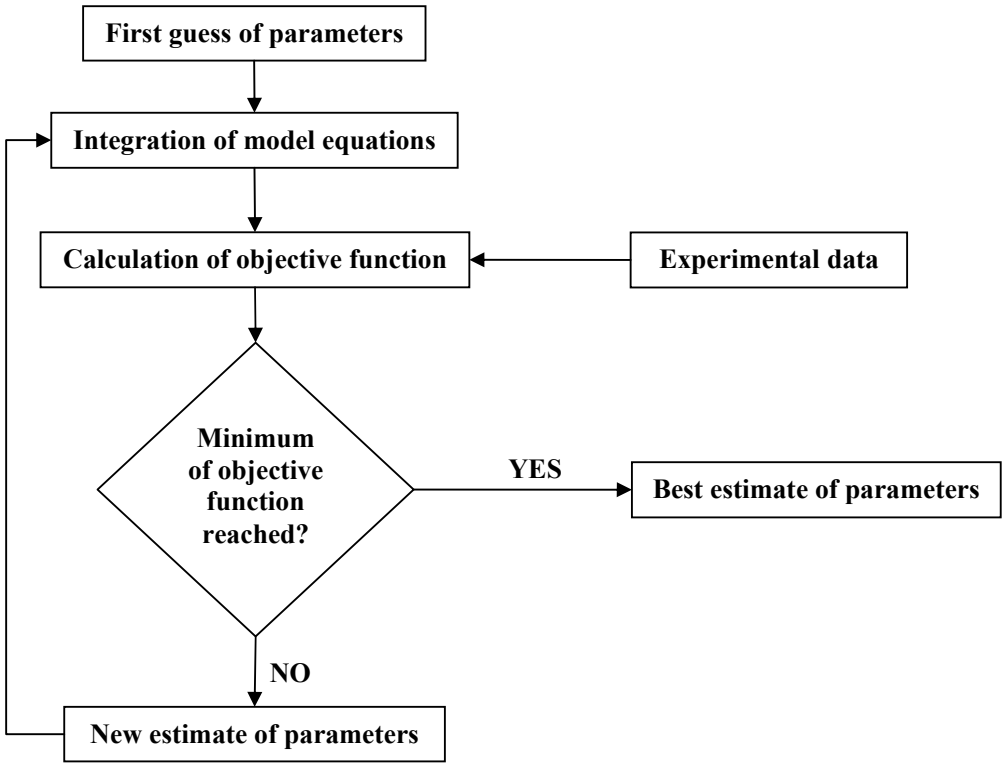

Figure 3-5: Flow diagram of parameter estimation routine adapted from (Wanner et al., 1992)

3.6.3 Using WEST for Parameter Estimation of BRE Model

The BRE model parameters were estimated using the WEST trajectory optimiser and respirometric experiment data. The WEST trajectory optimiser estimates a number of parameters by minimising a cost function, which is a measure for the difference between the simulated results and a measured data set. In this study the cost function variable is oxygen uptake rate (OUR) and the cost functions input is the OUR experiment data. The cost function is a relationship between the available data and the simulation results. A best fit is obtained when the cost function is minimised with respect to the parameters. During a trajectory optimisation several runs are executed and after each simulation run the cost function is evaluated. Two criteria are used to calculate the cost function:

- Squared error. This is the sum of squared errors, were the error is the difference between the simulated results and the measured data.
- Absolute error. This it the sum of absolute errors.

An optimal fit is reached when the cost function becomes minimal. The BRE model maximum specific growth rate and half saturation coefficient parameters for both heterotrophic and autotrophic biomass growth were estimated.

CHAPTER 4
BATCH RESPIROMETRIC EXPERIMENT

This chapter describes the batch respirometric experimental protocol developed to quantify the inhibitory effects of textile dyes. The respirometric protocol developed provides information rich data which reliable parameter estimation can be performed. Previous unsuccessful experimental designs used during the optimising of the experimental design are discussed. The batch respirometric experimental optimal design along with the results from this experiment design is presented.

4.1 Batch Respirometric Experiments Setup

The respirometric layout is presented in Figure 4-2; this respirometer is operated with a cyclic on-off air supply controlled by the oxygen uptake rate (OUR) meter. The OUR meter measures and stores the OUR data during the air supply off phase. A detailed description of the OUR meter is provided in **Section 4.1.2**. Since the OUR data is measured during the air supply off phase the respirometer can be described by the static gas – static liquid respirometer principles. The Batch Respirometric Experiment system consists of three components:

- the bioreactor and respirometer
- the Oxygen Uptake Rate (OUR) meter instrument
- computer system

4.1.1 The bioreactor and respirometer

The bioreactor is a 2 L cyclic aerated continuously stirred vessel which is shown in Figure 4-1. The bioreactor has a dissolved oxygen probe and temperature probe which are connected to the UCT DO/OUR meter; in addition the bioreactor has a pH probe which is connected to a pH meter. The air supply to the reactor is controlled by the OUR meter; the air supply is switched on when the dissolved oxygen concentration (DO) reaches the lower bound (LB) and switched off when the DO reaches the upper bound (UB). The respirometer follows the principle of static gas – static liquid, since the OUR data are measured during the air supply phase. The respirometer OUR meter is operated with a small difference between the UB and LB dissolved oxygen concentration values (acetate spikes UB = 5.0 mgO_2/L, LB = 4.5 mgO_2/L and ammonia spikes UB = 5.0 mgO_2/L, LB = 4.8 mgO_2/L); this prevents oxygen limitation conditions which

allows the respirometer to be operated with a high concentration sludge (low S_0/X_0 ratio), it also provides a high frequency of measurements of OUR and shorter duration of experiments. The high frequency measure of OUR data is a critical property for this study, since this data will be used for wastewater characterisation and in determination of activated sludge kinetics (Dochain and Vanrolleghem, 2001). Furthermore to prevent the transfer of oxygen through the liquid-air interface which occurs when using an open vessel, the liquid surface was covered with pieces of plastic (Wentzel et al., 1995). In addition a bubble sparger was used to produce effervescent small bubbles, hence preventing the formation of large bubble on the surface of the liquid which would result in surface aeration. The respirometer follows the static gas – static liquid principle (refer to **Section 2.3.1.2**) this type of respirometer is described by the mass balance presented in **Section 2.3.1.2,** Equation 2-3. The measured OUR data consists of two components as shown in **Section 2.3.1.2,** Equation 2-5; the exogenous oxygen uptake rate (OUR_{exo}) which is the uptake of the degradable substrate and the baseline endogenous oxygen uptake rate (OUR_{end}).

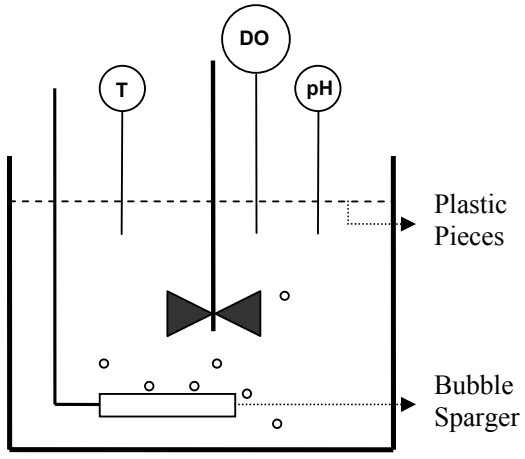

Figure 4-1: Schematic of respirometer used in Batch Respirometric Experiments

4.1.2 Oxygen Uptake Rate (OUR) Meter Instrument

The UCT DO/OUR meter (Randall et al., 1991) was used for the control of dissolved oxygen concentration and determination of oxygen uptake rate (OUR), an overview of the

components of this instrument is shown in Figure 4-2. The electronic controller unit coupled to a dissolved oxygen (DO) meter with probe controls the air supply with an on-off solenoid valve in such a way that the bioreactor is aerated intermittently to control the DO concentration between specified upper and lower limits. The OUR meter is connected to a host computer which stores the meters data with the DOMPC program.

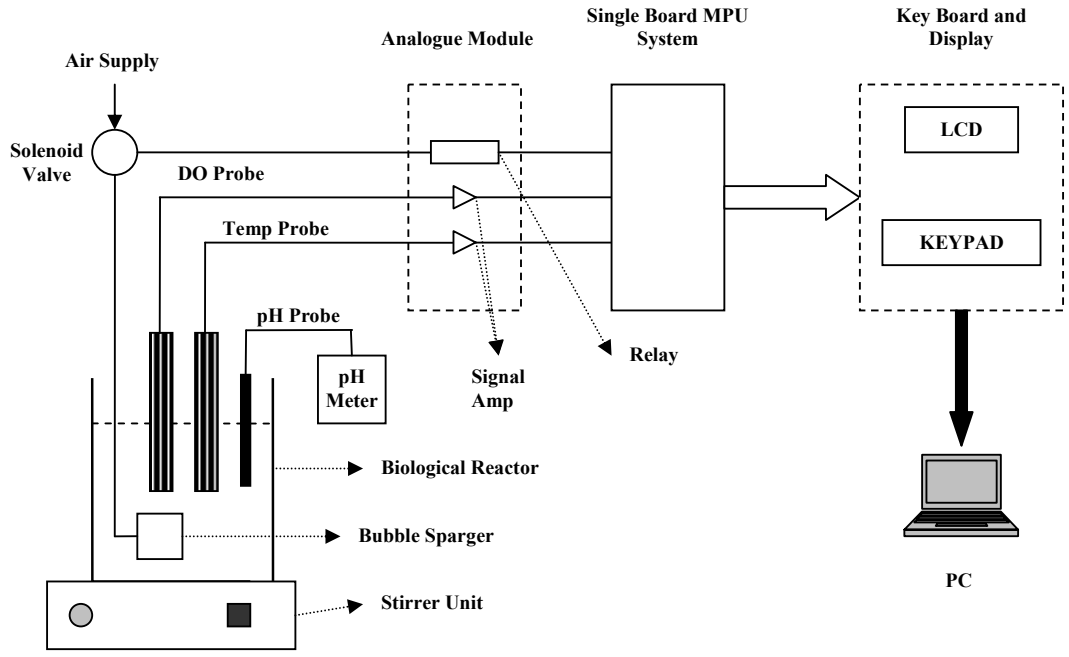

Figure 4-2: Overview of components of the Batch Respirometric Experiment adapted from (Randall et al., 1991)

Description of the UCT DO/OUR meter

The dissolved oxygen and temperature probe are connected to the UCT DO/OUR meter. The OUR meter consists of:

- controller
- crystal timer
- microprocessor for computing the OUR
- memory
- key pad for receiving instructions
- liquid crystal display (LCD) for displaying the results

The dissolved oxygen (DO) probe, meter and controller components serve to control the DO concentration between the selected upper and lower DO set points, with the aid of the microprocessor which is driven by a specially written program. The OUR is determined by collecting DO and time data pairs from the DO probe and crystal timer respectively at a pre selected time interval during the air-off period and performing a statistical linear least-square regression analysis on the accumulated data points. The LCD displays the current DO concentration, reactor temperature, the current OUR and the corresponding correlation coefficient. Various instructions can be given with the aid of the key-pad, these functions a discussed in **Appendix B**.

Hardware of the UCT DO/OUR meter

The schematic of the OUR meter component shown in Figure 4-2 and consists of an analogue module, microprocessor system and keyboard/display unit. The DO signal amplifier consist of a high stability amplifier with facilities for zero and gain adjustment which are required for calibration (calibration procedure is discussed in **Appendix B**). A second amplifier channel is on the board is for the temperature sensor. The solenoid valve control relay switches the air supply on and off in accordance with the upper and lower DO set points on the DO meter circuit board. The operation of all the input/output devices of the OUR meter is controlled by the microprocessor unit under program control. The microprocessor unit reads the analogue to digital conversions.

Determination of Oxygen Uptake Rate (OUR)

The method in which the Oxygen Uptake Rate (OUR) is determined is best describe by considering a complete cycle presented in the saw-tooth waveform in Figure 4-3, the dissolved oxygen concentration (DO) changes from upper bound (UB) to lower bound (LB) and back to

the upper bound during an on-off aeration cycle.

After the upper bound DO set point is reached the air supply is switched off and the DO starts to decrease due the biological uptake of oxygen. To ensure that at the time of aeration stopped no transient values affect the slope (OUR) calculation, the slope (OUR) is calculated by least squared linear regression method. The linear regression analysis of the collected DO-time data pairs is assisted by three statistical functions written in the microprocessor software for the variables time (X) and DO concentration (Y). The *ClearSigma* statistical function clears all variables at start of each curve fitting procedure, *UpdateSigma* function calculates running totals of X , Y , XY , X^2 , Y^2 and N (the number of data points collected) and *CalcStat* function calculates the following statistical parameters based on the current values of the running totals, average and standard deviation of X and Y values, m slope of the line (i.e. the OUR), c the Y intercept of the line, and r the correlation coefficient by linear least squared regression (Randall et al., 1991).

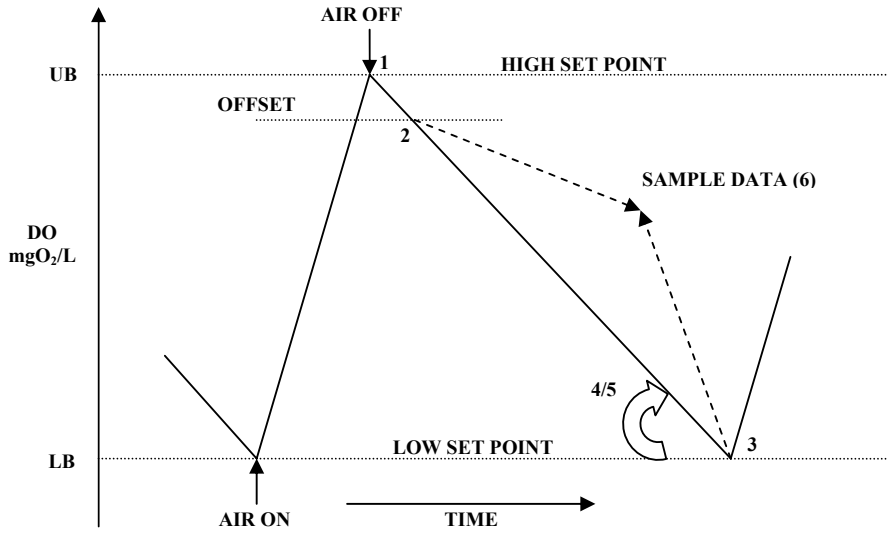

Figure 4-3: Saw-tooth waveform of the DO concentration-time trace obtained from on-off aeration adapted from (Randall et al., 1991)

Least Squares Linear Regression Method

For collected DO-time data collected the variable time (X) and DO (Y) are used in the least squares linear regression method to determine the statistical parameters. For data to fit a linear function presented in Equation 4-1:

$$Y = mX + c \tag{4-1}$$

The slope (i.e. the OUR), m ,of the linear function presented in Equation 3-7 is calculated from Equation 4-2:

$$m = \frac{N\left(\sum XY\right) - \sum X \cdot \sum Y}{N \cdot \sum X^2 - \left(\sum X\right)^2} \tag{4-2}$$

The Y intercept, c , of the linear function presented in Equation 3-7 is calculated from averages of the X and Y data sets as presented in Equation 4-3:

$$c = \frac{\sum Y}{N} - \frac{m \cdot \sum X}{N} \tag{4-3}$$

The correlation coefficient, r , which is used to determine the accuracy of the linear regression is calculated from Equation 4-4:

$$r = \frac{N \cdot \left(\sum XY\right) - \left(\sum X\right) \cdot \left(\sum Y\right)}{\left(\left[N \cdot \sum X^2 - \left(\sum X\right)^2\right] \cdot \left[N \cdot \sum Y^2 - \left(\sum Y\right)^2\right]\right)^{1/2}} \tag{4-4}$$

4.1.3 Computer System

The measured and calculated experiment data stored in the UCT DO/OUR meter was transferred to a personal computer (PC) by using a program named DOMPC. This data was then stored on disk and later analysed.

4.2 Analytical Tests

For the respirometric experiments conducted, the following analyses were performed according to Standard Methods (APHA, 1998):

- organic content (refer to **Appendix D**)
- total suspended solid (refer to **Appendix D**)
- volatile suspended solids (refer to **Appendix D**)

4.3 The OED Procedure Applied to the Batch Respirometric Experiment Design

The optimal experimental design procedure was applied in the design of the batch respirometric experiment. The objectives were to characterise the wastewater (obtained from Umbilo Wastewater Treatment Works) and obtain kinetic parameter estimates (emphases on the determination on maximum specific growth rate and half saturation constant).

The initial objectives of the batch respirometric experiments were to characterise the wastewater, determine autotrophic growth kinetics, heterotrophic growth kinetics and hydrolysis kinetics. In these experiments un-concentrated activated sludge and wastewater collected from Umbilo Wastewater Treatment Works aeration basin and the primary settler tops respectively were used. The preliminary respirometric experiment design consisted of two separate experiments; the first experiment was used to determine heterotrophic hydrolysis and growth kinetic by inhibiting nitrification, and the second experiment was used to determine autotrophic growth kinetics. Nitrification in the first experiment was inhibited using *Allylthiourea*. The hetetrophic kinetic parameter estimates determined in the first experiment was used as default values along with data collected from the second experiment, during the parameter estimation of the autotrophic kinetics. The bioreactor, respirometer and computer system mentioned in **Section 4.1** were used in these experiments; a sample (1.7 L) of un-concentrated activated sludge was placed in the bioreactor and 0.3 L wastewater was used as the substrate spike. The respirometer *OUR* meter was operated with a sample rate of 10 s, 5 mg O_2/L upper bound and 3 mg O_2/L lower bound dissolved oxygen concentration.

First Series of Respirometric Experiments:

The resultant parameter estimations of the measured data of first respirometric experiment design and the BRE model are presented in Table 4-1 and the model fits are Figure 4-4 to Figure 4-6. A second uninhibited nitrification experiment was performed in order to determine if there had been any change in the characteristics of the biomass or wastewater during the course of the experiments. It is observed from Figure 4-4 to Figure 4-6 that the substrate from the wastewater takes about 24-30 h to be consumed thereafter the activated sludge returns to endogenous respiration, hence a single experiment can be performed in a day and the total time taken for the three experiment runs was three days. Furthermore it is observed in Figure 4-4 to Figure 4-6 that insufficient data points are measured from the start of the spike to the maximum oxygen uptake value (OUR_{max}) and at the OUR_{max} value, resultantly unreliable parameter estimates of maximum specific growth and half saturation constants of heterotrophic and autotrophic biomass were obtained.

The curve fit of an experiment in which nitrification is inhibited is presented in Figure 4-4; it is observed that insufficient data points are measured to provide reliable parameter estimates of heterotrophic growth kinetics. The estimated parameters from the nitrification inhibited run are presented in Table 4-1; these parameter estimates are unreliable and no confidence interval information could be obtained. Furthermore, as presented in Table 4-1 the heterotrophic growth kinetic parameter estimates do not match those obtained in other studies (Insel et al., 2003, Vanrolleghem et al., 2004).

The curve fits presented in Figure 4-5 and Figure 4-6 are experiments in which nitrification is not inhibited these respirographic profiles have no clear indication of the degradation of the ammonia component, hence unreliable estimates (refer to Table 4-1) of ammonia kinetics were obtained. Furthermore, from Table 4-1 there is a high standard deviation between the nitrification parameter estimates of the two nitrification uninhibited runs, this could be as a result of a change in the characteristics of the biomass or wastewater during the course of the experiments or since the parameter estimates were unreliable.

Table 4-1: Estimated parameters obtained from the first experiment design data compared to those presented in literature

Experiment/Literature	μ_{mH} (1/d)	K_S (gCOD/m^3)	k_h (1/d)	K_X (gCOD/gCOD)	μ_{mA} (1/d)	K_{NH} (gNH$_3$-N/m^3)
Nitrification inhibited	0.952	0.687	2	0.322		
Nitrification uninhibited Run 1					0.420	1.887
Nitrification uninhibited Run 2					0.731	4.977
(Insel et al., 2003)	1.104	0.509	1.168	0.0106		
(Vanrolleghem et al., 2004)		0.66				
(Gernaey et al., 2001)					0.0047	0.299
(Spanjers and Vanrolleghem, 1995)						0.250

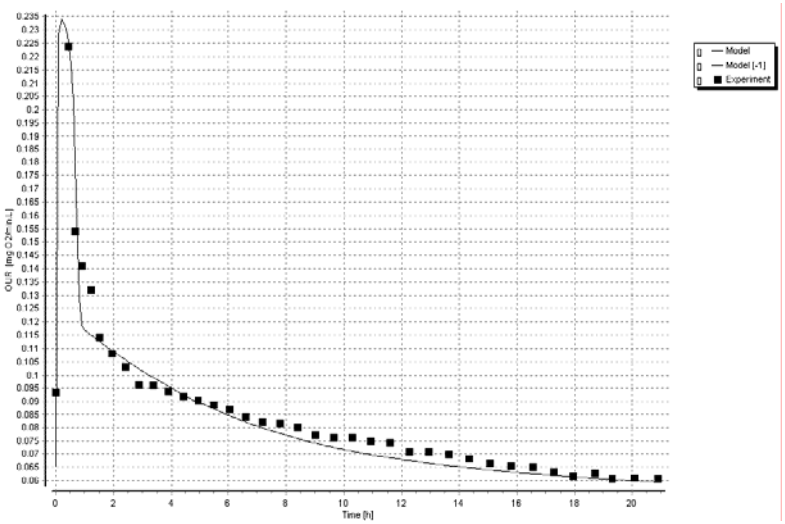

Figure 4-4: Regressed fits of OUR when nitrification is inhibited, after addition of 0.3 L wastewater into 1.7 L activated sludge for which the experimental data (squares) and BRE model (line)

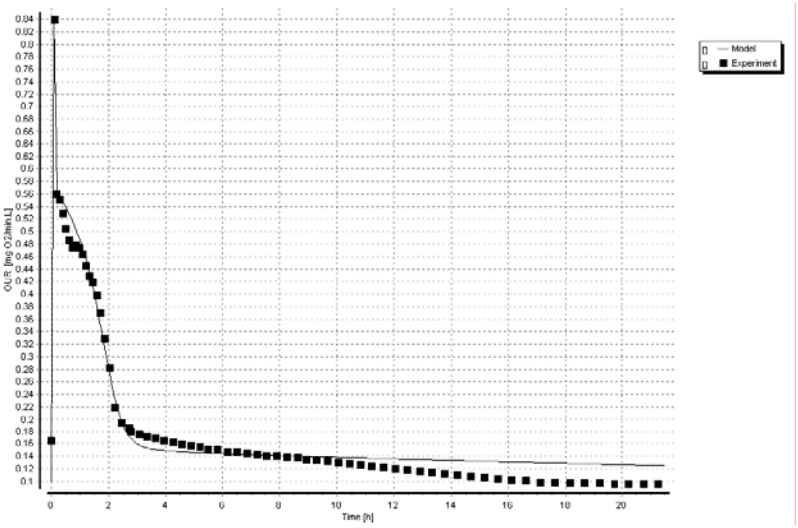

Figure 4-5: Regressed fits of OUR when nitrification is uninhibited, after addition of 0.3 L wastewater into 1.7 L activated sludge for which the experimental data (squares) and BRE model (line)

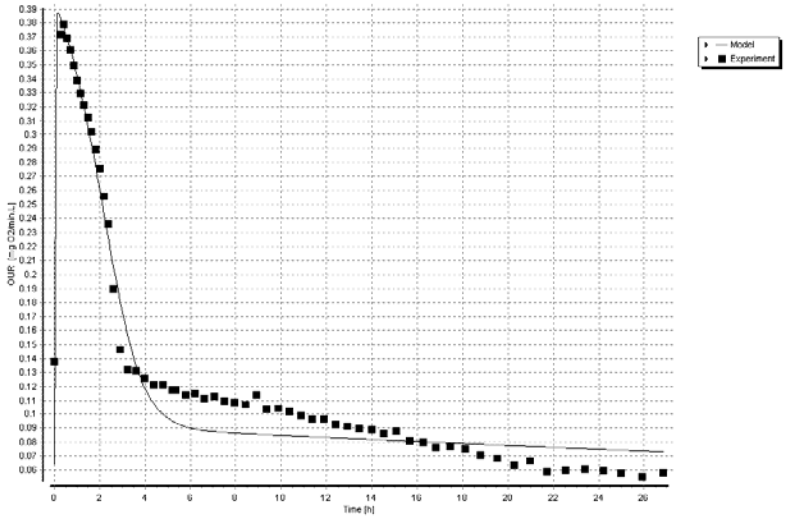

Figure 4-6: Regressed fits of OUR when nitrification is uninhibited, after addition of 0.3 L wastewater into 1.7 L activated sludge for which the experimental data (squares) and BRE model (line)

Second Series of Respirometric Experiments:

As stated above unreliable estimates of ammonia kinetics were obtained for the experiments in which nitrification is not inhibited presented in Figure 4-5 and Figure 4-6, since the respirographic profiles have no indication of the degradation of the ammonia substrate component. To solve this problem the identical experiment was performed as before, except 2 mg/L ammonium chloride along with the wastewater was added as the substrate spike to the activated sludge to produce a respirometric profile in which the degradation of ammonia and organic carbon components can be observed.

The resultant curve fit of this experiment to the model is presented in Figure 4-7; this respirometric profile has more measured data points at the maximum oxygen uptake rate value (OUR_{max}), but once again no clear differentiation can be observed between the degradation of ammonia and organic carbon substrates. The parameter estimation performed using this measured data and the estimated parameters are presented in Table 4-2; these parameter estimates are unreliable and no confidence information was obtained. Furthermore, as presented

in Table 4-2 the parameter estimates do not match those obtained in previous studies (Gernaey et al., 2001, Insel et al., 2003, Spanjers and Vanrolleghem, 1995, Vanrolleghem et al., 2004). Hence the addition of ammonia chloride with the wastewater had no positive effect for parameter estimation process.

Table 4-2: Estimated parameters obtained from the second experiment design data compared to those presented in literature

Experiment/Literature	μ_{mH} (1/d)	K_S (gCOD/m^3)	k_h (1/d)	K_X (gCOD/gCOD)	μ_{mA} (1/d)	K_{NH} (gNH$_3$-N/m^3)
Second respirometric design	0.5000	0.680	2	0.0004	0.223	1.999
(Insel et al., 2003)	1.104	0.509	1.168	0.0106		
(Vanrolleghem et al., 2004)		0.66				
(Gernaey et al., 2001)					0.0047	0.299
(Spanjers and Vanrolleghem, 1995)						0.250

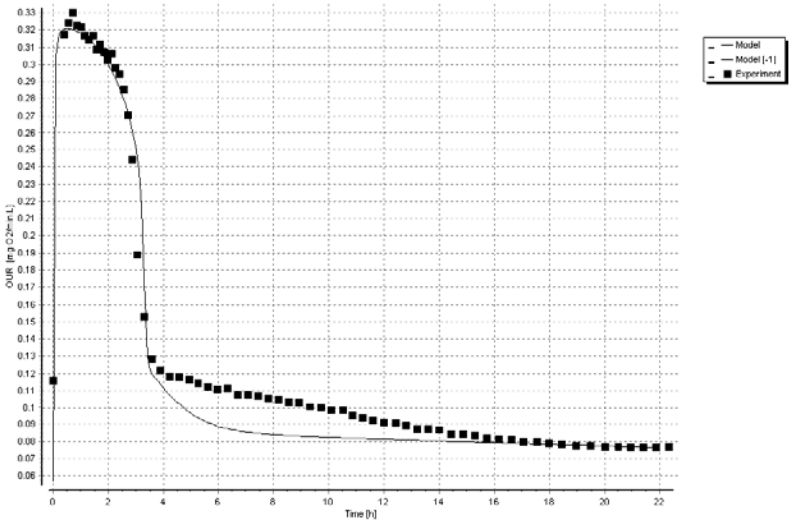

Figure 4-7: Regressed fits of OUR when nitrification is uninhibited, after addition of 0.3 L wastewater and 2 mg/L ammonium chloride into 1.7 L activated sludge for which the experimental data (squares) and BRE model (line)

Third Series of Respirometric Experiments:

As discussed earlier the time taken to perform the experiments of the preliminary respirometric experiment design was lengthy (refer to Figure 4-4 to Figure 4-6), since the biomass had a slow rate of consumption of the substrate in the wastewater. Furthermore unreliable parameter estimates of maximum specific growth and half saturation constants of heterotrophic and autotrophic biomass were obtained, since insufficient data points are measured from the start of the spike to the maximum oxygen uptake value ($OUR_{\max}$) and at the $OUR_{\max}$ value (refer to Figure 4-4 to Figure 4-6). A possible reason for these problems was that the activated sludge was too dilute, that is the biomass concentration in the bioreactor was too low. To solve this problem an identical experiment design was used as before, except activated sludge was concentrated by allowing to the activated sludge to settle thereafter half the volume of top layer of supernatant liquid was removed.

The resultant respirometric profile of this experiment are presented in Figure 4-8 and Figure 4-9; these respirometric profiles show the duration of the experiments was shorter, since

that the substrate in the wastewater is consumed in about 4 h. The parameter estimation performed using this measured data and the estimated parameters are presented in Table 4-3; these parameter estimates are unreliable and no confidence information was obtained. Furthermore, as presented in Table 4-3 the parameter estimates do not match those obtained in previous studies (Gernaey et al., 2001, Insel et al., 2003, Spanjers and Vanrolleghem, 1995, Vanrolleghem et al., 2004). Furthermore, from Table 4-3 there is a high standard deviation between the parameter estimates of the two concentrated activated sludge runs, once again this could be as a result of a change in the characteristics of the biomass or wastewater during the course of the experiments or since the parameter estimates were unreliable. The concentrating of the activated sludge did not aid in parameter estimation but had a significant effect on the duration of respirometric experiments; hence a greater number of experiments could be performed in a single day.

Table 4-3: Estimated parameters obtained from the third experiment design data compared to those presented in literature

Experiment/Literature	μ_{mH} (1/d)	K_S (gCOD/m^3)	k_h (1/d)	K_X (gCOD/gCOD)	μ_{mA} (1/d)	K_{NH} (gNH$_3$-N/m^3)
Concentrated activated sludge Run 1	4.228	0.580	5	0.0335	0.411	2.947
Concentrated activated sludge Run 2	3.954	0.680	5	0.0296	0.345	1.441
(Insel et al., 2003)	1.104	0.509	1.168	0.0106		
(Vanrolleghem et al., 2004)		0.66				
(Gernaey et al., 2001)					0.0047	0.299
(Spanjers and Vanrolleghem, 1995)						0.250

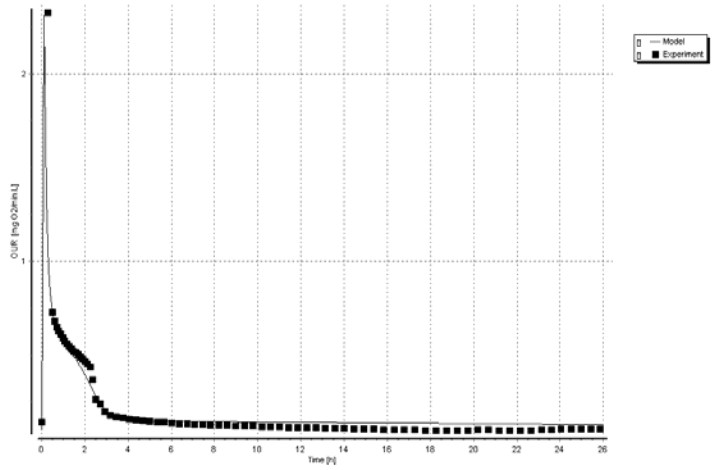

Figure 4-8: Regressed fits of OUR when nitrification is uninhibited, after addition of 0.3 L wastewater into 1.7 L concentrated activated sludge for which the experimental data (squares) and BRE model (line)

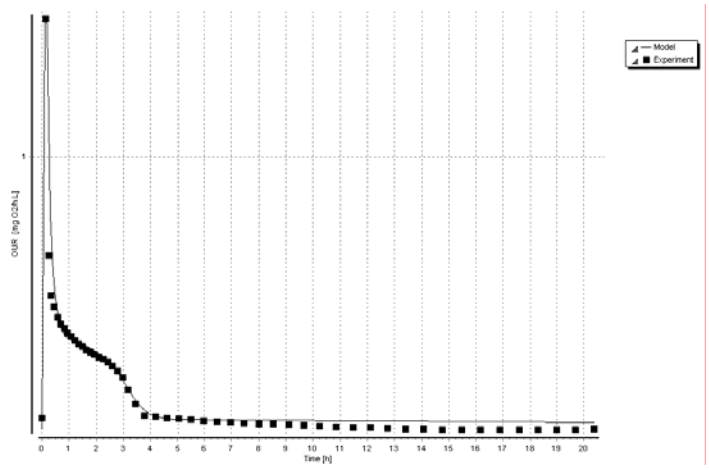

Figure 4-9: Regressed fits of OUR when nitrification is uninhibited, after addition of 0.3 L wastewater into 1.7 L concentrated activated sludge for which the experimental data (squares) and BRE model (line)

Fourth Series of Respirometric Experiments:

The previous three experiment design discussed above were time consuming and proved to be unable to produce sufficient measured data to provide reliable parameter estimates. The objectives of the respirometric experiment design were reassessed to possibly provide clearer set of objectives. Previous experiment design produced unreliable parameter estimates of maximum specific growth rates (μ_{mH} and μ_{mA}) and half saturation constants (K_S and K_{NH}) since insufficient data points from the start of the spike to the maximum oxygen uptake value ($OUR_{\max}$) and at the $OUR_{\max}$ value were measured, hence one of the major objectives of this experiment design is obtain more measured data points in those areas. As discussed in the section describing the third experiment design concentrating the activated sludge resulted in a shorter duration of experiments.

The initial objectives of characterising the wastewater and obtaining heterotrophic hydrolysis parameter estimates were not the critical sub objectives as the main objective of this study was to determine the inhibitory effect of textile dyes. The use of wastewater as a substrate was not essential; hence sodium acetate and ammonium chloride were used as substrates in the new set of experiments. Wastewater characterisation and heterotrophic hydrolysis kinetic parameters to be estimation were no longer objectives; therefore sodium acetate and ammonium chloride were used as substrate instead of wastewater, this reduced the number parameters to be estimated. From **Section 2.4.1**, Equation 2-7 by reducing the number of parameters (p) to be estimated more confident parameter estimate maybe obtained since the residual mean square (s^2) is reduced. Since the numbers of parameters to be estimated were reduced, more confident parameter estimates could be achieved. As hetetrophic hydrolysis reaction is a slow reaction by using readily biodegradable substrate like sodium acetate the hydrolysis process is eliminated, hence shorting the duration time for the consumption of a substrate and the duration of the experiment.

This respirometric experiment design consisted of two separate experiments; the first experiment was used to determine growth kinetic by inhibiting nitrification and adding sodium acetate as substrate, and the second experiment determined the autotrophic growth kinetics by adding ammonium chloride. Performing two separate experiments to determine heterotrophic and autotrophic parameter estimates has the disadvantage of being more time consuming since double the number of experiments need to be performed, but the advantage is that more confident parameter estimates will be obtained since separate parameter estimation will performed for hetetrophic and autotrophic kinetic parameters.

A major objective of this experimental design is to obtain sufficient measured data points in the area from the start of the spike to the maximum oxygen uptake value ($OUR_{\max}$) and at the $OUR_{\max}$ value. The previous experiment design produced insufficient data points from the start of the spike to the $OUR_{\max}$ and at the $OUR_{\max}$ value. The respirometer OUR meter previously was operated with a sample rate of 10 s, 5 mg O_2/L upper bound and 3 mg O_2/L lower bound dissolved oxygen concentration. To increase the number of measured data points in the first experiment design (i.e. the experiment performed with sodium acetate as substrate) the OUR meter upper and lower bound dissolved oxygen concentration was changed to 5 mg O_2/L and 4.5 mg O_2/L respectively, also the sample rate was increased to sample every 6 s. For the second experiment design (i.e. the experiment performed with ammonium chloride substrate) the OUR meter the sample rate was increased to sample every 1 s, upper and lower bound dissolved oxygen concentration was changed to 5 mg O_2/L and 4.8 mg O_2/L respectively, since ammonia spike has a lower $OUR_{\max}$ value.

The respirometric profiles of the sodium acetate and ammonium chloride substrate spikes of this experiment design is presented in Figure 4-10 and Figure 4-11 respectively. In both experiments the endogenous activated sludge was spiked twice with the respective substrate. The regressed fits of these substrate spikes are presented in Figure 4-12 and Figure 4-13, and resultant parameter estimates are shown in Table 4-4. This experimental design has achieved all the objectives stated above; sufficient measured data points in the area from the start of the spike to the maximum oxygen uptake value ($OUR_{\max}$) and at the $OUR_{\max}$ value were obtained, reliable parameter estimates of maximum specific growth rates (μ_{mH} and μ_{mA}) and half saturation constants (K_S and K_{NH}) and the duration of experiments were significantly shorter.

This experiment design respirometric profiles presented in Figure 4-12 and Figure 4-13 have significantly more data points in the area from the start of the spike to the maximum oxygen uptake value ($OUR_{\max}$) and at this peak $OUR_{\max}$. This was a critical objective achieved since more measured data points in this area were essential in obtaining reliable parameter estimates of maximum specific growth rates (μ_{mH} and μ_{mA}) and half saturation constants (K_S and K_{NH}).

Parameter estimation were performed using the measured respirometric data to obtain the maximum specific growth rates (μ_{mH} and μ_{mA}), half saturation constants (K_S and K_{NH}) and heterotrophic yield coefficient (Y_H). In previous studies it has been observed that autotrophic yield coefficient (Y_A) parameter estimates do not to vary significantly from system to system (Henze et al., 1987), hence this parameter was not estimated and fixed at a literature value of 0.24 g COD/g N was used (Henze et al., 1987). The estimated parameters and confidence intervals for both substrate experiments are presented in Table 4-4. The heterotrophic yield coefficient (Y_H) estimates of the first and second substrate spike do not vary significantly and these estimates (0.669 and 0.676 g COD/g COD) are relatively close to the activated sludge model No. 1 (ASM1) value of 0.67 g COD/g COD, hence in the future parameter estimations performed this value was fixed at 0.67 g COD/g COD.

The respirometric profiles for sodium acetate and ammonium chloride substrate spikes are presented in Figure 4-10 and Figure 4-11 respectively. These respirometric profiles show a significantly shorter duration for experiments, the sodium acetate substrate spikes are consumed in approximately 30 min and the ammonium chloride substrate is consumed in approximately 40 min. This higher substrate consumption rate will allow a series of substrate spikes to be performed in a single experiment; hence a series of dye-substrate spikes can be performed in a single experiment.

This respirometric experimental design was the optimal design which achieved all the objectives, hence this experimental design was used as the design for any further respirometric experiments performed in this study.

Table 4-4: Parameter estimate results and confidence intervals performed on experimental data obtained from sodium acetate and ammonium chloride experiments

Parameter	Sodium Acetate Experiment		Ammonium Chloride Experiment		Units
	First Spike	Second Spike	First Spike	Second Spike	
Maximum specific growth rate for heterotrophic biomass (μ_{mH})	2.650±0.435	2.617±0.410	-	-	1/d
Half saturation constant for heterotrophic biomass (K_S)	0.767±0.067	0.692±0.056	-	-	$gCOD/m^3$
Yield for heterotrophic biomass (Y_H)	0.669±0.039	0.676±0.023	-	-	gCOD/gCOD
Maximum specific growth rate for autotrophic biomass (μ_{mA})	-	-	0.271±0.029	0.376±0.041	1/d
Half saturation constant for autotrophic biomass (K_{NH})	-	-	0.069±0.085	0.170±0.092	$gNH_3\text{-}N/m^3$

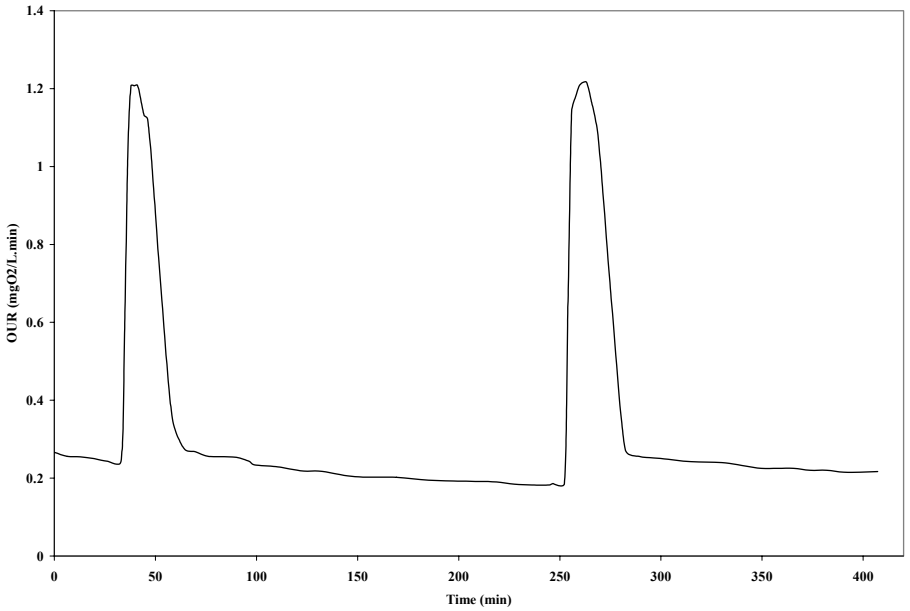

Figure 4-10: OUR profile with two sodium acetate (60mgCOD/L) substrate spikes

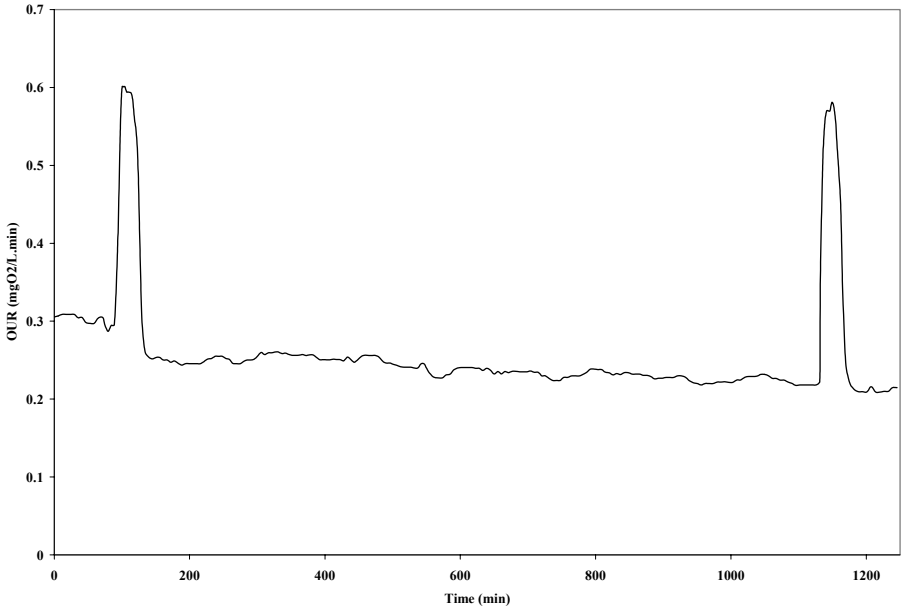

Figure 4-11: OUR profile with two ammonia chloride (4mgN/L) substrate spikes

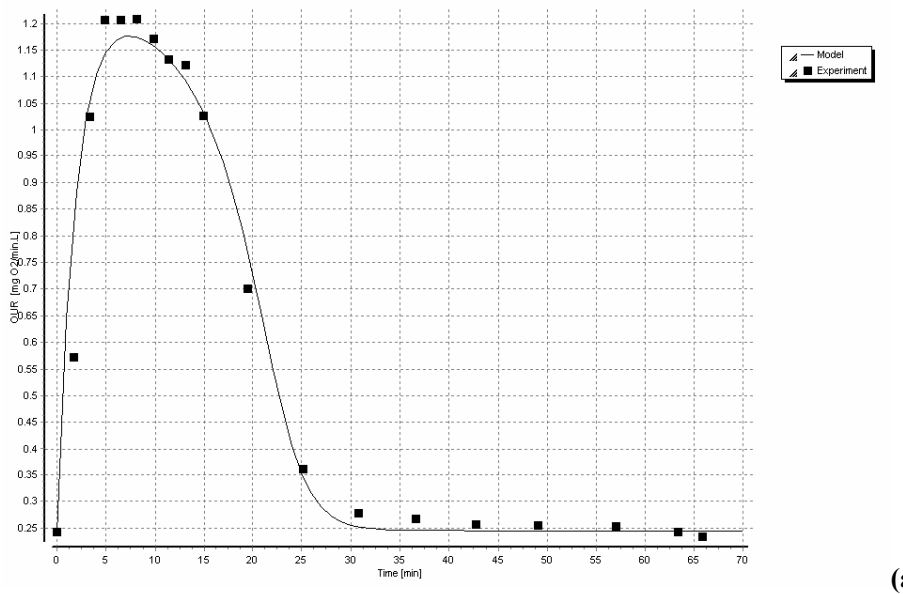

(a)

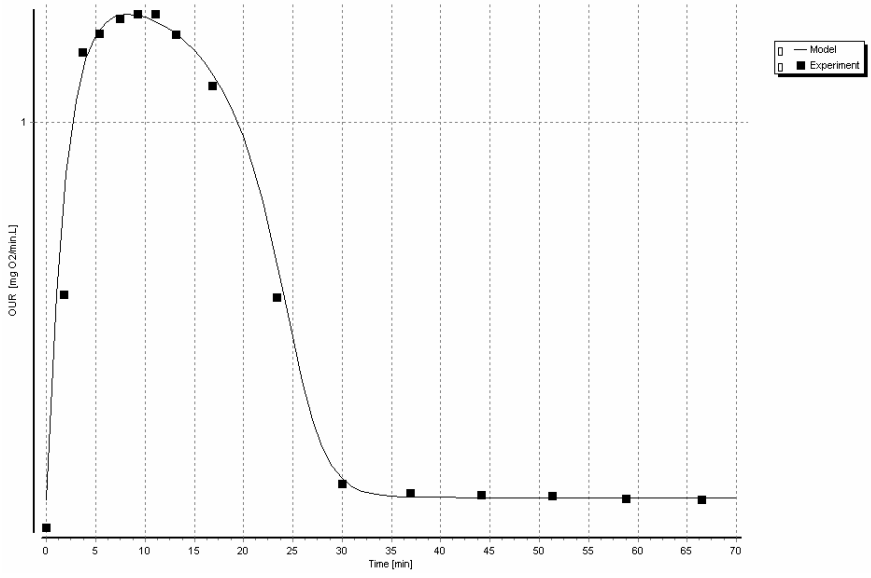

(b)

Figure 4-12: Regressed fits of OUR after addition of 60 mg/L sodium acetate into 1.7 L activated sludge for which the experimental data (squares) and BRE model (line), (a) First substrate spike and (b) Second substrate spike

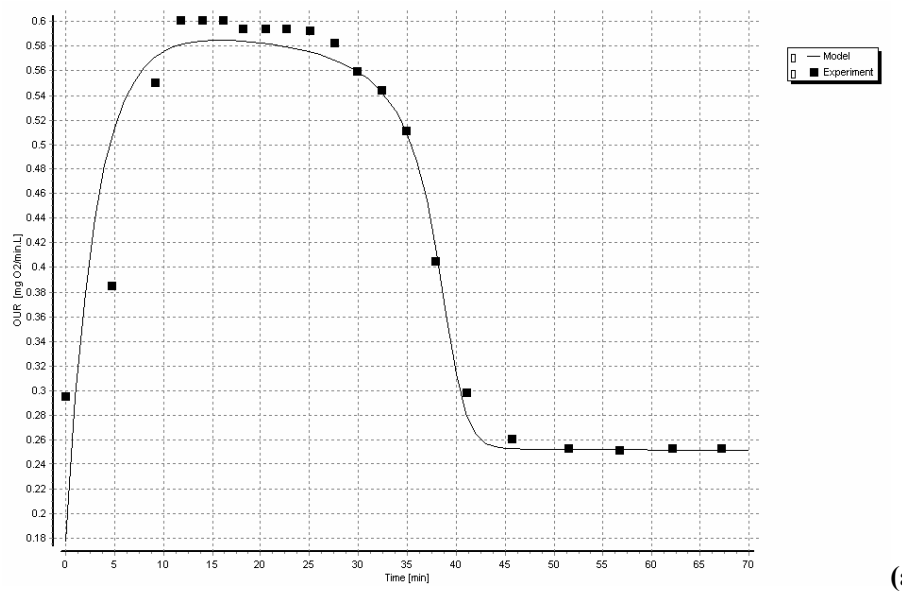

(a)

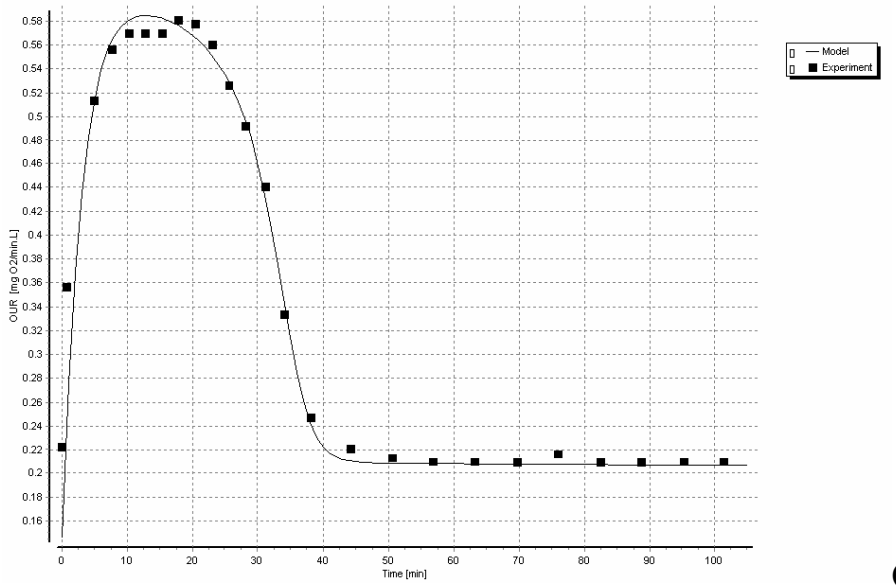

(b)

Figure 4-13: Regressed fits of OUR after addition of 4 mg/L ammonium chloride into 1.7 L activated sludge for which the experimental data (squares) and BRE model (line), (a) First substrate spike and (b) Second substrate spike

4.4 The Batch Respirometric Optimal Experiment Design

An optimal Batch Respirometric Experiment procedure was developed by implementing the

concept of Optimal Experimental Design (Dochain and Vanrolleghem, 2001) which has been discussed earlier. The experimental procedure consists of two main stages.

Before conducting the experiment the stock solutions for the reagents are prepared, details of the reagent preparation are presented in **Appendix A**. The pH in the bioreactor was monitored and maintained at a value of 7.5±0.2 by the prepared titrant reagents sodium hydroxide and hydrochloric acid. Sodium acetate and ammonium chloride were used as substrate spike reagents in separate experiments; the two substrates were used in separate experiments to ease the modelling process. Both the high and low scoring dyes used were scored according to the Score system. Furthermore both these dyes used in this study are azo dyes; since research has found that azo dyes are not degraded under aerobic conditions (**Section 2.1.2**). *Drimarene Violet K2-RL* was the high scoring dye used in the respirometric experiments; this dye has an A-score value of 1, B-score value of 3, C-score value of 2, a resulting exposure score of 6 and a toxicity score of 4. *Levafix Blue CA gran* was the low scoring dye used in the respirometric experiments; this dye has an A-score value of 1, B-score value of 4, C-score value of 1, a resulting exposure score of 4 and a toxicity score of 3.

Stage one of the experimental procedure consists of sampling concentrating of activated sludge. Grab samples of activated sludge were obtained from the Umbilo Wastewater Treatment Works aeration basins; this activated sludge was stored and concentrated under condition discussed in **Appendix D**.

The experimental procedure for stage two consists of the following steps (steps discussed in detail in **Appendix D)**:

- UCT DO/OUR meter start up
- pH probe calibration
- OUR meter calibration
- OUR meter set point adjustments
- Test monitoring
- OUR meter shut down

For the batch respirometric experiments the bioreactor was filled with 1.8 L of concentrated activated sludge. Acetate and ammonia were used as substrates since they are the predominant

substrates found in wastewater; for heterotrophic and autotrophic biomass growth respectively. The concentration of sodium acetate and ammonium chloride were 30 mg COD/L and 8 mg N/L respectively. To obtain representative data on the range of inhibition caused by the dyes the IC50 concentration value of the dyes used in the experiments were used as a guideline for the range of dye spike concentrations (Kong et al., 1996). The concentration of the dye spikes were doubled after each spike addition (Kong et al., 1996).

4.5 Results of Batch Respirometric Experiments

To obtain the required inhibition data the batch respirometric experiments were performed in a similar method to those of Kong et al. (1996). The resulting respirometric profile of the respirometric experiments performed using the high scoring dye and low scoring dye are presented in Figure 4-14 and Figure 4-15 respectively. Dye used in the respirometric experiments contained four to five concentrations. The cumulative concentration for the two dyes used in the respirometric experiments are summarised in Table 4-5. In all the experiments the first peak arises when endogenous activated sludge in the bioreactor is spiked with substrate only, the peaks thereafter are results of substrate and increasing concentrations of dye. The data collected from theses experiments were used in parameter estimations to assess the effect of the dyes in terms of kinetic parameters (refer to **Chapter 5**).

By observing the respirographic experiment profile peaks preliminary conclusions of whether the dyes have an inhibiting effect on the activated sludge processes were obtained, these conclusions can be obtained by observing the profiles maximum oxygen uptake rate ($OUR_{\max}$) and the area under the peaks. When observing the respirometric experiment profiles, the exogenous oxygen uptake rate (OUR_{exo}) is observed, that is the resultant respirometric profile (OUR) after substrate spike less the baseline initial endogenous respiration rate (OUR_{end}).

In all four respirographic profiles shown in Figure 4-14 and Figure 4-15, it observed as the concentration of dye increases the $OUR_{\max}$ and the area under the peaks decrease. Hence from these resultant experiment respirographic profiles it can be concluded that the dye spikes have an inhibitory effect on the activated sludge processes. The following observation are made when comparing acetate and ammonia spike respirometric profiles; in Figure 4-14 (b) as the concentration of dye increases a greater decrease in $OUR_{\max}$ and the area under the peaks is observed compared to Figure 4-14 (a). This is observed once again when comparing the respirometric profiles of Figure 4-15 (b) and Figure 4-15 (a). As previously discussed in

Chapter 2, previous studies have observed that the autotrophic biomass are more sensitive to toxic substances than heterotrophic biomass; this is concluded once again from the comparisons between acetate and ammonia substrate profiles.

A conclusion on whether the high scoring dye has a greater inhibitory effect than the low scoring dye can not be made by comparing the respective respirometric profiles. This conclusion can only be made once inhibitory kinetic parameters are obtained (refer to **Chapter 5**), and are used in the COST simulation benchmark (refer to **Chapter 6**) and the results from the COST simulation benchmark are analysed.

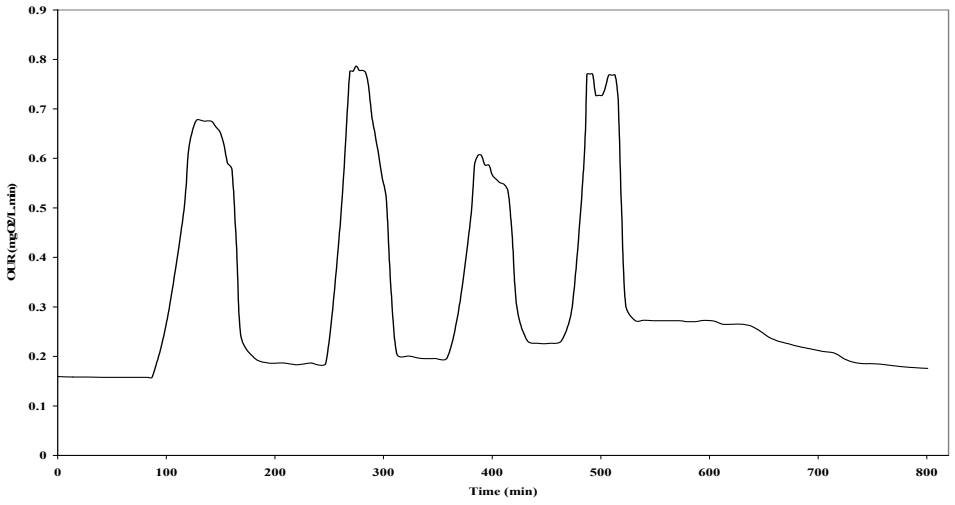

(a)

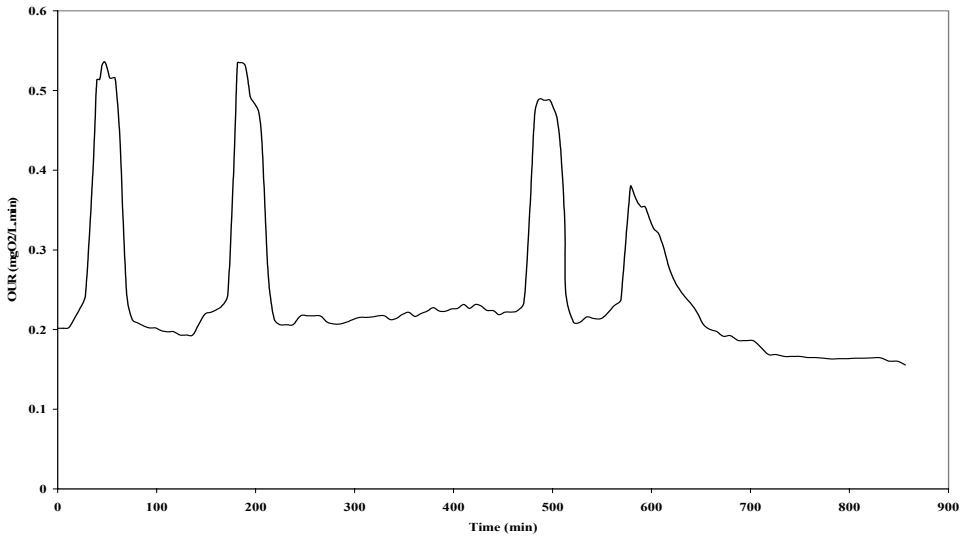

(b)

Figure 4-14: (a) OUR profile with sodium acetate (30mgCOD/L) substrate and high scoring toxicant dye Drimarene Violet K2-RL, first peak is pure sodium acetate followed by a series of mixtures of substrate and dye (b) OUR profile with ammonium chloride (8mgN/L) substrate and high scoring toxicant dye Drimarene Violet K2-RL, first peak is pure ammonium chloride followed by a series of mixtures of substrate and dye

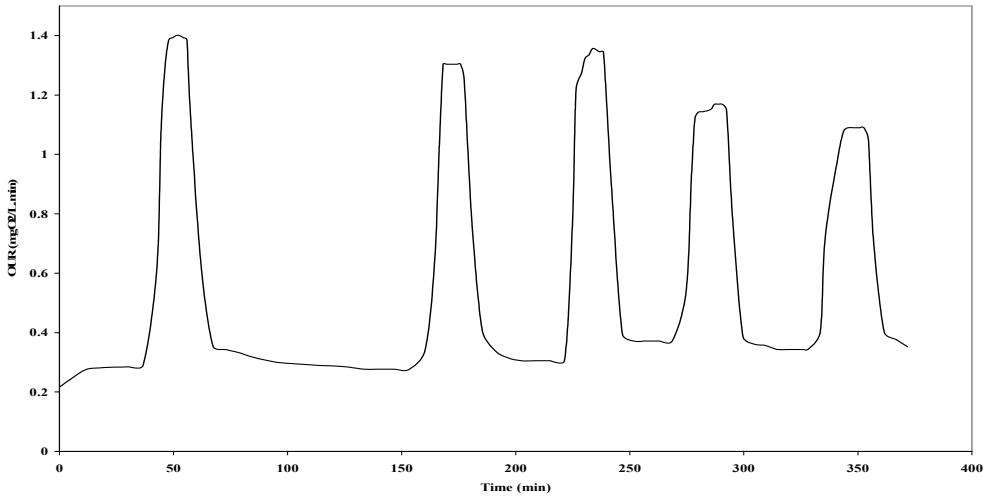

(a)

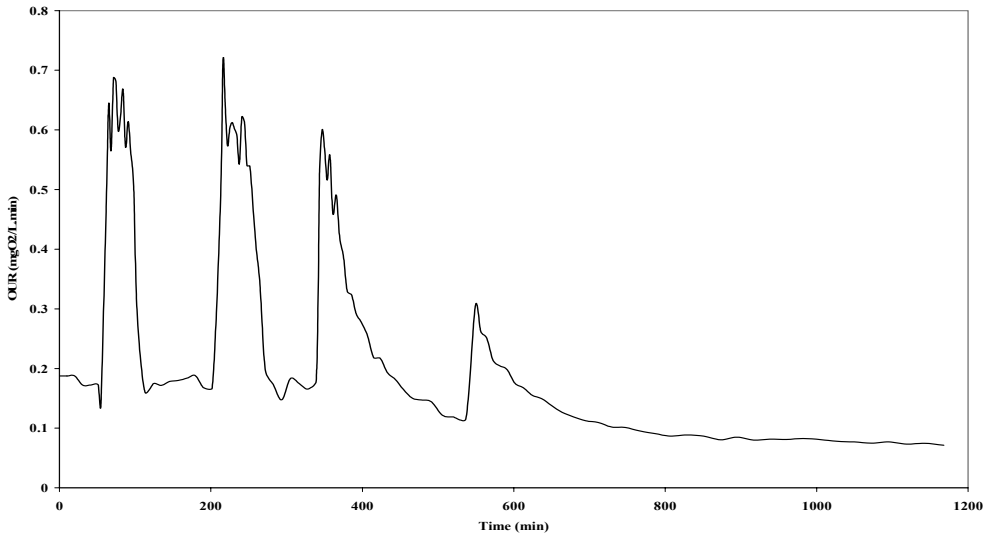

(b)

Figure 4-15: (a) OUR profile with sodium acetate (30mgCOD/L) substrate and low scoring toxicant dye Levafix Blue CA gran, first peak is pure sodium acetate followed by a series of mixtures of substrate and dye (b) OUR profile with ammonium chloride (8mgN/L) substrate and low scoring toxicant dye Levafix Blue CA gran, first peak is pure ammonium chloride followed by a series of mixtures of substrate and dye

Table 4-5: Cumulative dye concentrations used for respirometric experiments (mg/L)

Concentration Series	1	2	3	4	5
High scoring dye -Drimarene Violet K2-RL & Sodium Acetate	0	25	75	175	
High scoring dye -Drimarene Violet K2-RL & Ammonium Chloride	0	25	75	175	
Low scoring dye - Levafix Blue CA gran & Sodium Acetate	0	25	75	175	375
Low scoring dye - Levafix Blue CA gran & Ammonium Chloride	0	25	75	175	

CHAPTER 5
BRE MODEL SIMULATION RESULTS AND DISCUSSION

In this chapter the results from the identifiability study and parameter estimation performed on the BRE model are presented and discussed. The type of inhibition and the resultant inhibition kinetics of both dyes used in this study are presented.

5.1 Identifiability Study of BRE Model

An identifiability study was performed on the BRE model, the results of this identifiability analysis is presented in this section. The structural and practical identifiability of the BRE model was analysed.

5.1.1 Structural Identifiability of BRE Model

The identifiable parameter combinations for the BRE model heterotrophic and autotrophic growth are identical to that of the ASM1 model presented in **Section 3.5.1, Table 3-4** . In the batch respirometric experiments (BRE) performed no significant biomass growth occurred since the substrate pulses were at low concentrations relative to the sludge concentration. Therefore the identifiable parameter combinations for the BRE model will be the combinations found in the first column of **Table 3-4**.

5.1.2 Practical Identifiability of BRE Model

The output sensitivity function was used to evaluate the practical identifiability of the BRE model, because it is an important component in practical identifiability study, for reasons which have been discussed earlier in **Section 2.7.2 Section 3.5.2**. Sensitivity function data was generated in the sensitivity analysis mode in *WEST Experiment Environment*. WEST sensitivity analysis mode applies the numerical approximation method, discussed in **Section 3.3**, to determine the absolute and relative sensitivity. In the sensitivity analysis mode the absolute and relative sensitivity of the Oxygen Uptake Rate sensitivity variable due to change in sensitivity parameter was calculated. This was done for sensitivity function combinations of Oxygen Uptake Rate and chosen parameters. The absolute sensitivity of the OUR variable to change in parameter θ_i is calculated in WEST as follows:

$$SF = \frac{\partial OUR}{\partial \theta_i} = \frac{OUR(\theta_i) - OUR(\theta_i + \Delta\theta_i)}{\Delta\theta_i} \quad (5\text{-}1)$$

The relative sensitivity of the OUR variable to change in parameter θ_i is then calculated in WEST as follows:

$$RSF = \frac{\partial OUR}{\partial \theta_i} \cdot \frac{\theta_i}{OUR(\theta_i)} \quad (5\text{-}2)$$

Two different respirometric experiments were performed to determine nitrification and carbon reduction process kinetics independently, hence separate sensitivity analysis were performed on the BRE model nitrification and carbon reduction processes. The output sensitivity functions were calculated for μ_{mH}, K_S, k_h, K_X, τ_H, μ_{mA}, K_{NH} and τ_A these sensitivity plots are presented in Figure 5-1 and Figure 5-2.

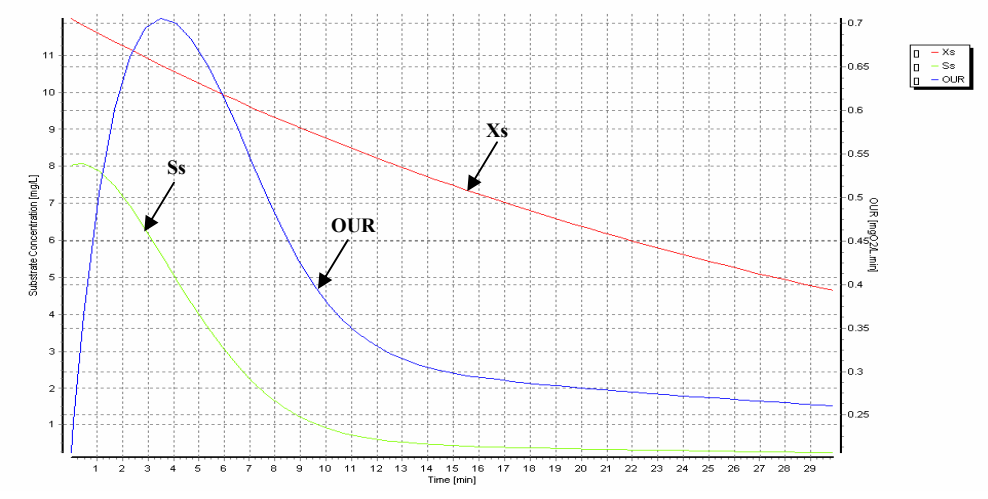

(a)

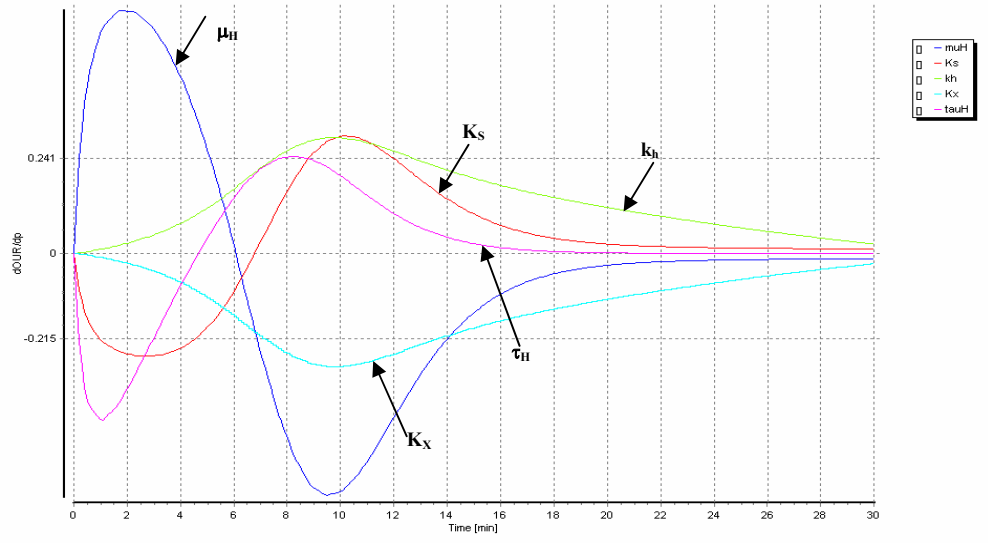

(b)

Figure 5-1: (a) OUR profile for BRE model heterotrophic biomass growth, (b) Output sensitivities for BRE model heterotrophic biomass growth

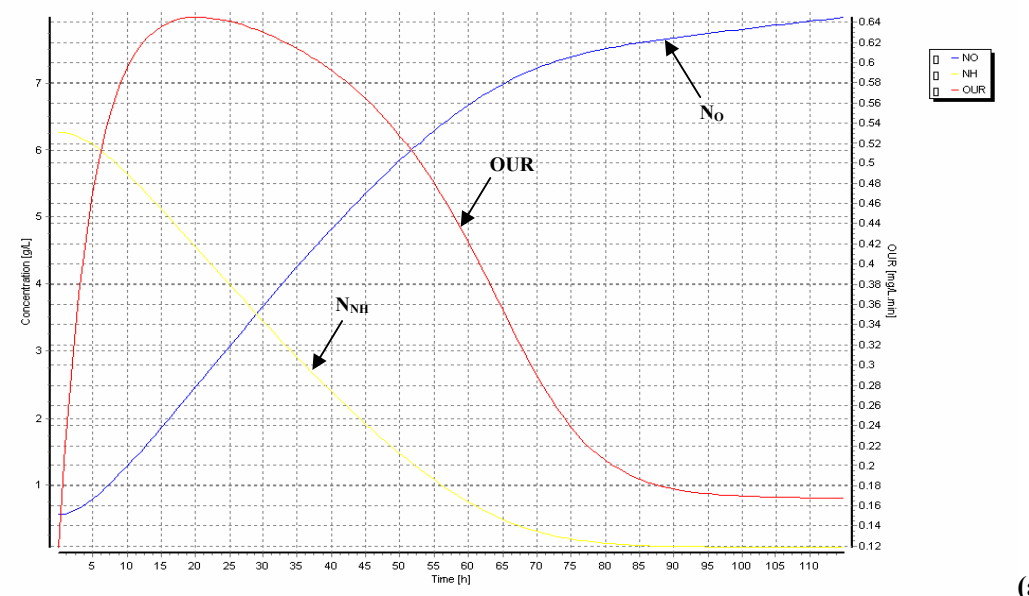

(a)

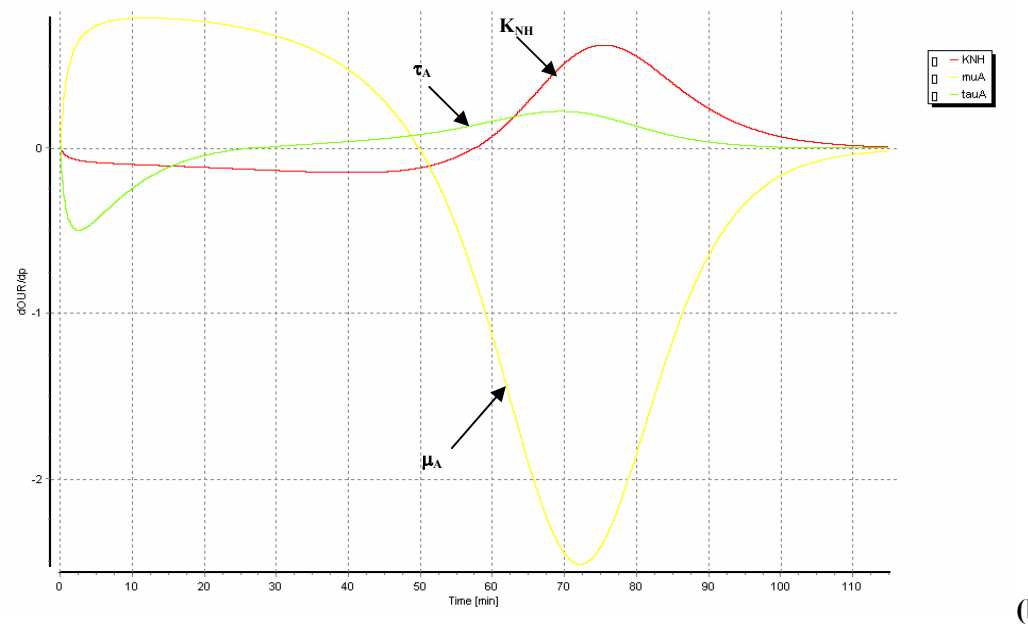

(b)

Figure 5-2: (a) OUR profile for BRE model autotrophic biomass growth, (b) Output sensitivities for BRE model autotrophic biomass Growth

From the above Figure 5-1 (b) it is observed that the heterotrophic hydrolysis process parameters k_h and K_X output sensitivity functions are correlated with each other, hence both parameters cannot be identified uniquely. Among the parameters considered the maximum specific growth rate for heterotrophic biomass μ_{mH} has the highest sensitivity. The Monod

parameters μ_{mH} and K_S output sensitivity functions show some correlation with each other, hence the initial values chosen for these parameters in parameter estimation will be critical task to obtain unique parameters estimates.

It is observed from the autotrophic sensitivity plots presented in Figure 5-2(b), that the maximum specific growth rate for autotrophic biomass μ_{mA} has the highest sensitivity. The autotrophic Monod parameters μ_{mA} and K_{NH} output sensitivity functions show a similar correlation relationship as the heterotrophic Monod parameters, resultantly great care must be taken in selecting initial values for these parameters when performing parameter estimation.

The sensitivity measure was performed using the output sensitivity function data obtained from the sensitivity analysis perform in WEST. A time interval of 0.1 min between data points was used in the sensitivity analysis simulations, since the respirometric experiment frequency at which OUR data is measured is limited to a time interval of 0.1 min. The sensitivity measure results for heterotrophic biomass growth are present in Table 5-1 and Figure 5-3. Sensitivity measure results for autotrophic biomass growth are present in Table 5-2 and Figure 5-4.

Table 5-1: Heterotrophic parameters ranked according to importance

Parameter j	**Sensitivity Measure** δ_j^{msqr}
μ_{mH}	0.313
k_h	0.159
K_X	0.156
K_S	0.150
τ_H	0.145

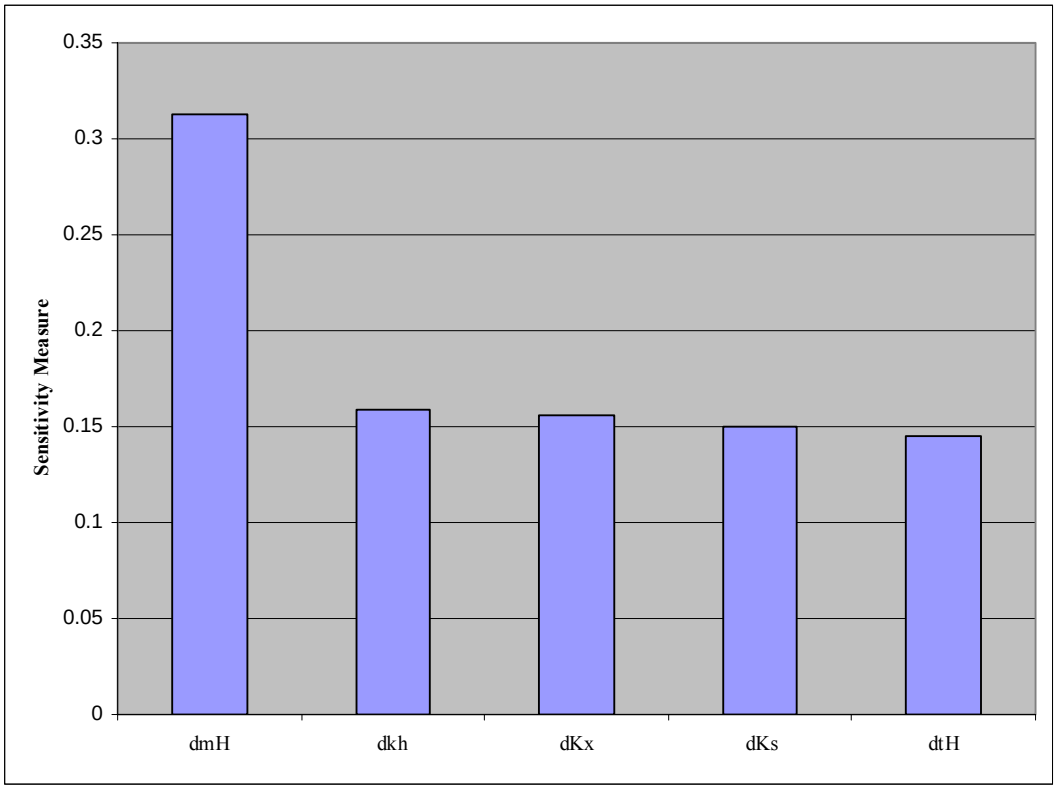

Figure 5-3: Heterotrophic parameters sensitivity measure

The heterotrophic parameter sensitivity measure results presented above, once again confirms that the maximum specific growth rate μ_{mH} has the highest average sensitivity to the output variable.

Table 5-2: Autotrophic parameters ranked according to importance

Parameter j	**Sensitivity Measure** δ_j^{msqr}
K_{NH}	0.313
μ_{mA}	0.159
τ_A	0.156

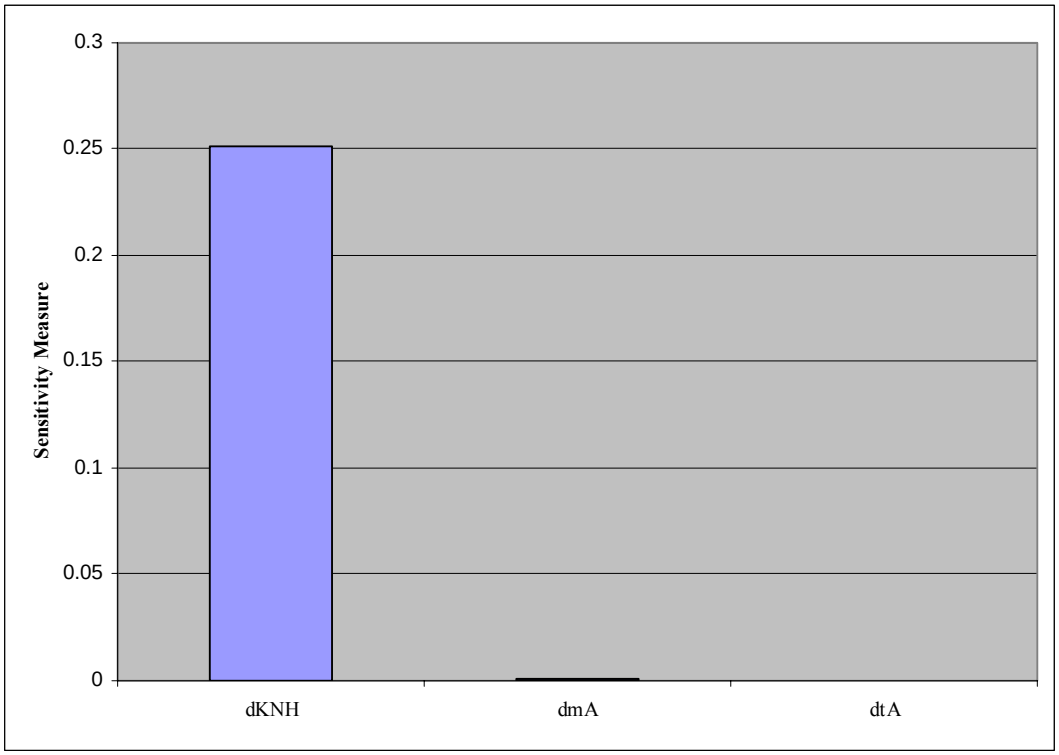

Figure 5-4: Autotrophic parameters sensitivity measure

The autotrophic parameter sensitivity measure results presented above indicates that K_{NH} has the highest average sensitivity to the output variable. This implies that both μ_{mA} and K_{NH} are significant parameter for parameter estimation.

5.2 Parameter Estimation of BRE Model

Parameter estimation was performed using the experimental data obtain from the Batch Respirometric Experiments (refer to **Section 4.5**) and the BRE model created in WEST. The parameters of the BRE model which were not estimated are presented along with the parameters default values in Table 5-3. The yield for heterotrophic biomass (Y_H) was estimated during the model calibration as was found to be the default value 0.67 found in literature (Henze et al., 1987). The *WEST Experimental Environment* trajectory optimiser was used for the parameter estimation. Regressed data fits for the high scoring dye - acetate and high scoring dye - ammonia mixtures are presented in Figure 5-5 and Figure 5-6 respectively. Also the regressed data fits for the low scoring dye - acetate and low scoring dye - ammonia mixtures are presented

in Figure 5-7 and Figure 5-8 respectively.

Table 5-3: BRE model parameters and defaults values

Parameter	Symbol	Value	Units	Reference
Yield for heterotrophic biomass	Y_H	0.67	gCOD/gCOD	(Henze et al., 1987)
Yield for autotrophic biomass	Y_A	0.24	gCOD/gN	(Henze et al., 1987)
Heterotrophic first-order time constant	τ_H	1.25	min	(Vanrolleghem et al., 2004)
Autotrophic first-order time constant	τ_A	3	min	(Spanjers and Vanrolleghem, 1995)
Mass of nitrogen per mass of COD in biomass	i_{XB}	0.086	gN/gCOD	(Henze et al., 1987)
Mass of nitrogen per mass of COD in products from biomass	i_{XP}	0.02	gN/gCOD	(Gujer et al., 1999)
Fraction of biomass leading to particulate products	f_P	0.2	-	(Gujer et al., 1999)

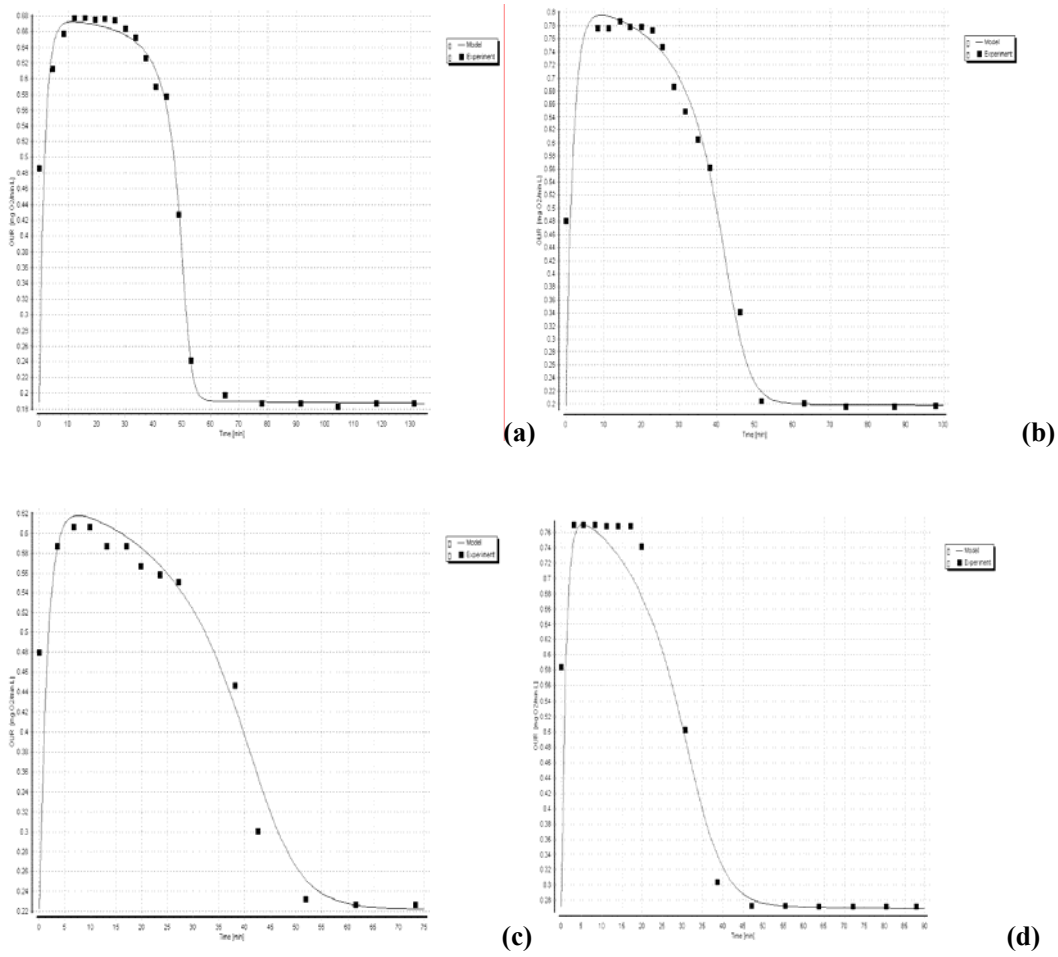

Figure 5-5: (a-d) Regressed fits of OUR for acetate substrate and high scoring dye runs for which the experimental data (squares) and BRE model (line), the concentration of the dye spikes increase from (a) to (d)

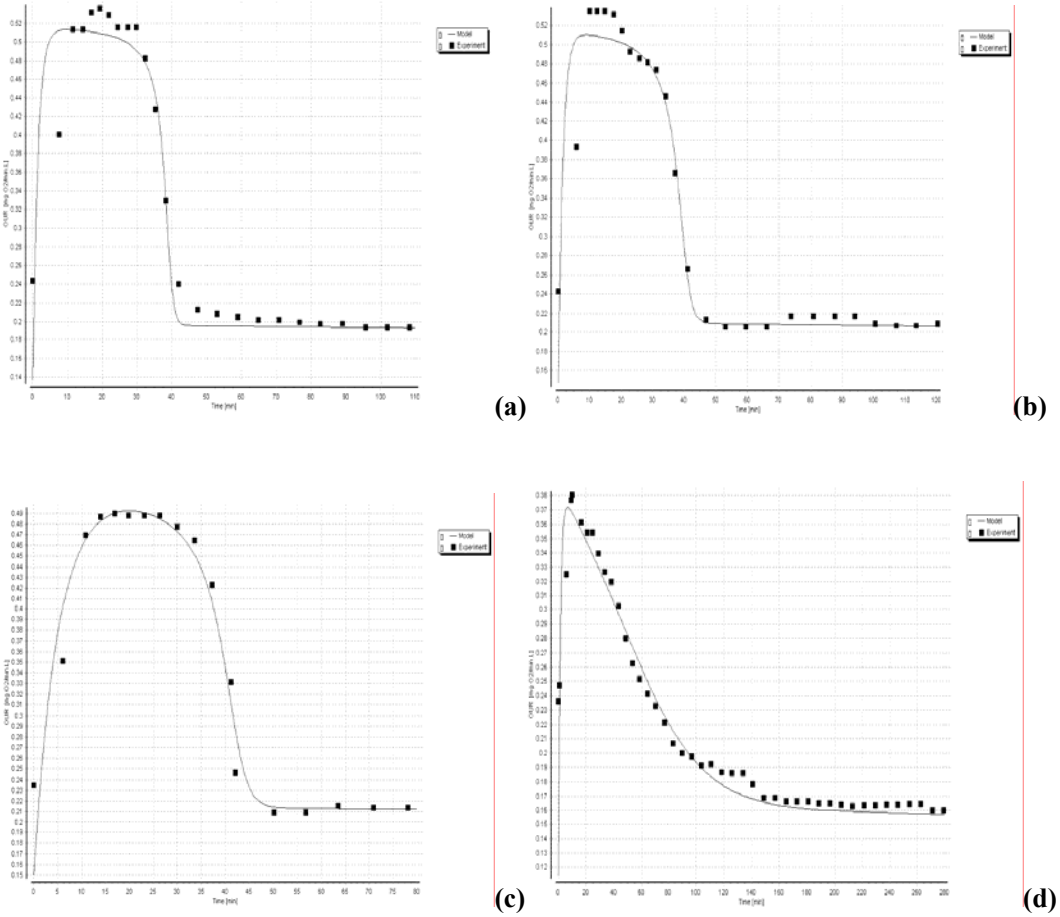

Figure 5-6: (a-d) Regressed fits of OUR for ammonia substrate and high scoring dye runs for which the experimental data (squares) and BRE model (line), the concentration of the dye spikes increase from (a) to (d)

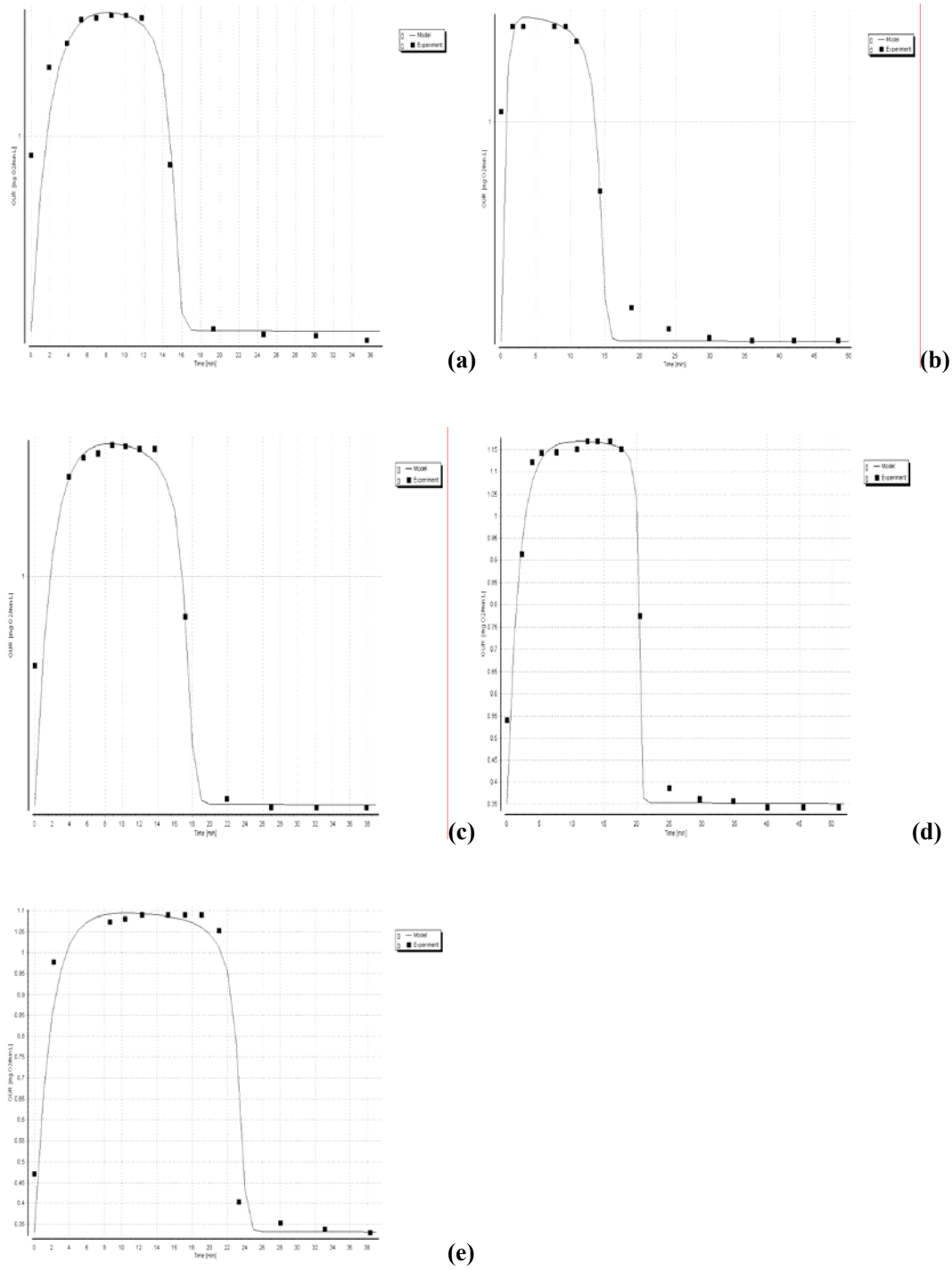

Figure 5-7: (a-e) Regressed fits of OUR for acetate substrate and low scoring dye runs for which the experimental data (squares) and BRE model (line), the concentration of the dye spikes increase from (a) to (e)

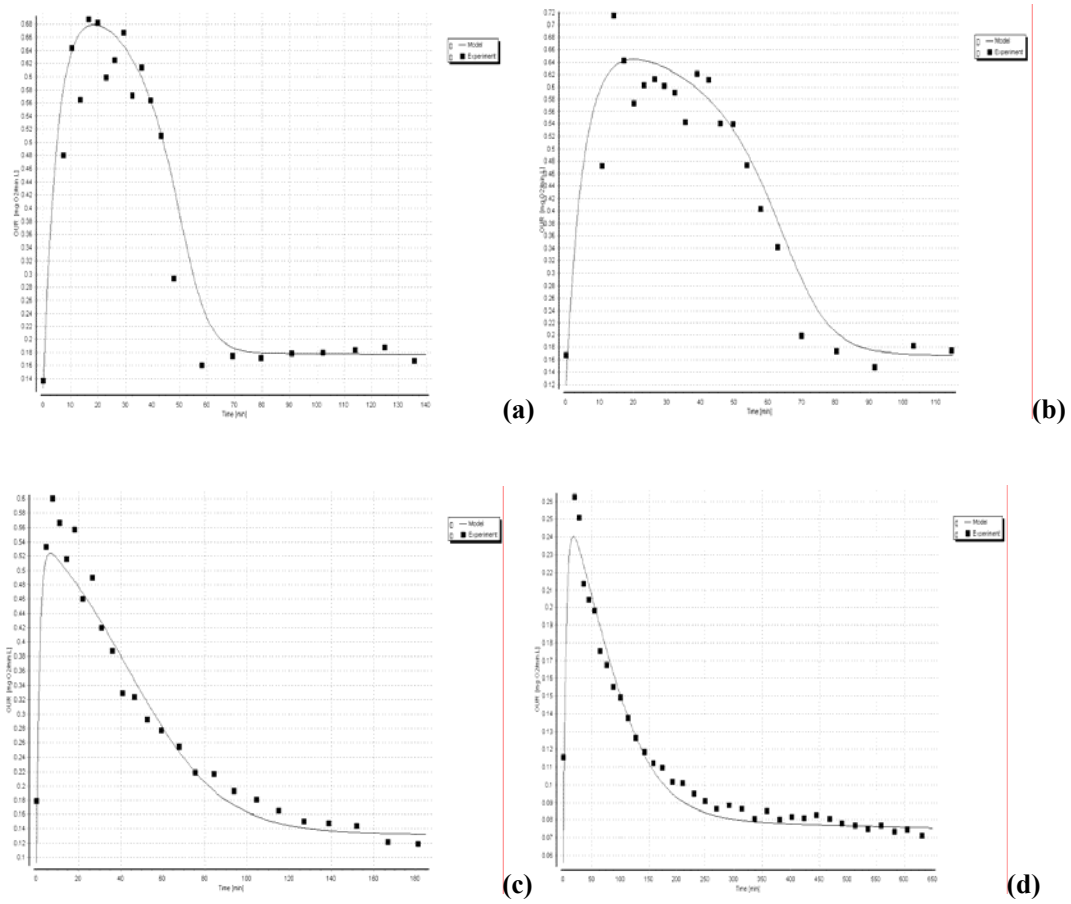

Figure 5-8: (a-d) Regressed fits of OUR for ammonia substrate and low scoring dye runs for which the experimental data (squares) and BRE model (line), the concentration of the dye spikes increase from (a) to (d)

The BRE model kinetic parameters for high and low scoring dyes obtained from the parameter estimation are shown in Table 5-4 and Table 5-5 respectively. It is observed from the estimated parameters that both dyes type of inhibition on the activated sludge processes of carbon reduction and nitrification process is the mixed inhibition type. This is so because both dyes cause a decrease in maximum specific growth rate and an increase in the half saturation constant (Volskay and Grady, 1988). Refer to **Section 3.1**, **Table 3-2** for the mixed inhibition type kinetic model.

Table 5-4: Parameter estimate results and confidence intervals performed on experimental data obtained from high scoring dye respirometric experiments

Parameter	Cumulative concentration of dye added (ppm)			
	0	25	75	175
Heterotrophic maximum specific growth rate μ_{mH}	0.620±0.025	0.605±0.032	0.574±0.068	0.520±0.093
Heterotrophic half saturation coefficient K_S	1.489±0.073	3.970±0.084	4.213±0.092	5.100±0.151
Autotrophic maximum specific growth rate μ_{mA}	0.337±0.021	0.290±0.022	0.234±0.018	0.187±0.017
Autotrophic half saturation coefficient K_{NH}	0.052±0.092	0.086±0.076	0.100±0.065	2.159±0.079

Table 5-5: Parameter estimate results and confidence intervals performed on experimental data obtained from low scoring dye respirometric experiments

Parameter	Cumulative concentration of dye added (ppm)				
	0	25	75	175	275
Heterotrophic maximum specific growth rate μ_{mH}	0.840±0.072	0.750±0.065	0.746±0.078	0.703±0.031	0.710±0.085
Heterotrophic half saturation coefficient K_S	0.609±0.081	0.685±0.093	0.691±0.085	0.151±0.075	0.461±0.090
Autotrophic maximum specific growth rate μ_{mA}	0.600±0.095	0.597±0.093	0.530±0.034	0.455±0.091	-
Autotrophic half saturation coefficient K_{NH}	0.641±0.064	0.824±0.073	3.100±0.045	5.187±0.075	-

The effect of mixed inhibition type on activated sludge processes can be quantified by Equation 5-3 and Equation 5-4.

$$\mu_{\max}^{*} = \frac{\mu_{\max}}{\left(1+\left(I/K_{I,m}\right)\right)} \tag{5-3}$$

$$K_S^{*} = K_S \cdot \left(1+\left(I/K_{I,S}\right)\right) \tag{5-4}$$

Using the data presented in Table 5-4 and Table 5-5 the $K_{I,m}$ and $K_{I,S}$ inhibition parameters were calculated through regression. These inhibition parameters for the high and low scoring dyes are presented in Table 5-6, the inhibition function and the respective parameters will be inputted into the *COST simulation benchmark model* (a detailed description of this model is provided in **Chapter 6**). The maximum specific growth rate is temperature dependent and obtained at the experiment temperature of 25°C, hence the this parameter was adjusted to satisfy a temperature condition of 15°C of the *COST simulation benchmark* by using the Arrhenius equation (Equation 5-5).

$$k(T) = k(T_r) \cdot e^{\theta(T-T_r)} \tag{5-5}$$

Table 5-6: Inhibition parameter values for high and low scoring dyes

Inhibiting Dye	Heterotrophic biomass growth		Autotrophic biomass growth	
	$K_{I,m}$	$K_{I,S}$	$K_{I,m}$	$K_{I,S}$
High scoring dye - Drimarene Violet K2-RL	921.800	61.113	194.246	5.103
Low scoring dye - Levafix Blue CA gran	1131.698	1.29×10^{9}	576.369	24.008

CHAPTER 6
ASSESSMENT OF WASTEWATER TREATMENT WORKS PERFORMANCE

In this chapter the impact of the textile dyes on the wastewater treatment works performance is assessed, the *COST simulation benchmark* was used for this assessment. Background information on COST and the concept of the COST simulation benchmark are discussed. The simulation benchmark model was used in this study to quantify the inhibitory effect of two dyes and determine whether the high scoring dye has a greater negative impact on wastewater treatment works performance than the low scoring dye.

6.1 Background on the COST and the COST Simulation Benchmark

COST (founded in 1971) is a European intergovernmental framework for co-operation in the field of scientific and technical research, allowing the coordination of European national funds. COST is the largest European framework for research co-operation, it has almost 200 Actions and involves nearly 30 000 scientists and more than 50 participating institution.

The *COST Simulation Benchmark Model* (Copp, 2002) is a publication which has been produced as a result of co-operation between two COST Actions. The two COST Actions; COST Action 682 'Integrated Wastewater Management' (1992-1998) which focused on biological wastewater treatment processes and the optimisation of design and operation based on process models, and COST Action 624 which is dedicated to the optimisation of the performance and cost-effectiveness of wastewater management systems. The goal of the *COST simulation benchmark* was to gain a greater understanding of the microbial system in wastewater treatment works and to evaluate different control strategies on the wastewater treatment works model.

The COST simulation benchmark protocol has been used in a number of studies to evaluate control strategies (Spanjers et al., 1998, Vanrolleghem and Gillot, 2002). The simulation benchmark model was used in this study since it is a well understood calibrated model, and the benchmark simulation protocol is clearly defined (Copp, 2002). The benchmark simulation model serves as a basis to evaluate the inhibitory impact of both dyes in this study (low scoring and high scoring dyes) on the process performance of a wastewater treatment works. The effluent requirements and treatment costs (that is labour costs) are often specific to a location,

this problem is prevented by using the benchmark model protocol, since the benchmark model uses a standard evaluation criteria.

6.2 Overview of COST Simulation benchmark

As discussed in the above section to obtain an unbiased comparison of the inhibition caused by both dyes, both dye inhibitions are evaluated under the same conditions, hence the clearly defined simulation benchmark protocol (Copp, 2002) is used. Also the simulation benchmark provides a suitable reference output. In this section an overview of the simulation benchmark model (Copp, 2002) is provided; the plant layout, process models and influent components are described.

6.2.1 Plant layout of simulation benchmark

A schematic representation of the simulation benchmark plant layout is shown in Figure 6-1, the plant design comprises of five reactors in series with a 10-layer secondary settling tank.

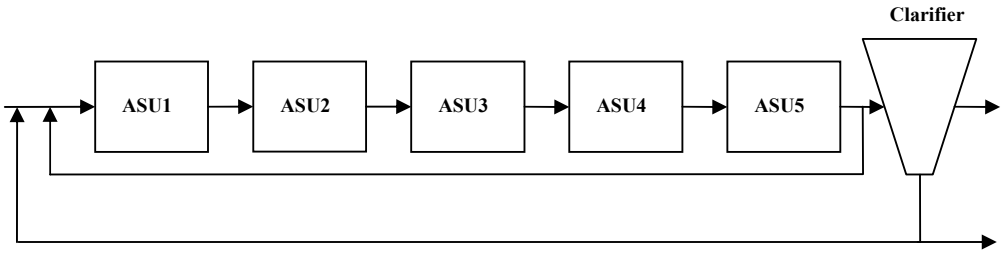

Figure 6-1: Schematic representation of the simulation benchmark plant layout showing activated sludge units (ASU) 1& 2 mixed and unaerated, ASU 3, 4 & 5 aerated, and 10 layer secondary settler

The physical attributes of the activated sludge units and settler are presented in Table 6-1 and the system variables are listed in Table 6-2. The simulation benchmark plant design consists of 5 activated sludge units in series with a secondary settler. Activated sludge units (ASU) 1& 2 each have a biological volume of 1 000 m^3 and are unaerated fully mixed reactors. ASU 3, 4 & 5 each have a biological volume of 1 333 m^3 and are aerated with saturated dissolved oxygen concentration (DO) value of 8 g O_2/m^3. The oxygen transfer coefficient ($K_L a$) value in ASU 3 & 4 are 10 1/h, whereas the $K_L a$ value in ASU 5 is 3.5 1/h. The secondary settler is a 10 layer

non-reactive settler with a volume of 6 000 m^3 (area of 1 500 m^2 and a depth of 4 m). The feed enters the settler in the middle of the sixth layer that is the feed point is 2.2 m from the bottom of the settler. The plant design has two internal recycles; a nitrate recycle from the fifth ASU to the first ASU at a rate of 55 338 m^3/d, and a activated sludge recycle from the underflow of the secondary settler to the first ASU at a flow rate of 18 446 m^3/d. The waste activated sludge is pumped continuously from the underflow at a rate of 385 m^3/d.

Table 6-1: Physical attributes of the activated sludge units and settler for the COST simulation benchmark plant configuration

Biological Process Unit	Physical Configuration	Units
Volume – Tank 1	1 000	m^3
Volume – Tank 2	1 000	m^3
Volume – Tank 3	1 333	m^3
Volume – Tank 4	1 333	m^3
Volume – Tank 5	1 333	m^3
Depth – Settler	4	m
Area – Settler	1 500	m^2
Volume - Settler	6 000	m^3

Table 6-2: System variables of the COST simulation benchmark plant configuration

System Variable	Default System Flow Rates	Units
Influent flow rate	18 446	m^3/d
Recycle flow rate	18 446	m^3/d
Internal recycle flow rate	55 338	m^3/d
Wastage flow rate	385	m^3/d
$K_L a$ – ASU 1	n/a	-
$K_L a$ – ASU 2	n/a	-
$K_L a$ – ASU 3	10	1/h
$K_L a$ – ASU 4	10	1/h
$K_L a$ – ASU 5	3.5	1/h

6.2.2 Process models of simulation benchmark

The COST benchmark simulation model uses two internationally accepted models to describe the biological process and settling process. The Activated Sludge Model 1 (ASM1) (Henze et al., 1987) is used as the biological process model and the double-exponential settling velocity function is used as the settler process model (Takacs et al., 1991).

6.2.2.1 Biological kinetic process model

As mention in **Section 2.5** a number of new activated sludge models have been proposed since ASM1 model was developed. These models include ASM2, ASM2d and ASM3. The ASM1 model is still the most popular model used internationally. There are a number of limitations to the ASM1 model which have been discussed in **Section 2.5.1**, but the worldwide appeal and practical confirmation of this model are the motivated reasons for it being used as the biological model for the simulation benchmark model. A detailed description and Petersen matrix representation of the ASM1 model are presented in **Section 2.5.1**.

The default stoichiometric and kinetic parameter values are presented in Table 6-3 and Table 6-4 respectively. The listed parameter estimates approximate those that are expected at the temperature of 15 °C.

Table 6-3: ASM1 stoichiometric parameter default values used in the simulation benchmark

Parameter	Value	Units
Autotrophic yield (Y_A)	0.24	gCOD/gN
Heterotrophic yield (Y_H)	0.67	gCOD/gCOD
Fraction of biomass to particulate products (f_p)	0.08	-
Fraction nitrogen in biomass (i_{XB})	0.08	gN/gCOD
Fraction nitrogen in particulate products (i_{XP})	0.06	gN/gCOD

Table 6-4: ASM1 kinetic parameter default values used in the simulation benchmark

Parameter	Value	Units
Maximum specific heterotrophic growth rate (μ_{mH})	4.00	1/d
Heterotrophic growth half-saturation coefficient (K_S)	10.00	$gCOD/m^3$
Heterotrophic oxygen half-saturation coefficient (K_{OH})	0.20	gO_2/m^3
Half-saturation coefficient for nitrate (K_{NO})	0.50	$gNO_3\text{-}N/m^3$
Heterotrophic decay rate (b_H)	0.30	1/d
Anoxic growth rate correction factor (η_g)	0.80	-
Anoxic hydrolysis rate correction factor (η_h)	0.80	-
Maximum specific hydrolysis rate (k_h)	3.00	gCOD/gCOD.d
Hydrolysis half-saturation coefficient (K_X)	0.10	g/gCOD
Maximum specific autotrophic growth rate (μ_{mA})	0.50	1/d
Autotrophic growth half-saturation coefficient (K_{NH})	1.00	$gNH_3\text{-}N/m^3$
Autotrophic decay rate (b_H)	0.05	1/d
Autotrophic oxygen half-saturation coefficient (K_{OA})	0.40	gO_2/m^3
Ammonification rate (k_a)	0.05	$m^3/gCOD.d$

6.2.2.2 Settling process model

The Takacs double-exponential settling velocity function (Takacs et al., 1991) was used as the settling process model for the simulation benchmark, since it is an internationally accepted settling process model. The double-exponential settling velocity function is shown in Equation 6-1; this function is based on the solid flux concept and is applicable to both hindered and flocculent settling conditions, unlike other settling models.

$$v_{sj} = v_0 e^{-r_h X_j^*} - v_0 e^{-r_p X_j^*} \quad (6\text{-}1)$$

Where:

v_{sj} is the settling velocity in layer j (m/d), subject to $0 \leq v_{sj} \geq v_0'$

X_j^* is the suspended solids concentration in layer j (g/m^3), subject to $X_j^* = X_j - X_{\min}$

X_j is the suspended solids concentration in layer j (g/m^3)

$X_{\min}$ is the minimum attainable suspended solids concentration (g/m^3), calculated from $X_{\min} = f_{ns} \cdot X_{in}$ (X_{in} is the mixed liquor suspended solids concentration entering the settler and f_{ns} is the non-settleable fraction)

The settler model parameters and default values are shown in Table 6-5.

Table 6-5: Settler model parameters and default values

Parameter	Value	Units
Maximum settling velocity (v_0')	250	m/d
Maximum Vesilind settling velocity (v_0)	474	m/d
Hindered zone settling parameter (r_h)	0.000576	m^3/g
Flocculent zone settling parameter (r_p)	0.00286	m^3/g
Non-settle able fraction (f_{ns})	0.00228	-

6.2.2.3 Influent composition

In the COST simulation benchmark protocol control strategies are evaluated by using three disturbances in the influent composition. The three disturbances are dry weather, storm event and rain event. The dry weather influent composition is used as the basis, the storm and rain event outputs are compared to the dry weather output. The ability of a control strategy to handle

these disturbances determines the performance of the control strategies.

In this study the impact of the two dye inhibitions are evaluated, hence the two dyes serve as the disturbances to the system while using the dry weather influent composition. The flow-weighted dry weather influent composition is presented in Table 6-6 (COST 624, 2005).

Table 6-6: Flow-weighted average dry weather influent composition (COST 624, 2005)

Component	Dry weather	Units
S_S	69.50	gCOD/m^3
X_{BH}	28.17	gCOD/m^3
X_S	202.32	gCOD/m^3
X_I	51.20	gCOD/m^3
S_{NH}	31.56	gN/m^3
S_I	30.00	gCOD/m^3
S_{ND}	6.95	gN/m^3
X_{ND}	10.59	gN/m^3
Q	18446	m^3/d

6.3 Modification made to simulation benchmark kinetic process model

In **Section 5.2** the type of inhibition and inhibition kinetics caused to activated sludge processes of the two dyes (i.e. high scoring dye *Drimarene Violet K2-RL* and low scoring dye *Levafix Blue CA gran*) which were examined in this study were determined. It was determined that both dyes exhibit a mixed inhibition type to both the activated sludge processes of carbon reduction and nitrification. The mixed inhibition type influence on the maximum specific growth rate and half saturation can be represented by Equation 6-2 and Equation 6-3 respectively.

$$\mu^*_{\max} = \frac{\mu_{\max}}{\left(1+\left(I/K_{I,m}\right)\right)} \tag{6-2}$$

$$K_S^* = K_S \cdot \left(1 + \left(I / K_{I,S}\right)\right) \quad (6\text{-}3)$$

As mention earlier in **Section 6.2.2.1** the Activated sludge model No.1 (ASM1) is the biological kinetic process model of the COST benchmark simulation model and the default stoichiometric and kinetic parameter values are presented in Table 6-3 and Table 6-4 respectively. The listed parameter estimates presented in Table 6-3 and Table 6-4 approximate those that are expected at the temperature of 15 °C, since the batch respirometric experiments were performed at 25 °C the parameter estimates were adjusted to represent 15 °C condition. The maximum specific growth rate was the only temperature dependent parameter; hence it was the only parameter adjusted to cater for the simulation benchmark temperature by using Arrhenius equation (refer to **Section 5.2**). The inhibition kinetic parameter values for both dyes obtained from regression of estimated parameter are presented in **Section 5.2,** Table 5-6.

The dye (inhibitor) concentration I shown in Equation 6-2 and Equation 6-3 was assumed to be a constant parameter value and not a concentration variable, this was assumed because both dyes are azo dyes and do not degrade under aerobic condition as discussed in **Section 2.1.2**.

The mixed inhibition function presented in Equation 5-2 and Equation 5-3, and the inhibition kinetic parameter values presented in Table 5-6 (**Section 5.2**) were inputted into the simulation benchmark biological kinetic model.

6.4 Simulation Procedure

The COST benchmark simulation model is an available model in WEST. The modifications discussed in **Section 6.3** to the simulation benchmark biological kinetic model were performed in the *WEST Model Editor*. The configuration of the benchmark model as it appears in *WEST Configuration Builder* is presented in Figure 6-2.

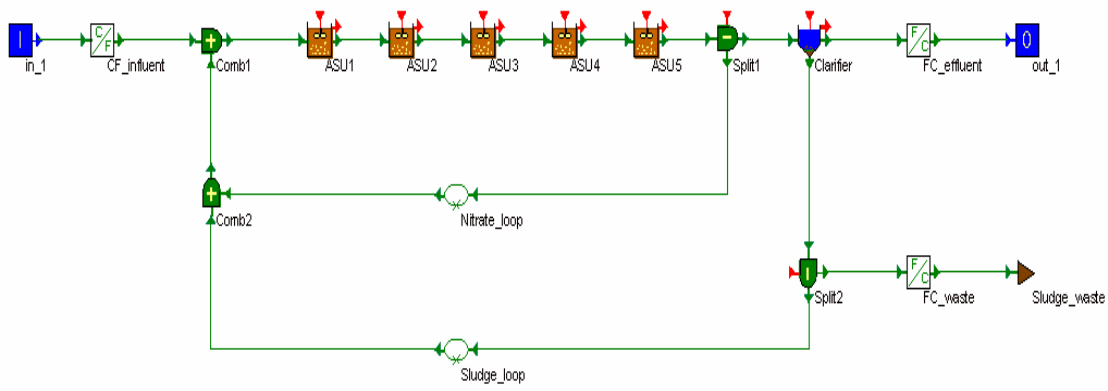

Figure 6-2: COST simulation benchmark model configuration as appears in WEST

A two step simulation procedure as defined in the simulation benchmark (Copp, 2002) were performed in *WEST Experimental Environmental*, these steps consists of a steady state simulation followed by a dynamic simulation using the dry weather influent input files.

6.4.1 Steady-state simulations

The first step in the simulation procedure is to simulate the simulation benchmark model under steady-state conditions using an influent of constant flow and composition. The flow-weighted dry weather data presented in Table 6-6 is used for this purpose and the simulation is performed for 60 d using a constant influent. Dynamic simulations follow the steady state simulation. This ensures a consistent starting point and should eliminate the influence of starting conditions on the generated dynamic output.

6.4.2 Dynamic simulations

The second step is the dynamic simulation which is performed using dynamic influent data (COST 624, 2005). Start the dynamic simulation from the steady state solution, using the dry weather dynamic influent file, simulate for 14 d. The resulting state variable values for all unit processes are saved and used to evaluate the dynamic performance of the plant to the inhibitor disturbance. The dynamic simulation output data generated during the last 7 d of simulation is used examine the dynamic performance of the plant. Output data is recorded at 0.01 d intervals.

The above two-step procedure was repeated for dye (inhibitor) concentration I in the range of 0 to 100 mg/L. The *WEST Scenario Analysis* function was used to reduce the time required to perform the above discussed simulations. *WEST Scenario Analysis* function allows multiple

simulations to be performed using a vector of parameter values, in this study the parameter vector is dye (inhibitor) concentration I. Two separate *Scenario Analysis* simulations were performed for the high scoring and low scoring dyes.

6.5 Performance index of simulation benchmark

The performance index aids in evaluation of the large amount of output data from the dynamic simulations and is specifically used to compare the impact of both dyes on the performance of the plant. The performance index is a set of geographically independent measures that combine the output data into a small number of composite terms called performance indices. The assessment of the plant process performance is quantified by the following three sub-levels:

- effluent quality index
- effluent violations
- operational costs

6.5.1 Effluent quality index

Effluent quality of the simulation benchmark model is considered through an effluent quality index (EQ), which quantifies into a single term the effluent pollution load to a receiving water body.

The composite variable used in the calculation of EQ are; TSS_e, COD_e, BOD_e, TKN_e, NO_e and $N_{tot,e}$, these variables are defined by Equation 6-4, 6-5, 6-6, 6-7, 6-8 and 6-9 respectively.

$$TSS_e = 0.75 \cdot \left(X_{S,e} + X_{BH,e} + X_{BA,e} + X_{P,e} + X_{I,e} \right) \tag{6-4}$$

$$COD_e = S_{S,e} + S_{I,e} + X_{S,e} + X_{BH,e} + X_{BA,e} + X_{P,e} + X_{I,e} \tag{6-5}$$

$$BOD_e = 0.25 \cdot \left(S_{S,e} + X_{S,e} + \left(1 - f_p\right) \cdot \left(X_{BH,e} + X_{BA,e} \right) \right) \tag{6-6}$$

$$TKN_e = S_{NH,e} + S_{ND,e} + X_{ND,e} + i_{XB} \cdot \left(X_{BH,e} + X_{BA,e} \right) + i_{XP} \cdot \left(X_{P,e} + X_{I,e} \right) \quad (6\text{-}7)$$

$$NO_e = S_{NO,e} \quad (6\text{-}8)$$

$$N_{tot,e} = TKN_e + NO_e \quad (6\text{-}9)$$

The effluent quality (EQ)is calculated by integrating through the final 7 days of the dry weather simulation as shown in Equation 5-10, the EQ units is kg pollution units per day (kgPU/d).

$$EQ = \frac{1}{1000 \cdot T} \int_{t_0}^{t_{7\,days}} \left[PU_{TSS}(t) + PU_{COD}(t) + PU_{BOD}(t) + PU_{TKN}(t) + PU_{NO}(t) \right] \cdot Q_e(t)\, dt \quad (6\text{-}10)$$

The composite variables used in Equation 6-10 to calculate effluent quality index, units are converted to pollution units by multiplying the composite variables by their respective β_i factors. These unit conversions for the respective composite variables are shown in Equation 6-11 to Equation 6-15.

$$PU_{TSS}(t) = \beta_{TSS} \cdot TSS_e(t) \quad (6\text{-}11)$$

$$PU_{COD}(t) = \beta_{COD} \cdot COD_e(t) \quad (6\text{-}12)$$

$$PU_{BOD}(t) = \beta_{BOD} \cdot BOD_e(t) \quad (6\text{-}13)$$

$$PU_{TKN}(t) = \beta_{TKN} \cdot TKN_e(t) \quad (6\text{-}14)$$

$$PU_{NO}(t) = \beta_{NO} \cdot NO_e(t) \quad (6\text{-}15)$$

The β_i factors presented in Table 6-7 were determined, in part, on empirical component weightings. The weightings are based on a Flanders effluent quality formula for calculating fines (Vanrolleghem et al., 1996). That formula is based on several terms including terms for organics, nutrients, metals and heat. The metals and heat terms are not of concern to the

simulation benchmark, but the organics and nutrient terms are related. Organic and nutrient terms can be calculated by using the Flanders equation and steady-state data from each of the layouts. From these terms it is then possible to determine the specific fraction that each term makes up of the fine formula, that is $\%nutrients = N_{nutrients} \Big/ \left(N_{nutrients} + N_{organics} \right)$. The β_i factors reflect these calculated fractions (Copp, 2002). For the COST benchmark layout, the steady state EQ was found to be weighted as 22% nutrients and 78% organics (Copp, 2002).

Table 6-7: β_i Factors for composite variables

β_i Factor	Value
β_{TSS}	2
β_{COD}	1
β_{BOD}	2
β_{TKN}	20
β_{NO}	20

6.5.2 Effluent Violations

The effluent violations are an additional measure to evaluate the performance of the wastewater treatment plant. The constraints for the five effluent components and the percentage of time that the constraints are not met are reported. The violations are calculated for five terms: ammonia, total nitrogen, BOD_5, total COD and suspended solids. The effluent constraint values for these five constraint terms are presented in Table 6-8.

Table 6-8: Effluent constraints values

Effluent Constraint	Adopted Effluent Constraint Value	Units
Ammonia ($S_{NH,e}$)	4	gN/m^3
Total Nitrogen ($N_{tot,e}$)	18	gN/m^3
BOD_5 (BOD_e)	10	$gBOD/m^3$
Total COD (COD_e)	100	$gCOD/m^3$
Suspended Solids (TSS_e)	30	gSS/m^3

The effluent violations are reported through two quantities which are calculated from the output data generated at 15 min intervals, these two quantities are; number of violations and percentage time plant is in violation.

Number of violations represents the number of times the wastewater treatment plant is in violation of the effluent constraints (i.e. the number of times the plant effluent increases above the effluent constraint). This value does not represent the length of time the wastewater treatment plant is in violation.

Percentage time plant in violation is a measure of the percentage of time the wastewater treatment plant is in violation of the effluent constraints.

6.5.3 Operational Variables

Operational issues are considered through three items; sludge production, pumping energy and aeration energy. Integrations are performed on the final 7 days of the dry weather simulations data.

Sludge Production

Sludge production consists of (i) sludge for disposal and (ii) total sludge production.

(i) Sludge for disposal (kg/d) is calculated from Equation 6-16.

$$P_{sludge} = \left[\Delta M \left(TSS_{system} \right) + M \left(TSS_W \right) \right] / T \quad (6\text{-}16)$$

Where:

$\Delta M \left(TSS_{system} \right)$ = change in system sludge mass for the final 7 days.

The change in system sludge mass is calculated using Equation 6-17 to Equation 6-19.

$$\Delta M \left(TSS_{system} \right) = M \left(TSS_{system} \right)_{day\,28} - M \left(TSS_{system} \right)_{day\,21} \quad (6\text{-}17)$$

$$M \left(TSS_{system} \right) = M \left(TSS_{reactors} \right) + M \left(TSS_{settler} \right) \quad (6\text{-}18)$$

$$M \left(TSS_w \right) = 0.75 \cdot \int_{t_0}^{t_{7\,days}} \left[X_{S,w}(t) + X_{BH,w}(t) + X_{BA,w}(t) + X_{P,w}(t) + X_{I,w}(t) \right] \cdot Q_w(t)\, dt \quad (6\text{-}19)$$

(ii) Total sludge production (kg/d) is calculated from Equation 6-20.

$$P_{total\_sludge} = P_{sludge} + M \left(TSS_e \right) / T \quad (6\text{-}20)$$

Where:

$$M \left(TSS_e \right) = 0.75 \cdot \int_{t_0}^{t_{7\,days}} \left[X_{S,e}(t) + X_{BH,e}(t) + X_{BA,e}(t) + X_{P,e}(t) + X_{I,e}(t) \right] \cdot Q_e(t)\, dt \quad (6\text{-}21)$$

Pumping Energy

The pumping energy (kWh/d) is calculated using Equation 6-22.

$$PE = \frac{0.04}{T} \cdot \int_{t_0}^{t_{7days}} \left[Q_a(t) + Q_r(t) + Q_w(t) \right] dt \quad (6\text{-}22)$$

Where:

$Q_a(t)$ = internal recycle flow rate at time t (m^3/d)

$Q_r(t)$ = return sludge recycle flow rate at time t (m^3/d)

$Q_w(t)$ = waste sludge flow rate at time t (m^3/d)

Aeration Energy

The aeration energy (kWh/d) is calculated using Equation 6-23.

$$AE = \frac{24}{T} \int_{t_0}^{t_{7days}} \sum_{i=1}^{i=5} \left[0.4032 K_L a_i(t)^2 + 7.8408 K_L a_i(t) \right] dt \quad (6\text{-}23)$$

Where: $K_L a_i(t)$ = the mass transfer coefficient (1/h) in i^{th} aerated reactor at time *t*

6.6 Results from COST benchmark simulations for both dyes

The COST simulation benchmark model was used in this study to quantify the inhibitory effect of two dyes (i.e. High scoring dye *Drimarene Violet K2-RL* and low scoring dye *Levafix Blue CA gran*) and determine whether the high scoring dye has a greater negative impact on wastewater treatment works than the low scoring dye. This evaluation is based on the performance indices (refer to **Section 6.5**) calculated using output data obtained from simulation performed on the modified COST simulation benchmark model (refer to **Section 6.3**). Simulations on the simulation benchmark model with both dye inhibition kinetics were performed, as stated previously using the scenario analysis function conditions of dye (inhibitor) concentration I in the range of 0 to 100 mg/L were simulated.

A comparison of effluent quality index (EQI) of both dyes in the dye concentration range of 0 to 100 mg/L is presented in Figure 6-3. From Figure 6-3 it can be concluded that both dyes have an inhibitory effect on wastewater treatment works processes, since as the concentration of both dyes increase the effluent quality index (EQI) increases. This implies the processes of

nutrient reduction are inhibited by the dyes, since greater amounts of nutrients are present in the effluent (i.e. higher EQI values). Furthermore it can be concluded that the high scoring dye (*Drimarene Violet K2-RL*) has a greater negative impact on the performance of the wastewater treatment works model than the low scoring dye (*Levafix Blue CA gran*), since in Figure 6-3 it is observed that as both dye concentration increases the EQI of the high scoring dye has a greater increase than the low scoring dye.

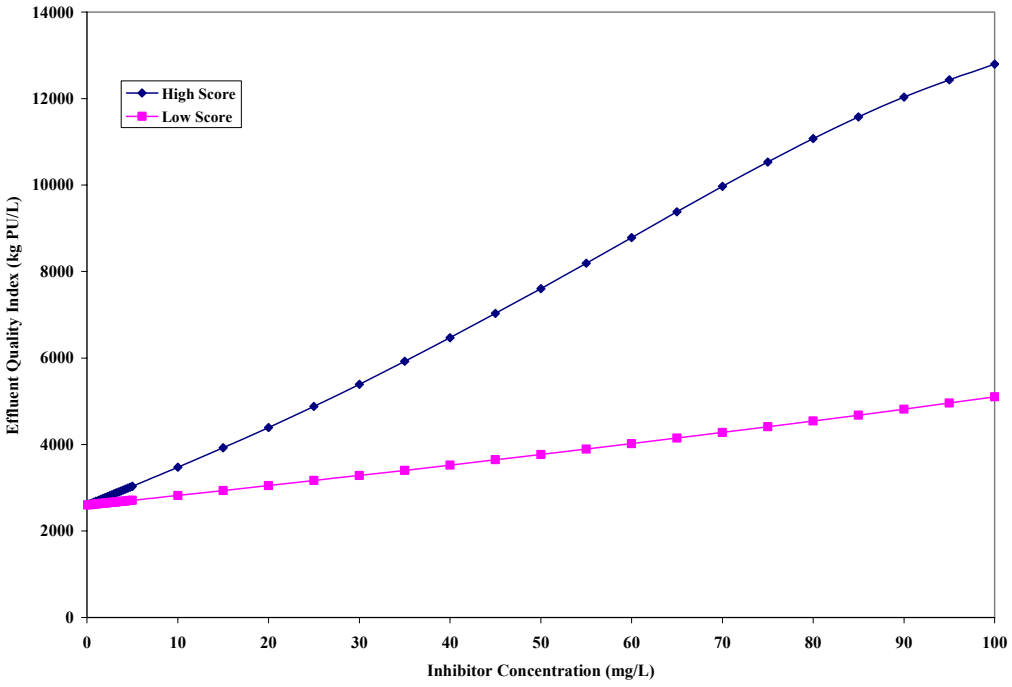

Figure 6-3: The relationship between effluent quality index and dye concentration for high and low scoring dyes.

The comparison of sludge disposal and total sludge production of both dyes in the dye concentration range of 0 to 100 mg/L is presented in Figure 6-4 and Figure 6-5 respectively. From Figure 6-4 and Figure 6-5 the conclusion of both dyes inhibiting the wastewater treatment works processes is reiterated since as the concentration of both dyes increase the sludge disposal and total sludge production decrease. This implies the activated sludge processes are inhibited by the dyes, since less sludge is produced and disposed (i.e. lower sludge disposal and total sludge production values). Once again it can be concluded that the high scoring dye (*Drimarene Violet K2-RL*) has a greater negative impact on the performance of the wastewater

treatment works model than the low scoring dye (*Levafix Blue CA gran*), since in Figure 6-4 and Figure 6-5 it is observed that as both dye concentration increases the sludge disposal and total sludge production respectively of the high scoring dye has a greater decrease than the low scoring dye.

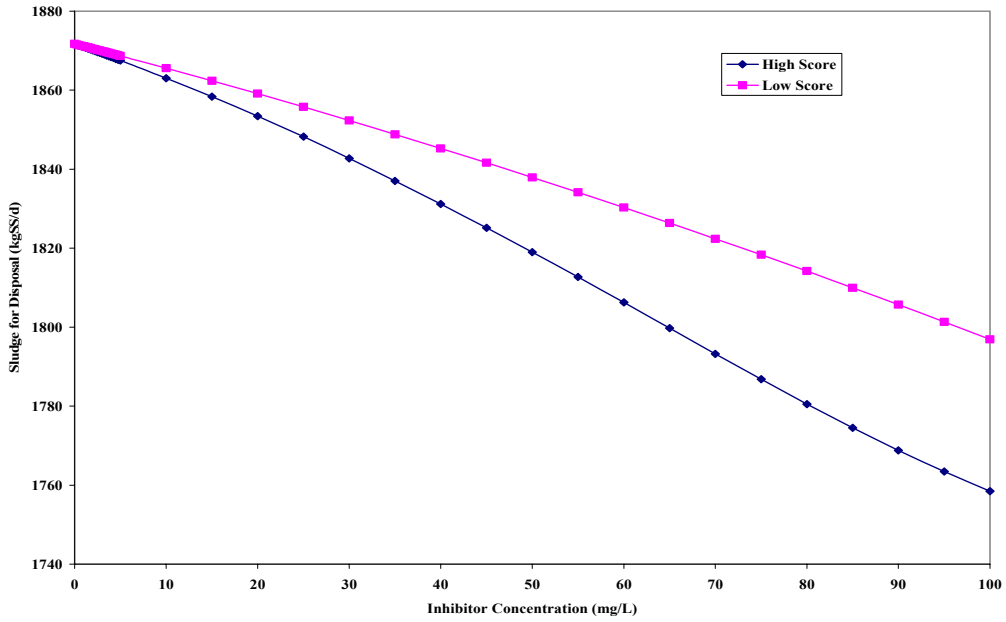

Figure 6-4: The relationship between sludge disposal and dye concentration for high and low scoring dyes.

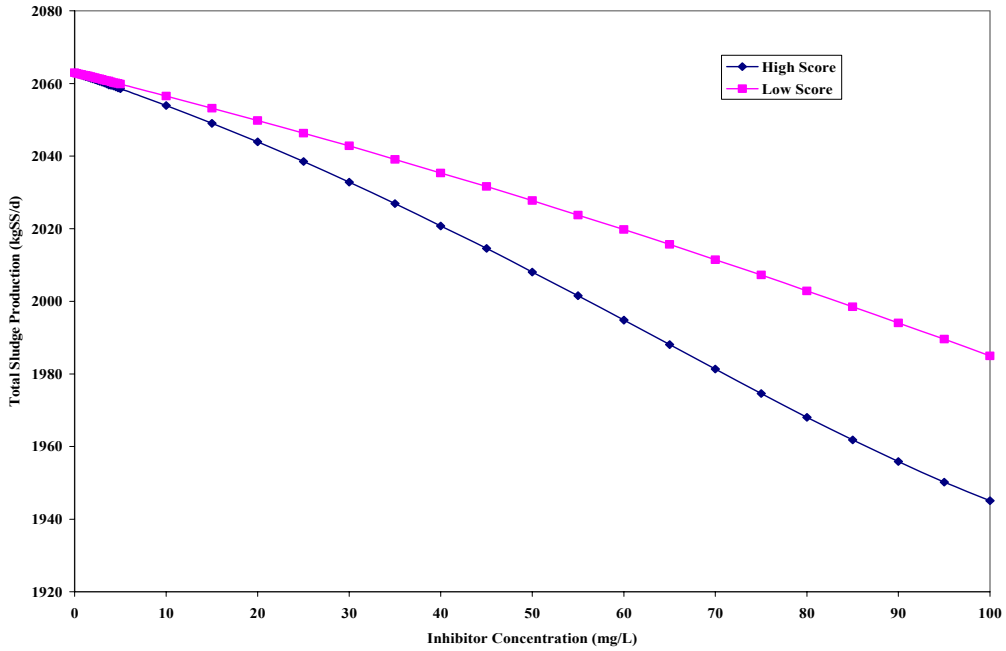

Figure 6-5: The relationship between total sludge production and dye concentration for high and low scoring dyes.

The comparison of number of violations and time in violation of both dyes in the dye concentration range of 0 to 100 mg/L is presented in Figure 6-6 and Figure 6-7 respectively. The conclusion stated above; that both dyes have an inhibitory effect on wastewater treatment works processes and that the high scoring dye (*Drimarene Violet K2-RL*) has a greater negative impact on the performance of the wastewater treatment works model than the low scoring dye (*Levafix Blue CA gran*), are reiterated once again when observing Figure 6-6 and Figure 6-7. Since in Figure 6-6 and Figure 6-7 the number of ammonia effluent violations and the percentage time that the plant is in violation of ammonia effluent constraints increase as the concentration of both dyes increase, and in Figure 6-6 and Figure 6-7 the high scoring dye has a greater number of ammonia effluent violations and the percentage time that the plant is in violation of ammonia effluent constraints is greater than the low scoring dye. Furthermore in Figure 6-6 and Figure 6-7 the number of violations and the percentage time in violation of ammonia and total nitrogen in effluent is effected by an increase in dye concentration, therefore it is concluded that the nitrification process experiences greater inhibition by the dyes than the carbon reduction processes. Since there is no BOD, COD and suspended solids effluent violations (refer to Figure 6-6); a negligible inhibitory effect of the dyes to the carbon reduction

processes can be concluded.

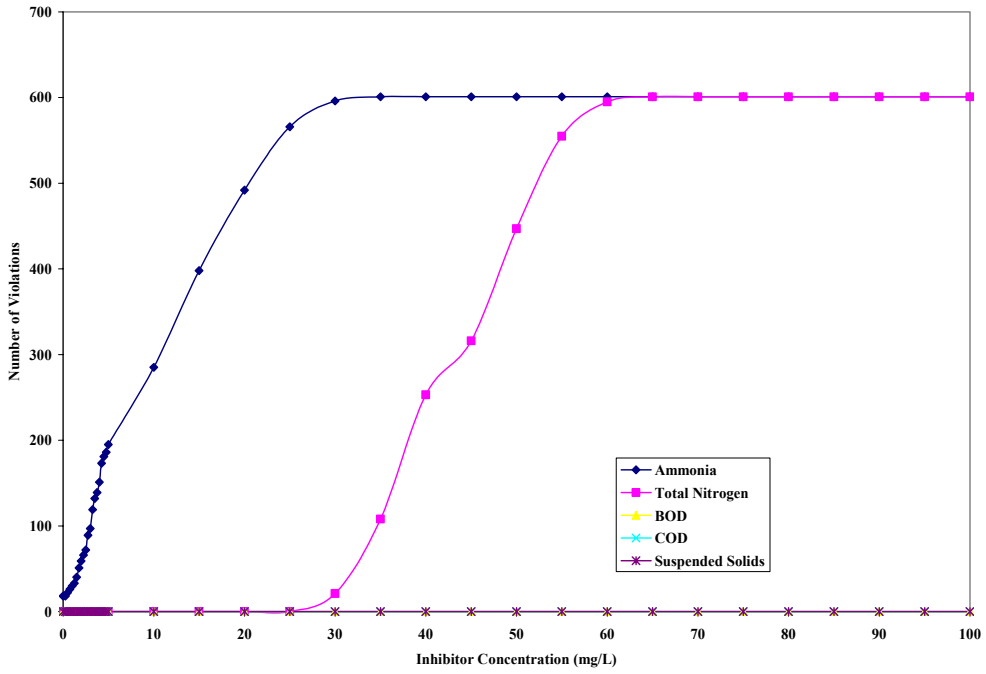

(a)

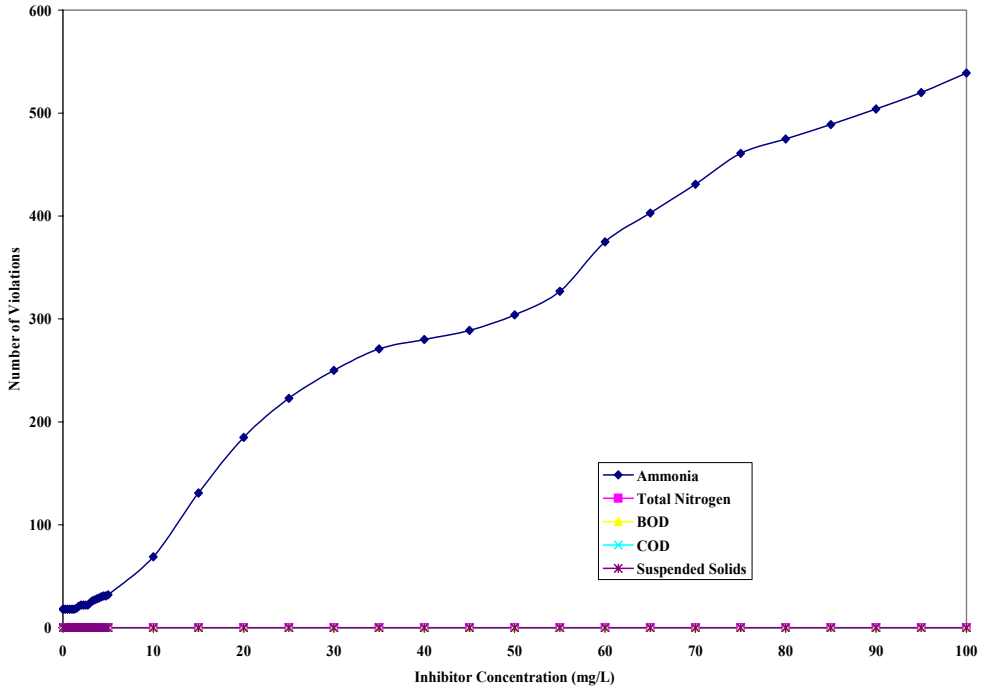

(b)

Figure 6-6: The relationship between Number of effluent violation and dye concentration for (a) high and (b) low scoring dyes.

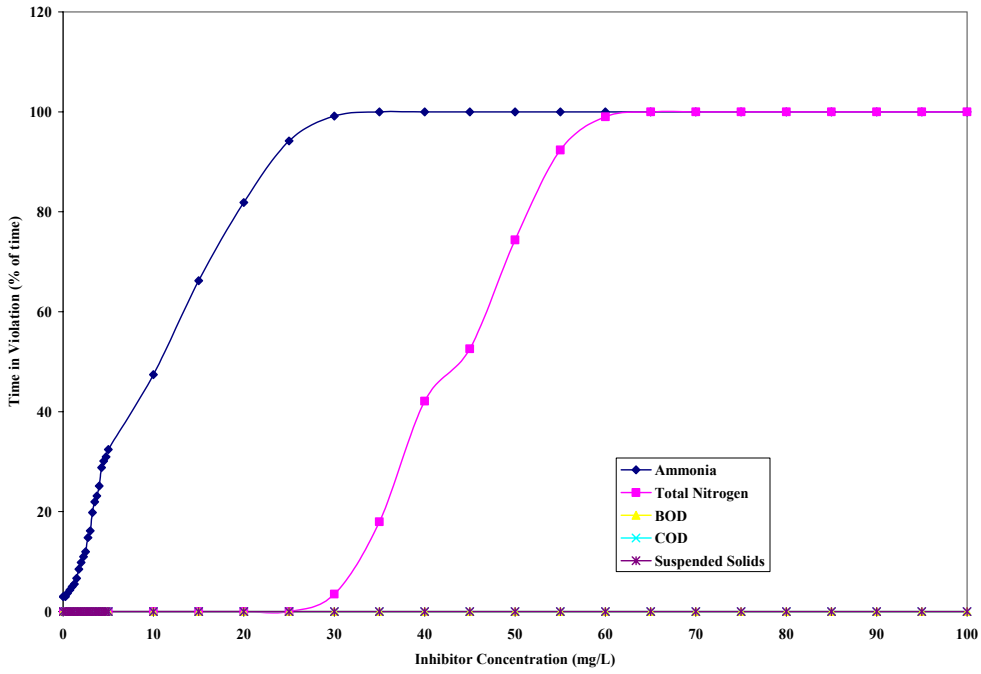

(a)

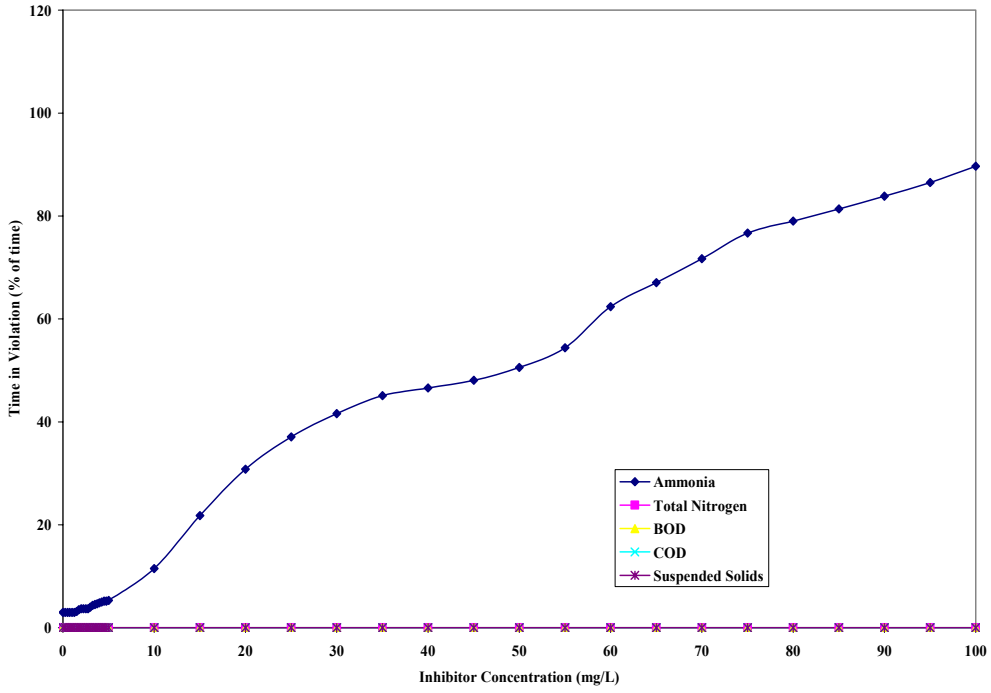

(b)

Figure 6-7: The relationship between time in violation and dye concentration for (a) high and (b) low scoring dyes.

Aeration energy and pumping energy are 6 476 kWh/d and 2 967 kWh/d respectively for both dyes. These energy values remain unaffected by the dyes since the pumping energy is calculated from respective constant flow rates (refer to Equation 6-22) are and the aeration energy is calculated from constant mass transfer coefficients (refer to Equation 6-23).

To summarise it has been concluded from simulation performed on the simulation benchmark model; that both dyes used in this study have an inhibitory effect on wastewater treatment processes and the high scoring dye has a greater negative impact than the low scoring dye on wastewater treatment works performance.

CHAPTER 7
DISCUSSION

In this chapter the broad spectrum impact of the results presented in the previous chapters are discussed. The formulation of the conclusion and recommendations of this study stated in **Chapter 8** is discussed.

7.1 Respirometric Experiments

The test activated sludge used in the batch respirometric experiments was obtained from the Umbilo wastewater treatment works (WWTW), this accounted for the normal operating conditions of the WWTW. Activated sludge in a wastewater treatment works acclimatises after prolonged exposure to toxic effluent, hence a more accurate measure of the inhibition caused by the toxic effluent probably could be to acclimatise the activated sludge to the test effluent before being used in the batch respirometric experiments. The reference substrate used in the experiments was sodium acetate and ammonium chloride, the primary components of wastewater. This was a conservative approach of selecting reference substrate, the use of a composite feed to the relevant WWTW accounts for normal operating conditions but wastewater entering the WWTW will have to be characterised to determine the composite feed. Pure dye was used as the test substance in these experiments to quantify the inhibition caused by the textile dye effluent. More accurately raw effluent from the textile companies should be used as the test substance. If the raw effluent is used as the test substance, a study into the biodegradability of the test substance needs to be performed since a biodegradation process will be required in the inhibition kinetic model.

The optimal experimental design (OED) (Dochain and Vanrolleghem, 2001) method of optimising data collection for model selection and calibration and was used in this study to design the batch respirometric experiment. This technique is used to obtain experiment designs which produce the most amount of information with the least amount of effort (Nopens et al., 2001), this method has been successfully used to design experiments and calibration of sensors in previous studies (De Pauw, 2005, Insel et al., 2003, Petersen, 2000, Sin, 2004). The OED method was effectively used in this study to design a batch respirometric experiment that produced information rich experimental data to facilitate reliable parameter estimates.

The batch respirometer used in this study followed the principle of static gas-static liquid respirometer (refer to **Section 2.3.1.2**). These respirometers are typically characterised by

low sampling frequency resulting in difficulties in determining kinetic parameters. By applying the OED technique the maximum amount of information was obtained from the batch respirometer utilised in this study. Although the measured data obtained from the batch respirometric experiment was sufficient to obtain reliable parameter estimates, the addition of a titrimetric measurement could definitely aid in the estimation of kinetic parameters. Titrimetry is a method for gaining information about the biological nitrogen removal processes of the activated sludge by monitoring pH. Nitrification and denitrification causes pH to decrease and increase respectively due to proton production and proton consumption respectively. The frequently used titrimetric method for monitoring the acid and base consumption rate to keep pH of the activated sludge constant (Ramadori et al., 1980) is effective for monitoring nitrification since nitrification has a clearly defined effect on pH (Gernaey et al., 1998). A combined respirometric-titrimetric experiment setup (Gernaey et al., 2002, Gernaey et al., 2001, Petersen, 2000, Sin, 2004) could allow the determination of both biological carbon source degradation and nitrogen removal information in a single experiment; hence the number of required experiments would be reduced.

This study only investigated the effect of the test substances on the aerobic activated sludge processes. The inclusion of an anoxic sensor similar to the sensor used in a previous study (Sin et al., 2003) to the experiment design would enable the impact of the test substances to the anoxic processes to be assessed.

7.2 Batch Respirometric Experiment (BRE) model

It was assumed that the same combination of the model parameters determined in the structural identifiability study by Taylor expansion method performed on the ASM1 model (Dochain and Vanrolleghem, 2001) applied for the BRE model. In a future study a structural identifiability analysis can be performed on the BRE model. There are many methods to determine structural identifiability (Dochain and Vanrolleghem, 2001, Petersen et al., 2003, Weijers and Vanrolleghem, 1997). If the experiment setup is changed to a respirometric-titrimetric design then some changes to the BRE model will be required; a proton concentration variable replacing the alkalinity concentration variable S_{ALK}, accounting for cumulative protons consumed or produced during biodegradation must be added (Gernaey et al., 1998), the nitrification process in the BRE model is also required, split into two processes to enable the titrimetric measured data to be used for parameter estimation (Gernaey et al., 2001) and including a carbon stripping process (Gernaey et al., 1998).

7.3 Assessment of Impact to WWTW Performance

The COST simulation benchmark model (Copp, 2002) is a activated sludge wastewater treatment model designed to evaluate different control strategies (De Pauw, 2005, Vanrolleghem and Gillot, 2002). Based on the features of the simulation benchmark a hundred scientific papers have been published world-wide (Jeppsson and Pons, 2004). In this study the benchmark model was adapted to assess the impact of the test substances concentration on the performance of the wastewater treatment works (WWTW) model. The assessment was based on performance indices which were calculated from the simulation data. From the results obtained from the simulations on the benchmark, indication are that for both test dyes as the concentration of the test substance increased a greater inhibition on performance of the WWTW model resulted, also the high scoring dye had a greater negative impact on the WWTW model performance than the low scoring dye. Hence this study concludes that the *score system* can be used confidently to administer toxic substances and their respective toxicity to WWTW. The limitation of the assessment was that the performance indices used in the assessment can not be converted to monetary values. A possible solution to this limitation is to include a control scheme as used in a previous study (Vanrolleghem and Gillot, 2002); were the dissolved oxygen concentration is controlled by manipulating the mass transfer coefficient ($K_L a$). The $K_L a$ variable is used in the benchmark protocol to calculate aeration cost which is in the form of power (kW/h); hence, a relationship between inhibitor concentration and aeration can be obtained, and the aeration cost can be easily converted to a monetary value. Therefore a relationship between test substance concentration and monetary values can be obtained; furthermore this relationship can be used in the design of tariff.

The COST benchmark simulation model is not an actual municipal WWTW, in a future study the COST benchmark simulation procedure can be used on an actual municipal WWTW (e.g. Umbilo WWTW). In this study the COST benchmark simulation model was sufficient to investigate the effect of the test substances. If an actual municipal WWTW model was used along with the COST benchmark procedure a more accurate assessment of the test substances on performance of WWTW could be obtained. The use of an actual WWTW would only be necessary if the information was to be used in a tariff calculation.

CHAPTER 8
CONCLUSIONS AND RECOMMENDATIONS

It has been concluded from the results of this study that:

1. The score system which is an administrative method of sorting organic chemicals based on the consumption and environmental behaviour of the organic chemicals; effectively identified textile dyes that have a negative impact on the environment and should be subject to closer examination.

2. The optimal experimental design method was an efficient method in designing the batch respirometric experiment. The batch respirometric experiment design provides rapid and reliable experimental data that can be used to obtain reliable parameter estimates.

3. The conservative approach used in this study of selecting test sludge, reference substrate and test substance, was successful in providing respirometric experiment data. Un-acclimatised activated sludge Umbilo wastewater treatment works (WWTW), was used as test sludge, reference substrate used in the experiments was sodium acetate and ammonium chloride, and the test substance used in the experiments was pure dye.

4. Autotrophic biomass responsible for nitrification process is more sensitive to toxic substances (in this study, textile dyes) than the hetetrophic biomass which is responsible for the carbon source degradation process.

5. The traditionally used activated sludge model No. 1 (ASM1) and ASM3 was determined to be too rigorous to obtain reliable parameter estimates with the current batch respirometric design. The batch respirometric experiment (BRE) model was developed with the objective of obtaining accurate estimates. This model is a more simplified model, and is a combination of ASM1 and ASM3 model concepts.

6. The batch respirometric experiment (BRE) activated sludge model and the respirometric experiment data successful obtained kinetic data which represented the inhibition caused by textile dyes.

7. The COST benchmark model standard evaluation criteria successfully investigated the effect of the test substances on a municipal WWTW performance.

Based on the work conducted in this study, the following is recommended:

1. A more rigorous approach to selecting test sludge, reference substrate and test substance. This may produce respirometric experiment data that more accurately represent the bioprocesses. A more rigorous selection to select acclimatised activated sludge to the test effluent as test sludge, composite feed to the relevant WWTW as reference substrate, and raw effluent from the textile companies as test substance.

2. To reduce the number of experiments required; a combined respirometric-titrimetric experiment setup would allow the determination of both biological carbon source degradation and nitrogen removal information in a single experiment, hence reducing the number of required experiments.

3. The inclusion of an anoxic sensor to the experiment design would enable the impact of the inhibitory substances to the anoxic processes to be assessed.

4. A structural identifiability analysis be performed on the BRE model.

5. Design of tariff for inhibitory substance discharged by industries to WWTW and application of the COST benchmark simulation procedure on an actual municipal WWTW that receives inhibitory substances (e.g. Umbilo WWTW). Also obtain a relationship between inhibitory substance concentration and economic values.

REFERENCES

APHA (1998) Standard methods for the examinaiton of water and wastewater (20th). *United Book Press Inc.* Baltimore, Maryland.

BANDYOPADHYAY B, HUMPHREY A and TAGUCHI H (1967) Dynamic measurement of the volumetric oxygen transfer coefficient in fermentation systems. *Biotechnol Bioeng* **9** 533-544.

BECK M. (1989) System identification and control (PATRY G and CHAPMAN D, eds.)*In Dynamic modelling and expert systems in wastewater engineering*, pp. 261-323, Lewis Publishers, Chelsea, Michigan.

BLOK J (1974) Respirometric measurements on activated sludge. *Water Res* **8** 11-18.

BLUM D and SPEECE R (1991) A database of chemical toxicity to environmental bacteria and its use in interspecies comparisons and correlations. *Res. J. Wat. Pollut. Control Fed.* **63** 198-207.

BOYLE W and BERTHOUEX P (1974) Biological wastewater treatment model building: fits and misfits. *Biotechnol Bioeng* **16** 1139-1159.

BRUN R, KUHNI M, SIEGRIST H, GUJER W and REICHERT P (2002) Practical identifiability of ASM2d parameters-systematic selection and tuning of parameter subsets. *Water Res* **36** 4113-4127.

CASTENSEN J, VANROLLEGHEM P, RAUCH W and REICHERT P (1997) Terminology and methodology in modelling for water quality management - a review. *Water Sci Technol* **36** (5) 157-168.

CECH J, CHUDOBA J and GRAU P (1984) Determination of kinetic constants of activated sludge microorganisms. *Water Sci Technol* **17** (2-3) 259-72.

COPP J (2002) The COST simulation benchmark - Description and simulator manual. *European Communities*. Luxembourg, Belgium.

COST 624 (2005) http://www.ensic.inpl-nancy.fr/COSTWWTP/.

DE PAUW D (2005) Optimal experimental design for calibration bioprocess models: A validated software toolbox. PhD thesis. Department of applied mathematics, biometrics and process control. Gent University. Gent. 263p.

DOCHAIN D and VANROLLEGHEM P (2001) Dynamical modelling and estimation in wastewater treatment processes. *IWA Publishing*. London, UK.

DOCHAIN D, VANROLLEGHEM P and VAN DAELE M (1995) Structural identifiability of biokinetic models of activated sludge respiration. *Water Res* **29** (11) 2571-2578.

DOLD P (1980) A general model for the activated sludge process. *Prog. Wat. Tech.* **12** (6) 47-77.

ELLIS T, BARBEAU D, SMETS B and GRADY C (1996) Respirometric techniques for determination of extant kinetic parameters describing biodegradation. *Water Environ Res* **38** 917-926.

FARKAS P (1981) The use of respirography in biological treatment plant control. *Water Sci Technol* **13** 125-131.

FLEGE R (1970) Determination of degraded dyes and auxiliary chemicals in effluents from textile dyeing processes. OWRR Project No. B-027-GA,

GERNAEY K, PETERSEN B, DOCHAIN D and VANROLLEGHEM P (2002) Modeling aerobic carbon source degradation processes using titrimetric data and combined

respirometric-titrimetric data: structural and practical identifiablity. *Biotechnol Bioeng* **79** (7) 754-766.

GERNAEY K, PETERSEN B, NOPENS I, CORNEAU Y and VANROLLEGHEM P (2002) Modeling aerobic carbon source degradation processes using titrimetric data and combined respirometric-titrimetric data: experimental data and model structure. *Biotechnol Bioeng* **79** (7) 741-753.

GERNAEY K, PETERSEN B, OTTOY J and VANROLLEGHEM P (2001) Activated sludge monitoring with combined respirometric-titrimetric measurements. *Water Res* **35** (5) 1280-1294.

GERNAEY K, VANROLLEGHEM P and VERSTRAETE W (1998) On-line estimation of nitrosomonas kinetic parameters in activated sludge samples using titration in-sensor-experiments. *Water Res* **32** (1) 71-80.

GERNAEY K, VERSCHUERE L, LUYTEN L and VERSTRAETE W (1997) Fast and sensitive acute toxicity detection with an enrichment nitrifying culture. *Water Environ Res* **69** 1163-1169.

GODEFROY S (1993) The regional treatment of textile and industrial effluent. Project No. 456,

GODFREY K and DI STEFANO III J. (1985) Identifiability of model parameters *In Identification and System Parameter Estimation*, pp. 89-114, Pergamon Press, Oxford.

GUJER W, HENZE M, MINO T and VAN LOOSDRECHT MCM (1999) Activated sludge model No. 3. *Water Sci Technol* **39** (1) 183-193.

HARTMANN L and LAUBENBERGER G (1968) Toxicity measurements in activated sludge. *J. San. Engr. Div. Proc. Am. Soc. Civ. Eng* **94** 247.

HENZE M, GRADY CPL J, GUJER W, MARAIS G and MATSUO T (1987) Activated sludge

model No.1. Sci. and Tech. Reports,

HENZE M, GUJER W, MINO T, MATSUO T, WENTZEL M and MARAIS G (1995) Activated Sludge Model No. 2. Sci. and Tech. Reports,

HENZE M, GUJER W, MINO T, WENTZEL M, VAN LOOSDRECHT MCM, MARAIS G and MATSUO T (1999) Activated sludge model No. 2d, ASM2d. *Water Sci Technol* **39** (1) 165-182.

HOLMBERG A (1982) On the paractical identifiability of microbial growth models incorporating Michaelis-Menten type nolinearities. *Math. Biosci.* **62** 23-43.

INSEL G, ORHON D and VANROLLEGHEM P (2003) Identification and modelling of aerobic hydrolysis - application of optimal experimental design. *J Chem Tech Biotech* **78** 437-445.

JEPPSSON U and PONS M (2004) The COST benchmark simulation model - current state and future perspective. *Contr Eng Pract* **12** (Control Engineering Practice) 299-304.

KAPPLER J and GUJER W (1992) Estimation of kinetic parameters of heterotrophic biomass under aerobic conditions and characterization of wastewater for activated sludge modelling. *Water Sci Technol* **25** (6) 125-139.

KONG Z, VANROLLEGHEM P, WILLEMS P and VERSTRAETE W (1996) Simultaneous determination of inhibition kinetics of carbon oxidation and nitrification with a respirometer. *Water Res* **30** (4) 825-836.

KRISTENSEN G, JORGENSEN P and HENZE M (1992) Charaterization of functional microorganism groups and substrate in activated sludge and wastewater by AUR, NUR and OUR. *Water Sci Technol* **25** (6) 43-57.

LAING (1991) The impact of effluent regulations on the dyeing industry. *Rev. Prog. Coloration* **21** 56-71.

LAURSEN S, KNUDSEN H, HANSEN J and ANDERSEN T (2002) Danish experience. Best Available Techniques – BAT - in the clothing and textile industry. Working Report no. 10, 2002,

LJUNG L (1999) System Identification - Theory for the User *Prentice-Hall*. Englewood Cliffs, NJ.

MUNACK A (1989) Optimal feeding strategy for identification of Monod-type models by fed-batch experiments. *Proc. Comp. Appl. in Ferm. Techn.: Mod. and Control of Biotech. Proc.* 195-204.

MUNACK A (1991) Optimization of sampling. *Biotechnology, aMulti-volume Comprehensive Treatise* **4** 251-264.

NOPENS I, HOPKINS L and VANROLLEGHEM P (2001) An overview of the posters presented at Watermatex 2000. III: Model selection and calibration/optimal experimental design. *Water Sci Technol* **43** (7) 387-389.

NOVAK L, LARREA L and WANNER J (1994) Estimation of maximum specific growth rate of heterotrophic and autotrophic biomass: A combined technique of mathematical modelling and batch cultivations. *Water Sci Technol* **30** (11) 171-180.

PAGGA U and BROWN D (1986) The degradation of dyestuffs: Part II; Behaviour of dyestuffs in aerobic biodegradation tests. *Chemosphere* **15** (4) 479-491.

PATTERSON J and BREZONIK P (1969) Discussion of 'Toxicity Measurements in Activated Sludge'. *J. San. Engr. Div. Proc. Am. Soc. Civ. Eng* **95** (775)

PETERSEN B (2000) Calibration, identifiablity and optimal experimental design of activated sludge models PhD thesis. Department of applied mathematics, biometrics and process control. Universiteit Gent. Gent. 364p.

PETERSEN B, GERNAEY K, DEVISSCHER M, DOCHAIN D and VANROLLEGHEM P (2003) A simplified method to assess structurally identifiable parameters in Monod-based activated sludge models. *Water Res* **37** 2893-2904.

RAMADORI R, ROZZI A and TANDOI V (1980) An automated system for monitoring the kinetics of biological oxidation of ammonia. *Water Res* **14** 1555-1557.

RANDALL E, WILKINSON A and EKAMA G (1991) An instrument for the direct determination of oxygen utilization rate. *Water SA* **17** (1) 11-18.

RAZO-FLORES E (1997) Biotransformation and biodegradation of azo dyes by anaerobic granular sludge bed reactors. *Appl. Microbiol. and Biotechnol* **47** 83-90.

ROBINSON J (1985) Determining microbial parameters using nonlinear regression analysis: Advantages and limitations in microbial ecology. *Adv. Microb. Ecol.* **8** 61-114.

ROS M, DULAR M and FARKAS P (1988) Measurement of repiration of activated sludge. *Water Res* **22** 1405-1411.

SIN G (2004) Systematic calibration of activated sludge models PhD thesis. Department of applied mathematics, biometrics and process control. Gent University. Gent. 372p.

SIN G, MALISSE K and VANROLLEGHEM P (2003) An integrated sensor for the monitoring of aerobic and anoxic activated sludge activities in biological nitrogen removal plants. *Water Sci Technol* **47** (2) 141-148.

SPANJERS H (1993) Respirometry in activated sludge. PhD thesis. Landbouwuniversiteit. Wageningen, Netherlands. 199p.

SPANJERS H and VANROLLEGHEM P (1995) Respirometry as a tool for rapid characterisation of wastewater and activated sludge. *Water Sci Technol* **31** (2) 105-114.

SPANJERS H, VANROLLEGHEM P, NGUYEN K, VANHOOREN H and PATRY G (1998) Towards a simulation-benchmark for evaluating respirometry-based control strategies. *Water Sci Technol* **37** (12) 219-226.

SPANJERS H, VANROLLEGHEM P, OLSSON G and DOLD P (1998) Respirometry in control of the activated sludge process. *International Association on Water Quality*. London, UK.

SPEECE R (1996) Anaerobic biotechnology for industrial wastewaters *Archae Press*. Nashville, Tennessee.

SUSCHKA J and FERREIRA E (1986) Activated sludge respirometric measurements. *Water Res* **20** 137-144.

TAKACS I, PATRY G and NOLASCO D (1991) A dynamic model of the clarification thickening process. *Water Res* **25** (10) 1263-1271.

TAKAMATSU T, SHIOYA S, MORISAKI K and IHARA D (1982) On-line monitoring and control of an activated sludge process for wastewater using 'MMOUR'. *Eur J Appl Microbiol Biotech* **14** 187-192.

VANHOOREN H, MEIRLAEN J, AMERLINCK Y, CLAEYS F, VANGHELUWE H and VANROLLEGHEM P (2003) WEST: modellling biological wastewater treatment. *J Hydro* **5** (1) 27-50.

VANROLLEGHEM P and GILLOT S (2002) Robustness and economic measures as control benchmark performance criteira. *Water Sci Technol* **45** (4-5) 117-126.

VANROLLEGHEM P, JEPPSSON U, CARSTENSEN J, CARLSSON B and OLSSON G (1996) Integration of wastewater treatment plant design and operation - a systematic approach to cost functions. *Water Sci Technol* **34** (3-4) 159-171.

VANROLLEGHEM P, KONG Z, ROMBOUTS G and VERSTRAETE W (1994) An on-line respirographic sensor for the characterization of load and toxicity of wastewaters. *J Chem Tech Biotechnol* **59** 321-333.

VANROLLEGHEM P, SIN G and GERNAEY K (2004) Transient response of aerobic and anoxic activated sludge activities to sudden substrate concentration changes. *Biotechnol Bioeng* **86** (3) 277-290.

VANROLLEGHEM P and SPANJERS H (1998) A hybrid respirometric method for more reliable assessment of activated sludge model parameter. *Water Sci Technol* **37** (12) 237-246.

VANROLLEGHEM P, SPANJERS H, PETERSEN B, GINESTET P and TAKACS I (1999) Estimating (combinations of) activated sludge model No.1 parameters and components by respirometry. *Water Sci Technol* **39** (1) 195-214.

VOLSKAY V and GRADY C (1988) Toxicity of selected RCRA compounds to activated sludge microorganisms. *J Water Poll Cont Fed* **60** (10) 1850-1856.

WANNER O, KAPPLER J and GUJER W (1992) Calibration of an activated sludge model based on human expertise and on a mathematical optimization technique - A comparison. *Water Sci Technol* **25** (6) 141-148.

WATTS J and GARBER W (1993) On-line respriometry: A powerful tool for activated sludge plant operation and design. *Water Sci Technol* **28** (11-12) 389-399.

WEIJERS S and VANROLLEGHEM P (1997) A procedure for selecting best identifiable parameters in calibrating activated sludge model no.1 to full-scale plant data. *Water Sci Technol* **36** (5) 69-79.

WENTZEL M, MBEWE A and EKAMA G (1995) Batch test for measurement of readily biodegradable COD and active organism concentrations in municipal waste waters. *Water SA* **21** (2) 117-124.

WILLETTS J (1999) Thermophilic treatment of textile dye wastewater. PhD Thesis. School of Civil and Environmental Engineering. University of New South Wales.

WWW.HEMMIS.COM. (2006), http://www.hemmis.com/products/west/history_west.htm

APPENDIX A

REAGENT PREPARATION

Hydrochloric Acid Titrant

$[HCl]_{aq}$	=	0.01 M
[ ]	=	n / V
n	=	[ ] . V
	=	(0.01 x 1) mol/Lx L
	=	0.01 mol
n	=	m / M_m
M_m	=	36.46 g/mol
m	=	(0.01 x 36.46) mol x g/mol
	=	0.3646 g

Using a 32% (w/w) solution of HCl

0.32	:	0.3646 g
1	:	X
X	=	1.1394 g

Sodium Hydroxide Titrant

$[NaOH]_{aq}$ = 0.01 M

n = [ ] . V

= (0.01 x 1) mol/L x L

= 0.01 mol

Using Sodium Hydroxide pellets of 98% purity.

n = m / M_m

M_m = 40.00 g/mol

m = (0.01 x 40.00) mol x g/mol

= 0.40 g

Sodium Acetate Spike

$[C_2H_3NaO_2]$ = 0.18 g COD/L

n = [ ] . V

= (0.18 x 1) mol/L x L

= 0.18mol

Using Sodium Acetate Anhydrous of 98% purity.

n = m / Mm

M_m = 82.03 g/mol

m = (0.18 x 82.03) mol x g/mol

= 14.7654 g

Ammonium Chloride Spike

$[NH_4Cl]_{aq}$ = 0.07 M

n = [ ] . V

= (0.07 x 1) mol/L x L

= 0.07 mol

Using Ammonium Chloride Anhydrous of 98% purity.

n = m / M_m

M_m = 53.50 g/mol

m = (0.07 x 53.50) mol x g/mol

= 3.7450g

Textile Dye Spike

Using the required dye.

[dye] = 10.00 g/L

m = [ ] . V

= (10.00 x 1) g/L x L

= 10.00 g

APPENDIX B

EQUIPMENT

DISSOLVED OXYGEN PROBE

Type:	YSI 5739 Field Probe
Membrane:	FEP Teflon
Cathode:	Gold
Anode:	Silver
Electrolyte:	Half-saturated KCL
Temperature Range:	-5 to 45 °C
Polarizing Voltage:	0.8 V
Probe Current:	19mA

OXYGEN UPTAKE RATE METER

Type: UCT DO/OUR Meter

Key Pad Functions:

- When in Mode A – press the "B" key. Display confirms – Mode B Selected.
- When in operation display indicates; DO (mg/L), Temperature (°C), Hi Limit and Lo Limit (mg O_2/L).
- Set Hi and Lo limits by holding down the following keys:

  C - Increases Hi Limit

  D - Decreases Hi Limit

  E - Increases Lo Limit

  F - Decreases Lo Limit

- Re-selecting Mode A clears all accumulated data.
- The 10 most recent OUR determinations are available via the LCD.

  Hold down "0" key – display current cycle OUR

  Hold down "1" key – display current cycle – 1 OUR

  .. ..

  Hold down "9" key – display current cycle - 9 OUR

EQUIPMENT CALIBRATION

OXYGEN UPTAKE RATE METER

Requirements:

- Sodium sulphite solution of 27 g/L concentration.
- Beaker of distilled Water.

Procedure:

- Connect DO electrode to the "probe" socket and temperature probe to "temp" socket.
- Switch on instrument.
- Push the "A" key to get meter in Mode A, instrument displays dissolved oxygen concentration (mg/L) and temperature (°C).
- To set DO zero, place DO probe in sodium sulphite solution (27 g/L) and leave in solution until dissolved oxygen concentration (DO) reading is stable for about 1 minute. Adjust ZERO pot on rear of instrument such the DO reading is 0.0 mg/L.
- Remove DO probe from sodium sulphite solution and flush in distilled water.
- To set DO gain, place DO probe in beaker of distilled water. Bubble air into the water such that the water becomes saturated with oxygen. Continue bubbling air until reading is constant. Use the temperature probe to measure the water temperature. Refer to Table B-1 to determine the saturated value of DO at the current temperature. A correction factor for the atmospheric pressure should be included, see Table B-2.

  Example

  DO = 9.00 mg/L at 21 ^{o}C (at 1 atmosphere)

  DO = (9.00 x 0.88) = 7.92 mg/L (at 669 mmHg)

  Adjust GAIN pot on rear of instrument such that the DO reading is correct.
- Verify the zero setting by replacing the probe in the sodium sulphite solution.

Table B-9: Oxygen Solubility (at Sea Level)

Temperature (°C)	Dissolved Oxygen (mg/L)	Temperature (°C)	Dissolved Oxygen (mg/L)
1	14.60	23	8.70
2	14.20	24	8.50
3	13.90	25	8.40
4	13.50	26	8.20
5	13.20	27	8.10
6	12.80	28	7.90
7	12.40	29	7.80
8	11.90	30	7.70
9	11.60	31	7.50
10	11.30	32	7.40
11	11.10	33	7.30
12	10.80	34	7.20
13	10.60	35	7.10
14	10.40	36	7.00
15	10.20	37	6.80
16	9.90	38	6.70
17	9.70	39	6.60
18	9.50	40	6.50
19	9.30	41	6.40
20	9.20	42	6.30
21	9.00	43	6.20
22	8.80	44	6.10

Table B-10: Atmospheric Pressure Correction Factors

Atmospheric Pressure (mmHg)	Correction Factor
760	1.00
745	0.98
730	0.96
714	0.94
699	0.92
684	0.90
669	0.88
654	0.86
638	0.84
623	0.82
608	0.80
593	0.78
578	0.76
562	0.74
547	0.72
532	0.70
517	0.68
502	0.66

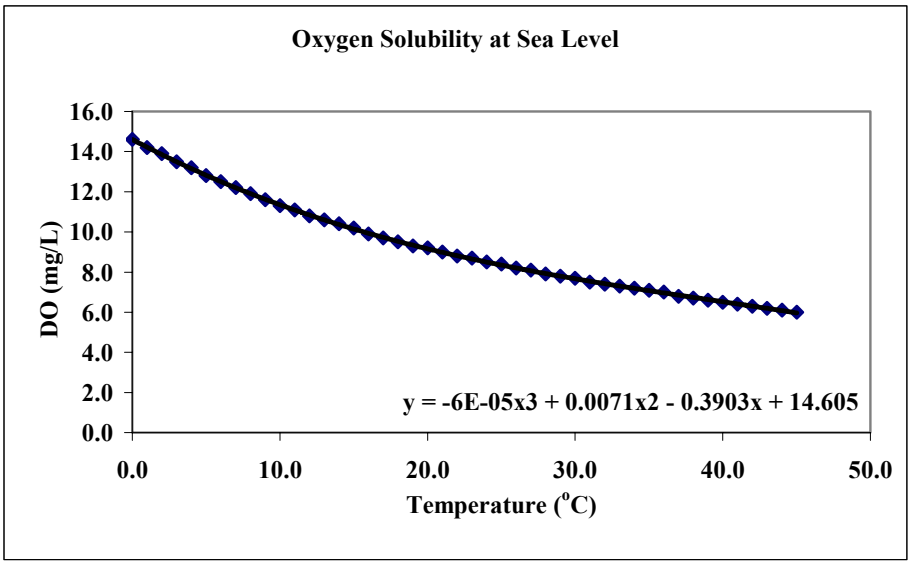

Figure B-8: Oxygen Solubility at Sea Level

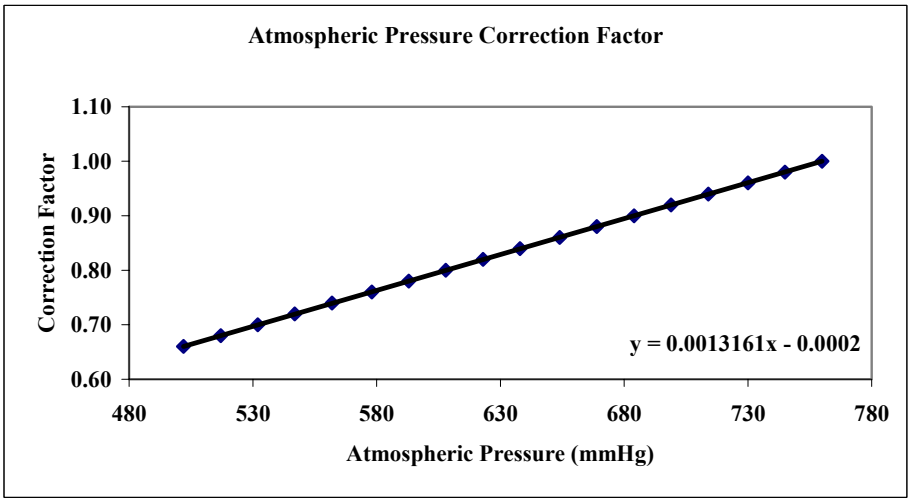

Figure B-9: Atmospheric Pressure Correction Factor

APPENDIX C

THEORETICAL METHODS

Estimating Chemical Oxygen Demand (COD) Content

The theoretical COD can be determined by using the following equation:

$$C_nH_aO_bN_c + dCr_2O_7^{2-} + (8d + c)H^+ \longrightarrow nCO_2 + \frac{a + 8d - 3c}{2}H_2O + cNH_4^+ + 2dCr^{3+} \quad \text{(C-1)}$$

Where:

$$d = \frac{2n}{3} + \frac{a}{6} - \frac{b}{3} - \frac{c}{2} \quad \text{(C-2)}$$

$$COD = (3/2)d \quad \text{(C-3)}$$

An example of the calculation to determine the theoretical COD is presented and the results summarised in Table C-2.

The molecular weights of the reacting species are required for this calculation and are shown below in Table C-1.

Table C-11: Compound Molecular Formulae and Weights

Compound	Formula	Molecular Weight g/mol
Acetate	CH_3COONa	82
Biomass	$C_5H_7O_2N$	113

Acetate:

n = 2

a = 3

b = 2

c = 1

Substituting into equation (C-2):

d = 0.67 moles of O_2

Resultantly equation (C-1) is:

$$C_2H_3O_2Na + 0.66Cr_2O_7^{2-} + 6.28H^+ \longrightarrow 2CO_2 + 5.28H_2O + Na^+ + 1.32Cr^{3+}$$

Hence, using equation (C-3):

1 mole CH_3COONa = (3/2)d

= 1 mole of O_2

But, 1 mole CH_3COONa = 82 g

1 mole O_2 = 32 g

Thus for the complete oxidation of 82 g of CH_3COONa, 32 g of oxygen is required.

Therefore: 1g CH_3COONa requires 0.392 gO_2 or equivalently 0.392 gCOD.

Table C-12: Theoretical Estimates of Chemical Oxygen Demand

Compound	Formula	n	a	b	c	d	gCOD
Acetate	CH_3COONa	2	3	2	1	0.67	0.392
Biomass	$C_5H_7O_2N$	5	7	2	1	3.33	1.416

APPENDIX D

OPERATIONAL MANUAL

STAGE ONE

The activated sludge sampled from the aeration basin maybe stored for no more than 2 weeks before concentration. The sludge must be kept in a dark cold room set at 4°C with no substrate.

Biomass Concentration

- Remove raw activated sludge from 4°C cold room.
- Allow particulates to settle in container.
- Concentrate activated sludge by removing as much supernatant liquid from container.
- Place container of sludge in warm bath, leave in bath until sludge reaches 25°C. The sludge is now ready to be used in reactor.

STAGE TWO

Start up

- Locate UCT DO/OUR meter main socket. Ensure that the amplifier and computer are plugged in.
- Check that the computer and amplifier are connected to UCT DO/OUR meter.
- Switch on UCT DO/OUR meter at main switch, the LCD displays:

  DO Meter V2.1

  UCT Chem Eng 1992
- Switch on computer and in DOS mode start the programme i.e. (C:\doprogs\DOMPC.exe).
- A blue main menu screen should appear.

Probe Calibration

The pH electrode is calibrated using pH4 and pH 7 buffer solutions. The pH probe is immersed in the lower pH buffer solution then into the higher pH buffer solution. The temperature probe

does not require calibration.

OUR Meter Calibration

Calibrate UCT DO/OUR meter as described in Appendix B.

Set point Adjustment

The set points adjustments for sodium acetate spikes and ammonium chloride spikes experiments are different. This is so as a result of noise effects and the differing rates at which the two substrates are consumed.

Sodium Acetate Spike Experiments:

- The Hi and Lo limits for dissolved oxygen (DO) concentration must be set on the DO/OUR meter.
- Press “B” key on the meter to get into Mode B.
- The Hi limit for DO concentration is increased by pressing “C” key and decreased by pressing “D” key. Set Hi Limit of DO concentration to 5.00 mg/L.
- The Lo limit for DO concentration is increased by pressing “E” key and decreased by pressing “F” key. Set Lo Limit of DO concentration to 4.50 mg/L.
- The offset DO value and the sample rate are adjusted in the main menu of the DOMPC programme.
- Select the “Offset” option in the main menu.
- Set offset to a value of zero. Press ENTER to return to the main menu.
- Select the “Sample rate” option in the main menu.
- Set Sample rate to 6 s. Press ENTER to return to the main menu.

Ammonium Chloride Spike Experiments:

- The Hi and Lo limits for dissolved oxygen (DO) concentration must be set on the DO/OUR meter.
- Press “B” key on the meter to get into Mode B.
- The Hi limit for DO concentration is increased by pressing “C” key and decreased by pressing “D” key. Set Hi Limit of DO concentration to 5.00 mg/L.

- The Lo limit for DO concentration is increased by pressing “E” key and decreased by pressing “F” key. Set Lo Limit of DO concentration to 4.80 mg/L.
- The offset DO value and the sample rate are adjusted in the main menu of the DOMPC programme.
- Select the “Offset” option in the main menu.
- Set offset to a value of zero. Press ENTER to return to the main menu.
- Select the “Sample rate” option in the main menu.
- Set Sample rate to 1 s. Press ENTER to return to the main menu.

Test Monitoring

- The pH of the reactor must be monitored continually and controlled at a value of pH 7.5 (± 0.2), using the hydrochloric acid and sodium hydroxide 0.01 M titrate solutions.
- At intervals of 3 hr or sooner depending on the rate of activity, OUR data should be analysed until endogenous respiration conditions are observed.
- After spiking with substrate the OUR data should be analysed at intervals of about 30 min, once again depending on the rate of activity.
- Select the “Collect Historic data” option in the main menu.
- Choose the “Write disk only” option. Press ENTER to return to the main menu.

Shut down

- Collect the remaining OUR data.
- Exit from DOMPC program. Select “Quit to DOS” option.
- Remove all probes from reactor.
- Rinse pH probe with distilled water and cap it. Place some potassium chloride solution into cap before placing it over the probe.
- Rinse DO probe with distilled water and place probe in bottle. Ensure moist sponge is in the bottle.
- Rinse Temperature probe.

ANALYTICAL TEST PROCEDURES

Organic Content

The Chemical oxygen demand (COD) was used as a measure of the oxygen equivalent of the organic matter content of samples that were susceptible to oxidation by a strong chemical oxidant.

COD Open Reflux Method:

This method is suitable for wastes where a larger, more concentrated sample is preferred. The test was used to evaluate the COD of the wastewater which was used as a substrate in the respirometric experiments. A sample is refluxed in strong acid solution with a known excess of potassium dichromate ($K_2Cr_2O_7$). After digestion, the remaining unreduced $K_2Cr_2O_7$ is titrated with ferrous ammonium sulphate to determine the amount of $K_2Cr_2O_7$ consumed and the oxidizable matter is calculated in terms of oxygen equivalent. The procedure of the open reflux method is presented below.

A 250 mL sample of the test substance was diluted to 500 mL in a volumetric flask. The dilution is necessary because the sample COD could be greater than 900 mg O_2/L. A 10 mL aliquot of this was placed into a 250 mL refluxing flask. To this was added 0.04 g of mercuric sulphate, several glass beads and 5 mL aliquot of potassium dichromate solution (0.0417 M) was added. A 5 mL of sulphuric acid reagent was added to this. The flask was attached to the condenser and cooling water turned on. The mixture was refluxed for 2 h. A blank consisting of 10 mL distilled water, instead of the substrate, was refluxed in the same way. The samples were allowed to cooled and the condenser was rinsed with 80 mL distilled water. Thereafter, they were titrated with ferrous ammonium sulphate solution (FAS) using ferroin indicator.

The COD of the sample was evaluated using Equation.

$$COD = \frac{(A-B)\cdot C \cdot 8000}{V_S} \qquad \text{(D-1)}$$

A = FAS (Blank) [mL]

B = FAS (Sample) [mL]

C = Molarity of FAS [M]

V_S = Volume of Sample [mL]

Total Suspended Solids:

The test was used to evaluate the total solid content of the activated sludge which was used in the respirometric experiments. A well-mixed sample is filtered through a weighed standard glass-fiber filter and the residue retained on the filter is dried to a constant weight at 103 °C. The increase in weight of the filter represents the total suspended solids. The procedure of the total suspended solids test is presented below.

10 mL, 20 mL and 30 mL well-mixed samples of activated sludge were filtered separately through 3 weighed standard glass-fiber filter papers respectively and the residue retained on the filters is dried to a constant weight at 103 °C. The filter with this residue is allowed to cool in a desiccator then weighed.

The total suspended solids of the sample were evaluated using Equation.

$$TSS = \frac{(A - B) \cdot 1000}{V_S} \tag{D-2}$$

A = weight of filter + dried residue [mg]

B = weight of filter [mg]

V_S = Volume of Sample [mL]

Volatile Suspended Solids:

This measurement of volatile solids is an approximation of the amount of organic matter present in the solid fraction of the activated sludge. The residue from the TSS test is ignited at

550 °C for 2 h. The remaining solids represent the fixed total, dissolved, or suspended solids while the weight lost on ignition is the volatile solids. The procedure of the volatile suspended solids test is presented below.

The residue of the 3 samples from the TSS test is ignited at 550 °C for 2 hr. The filter with this residue after ignition is allowed to cool in a desiccator then weighed.

The volatile suspended solids of the sample were evaluated using Equation.

$$VSS = \frac{(A - B) \cdot 1000}{V_S} \tag{D-3}$$

A = weight of filter + dried residue after ignition [mg]

B = weight of filter + dried residue before ignition [mg]

V_S = Volume of Sample [mL]

APPENDIX E

EXPERIMENTS DATA AND SAMPLE CALCULATION

The respirometric experiment raw data is presented in **Annexure 1**; CD-Rom Annex1_Respirometric Experiment Data.xls file. Results and the calculations from COD and Solids tests are presented in **Annexure 2**; CD-Rom Annex2_COD& Solid Tests.xls file.

PARAMETER ESTIMATION SIMULATION DATA

The BRE model kinetic parameters obtained from parameter estimation performed on WEST and the conversions calculation required so that the parameters can be inputted into COST benchmark model are presented in **Annexure 3**; CD-Rom Annex3_BRE Kinetic process parameters.xls file.

ASSEMENT OF WASTEWATER TREATMENT WORKS PERFORMANCE DATA

The raw data obtained simulation performed on the COST benchmark simulation model and the COST benchmark calculation used to obtain performance indices are presented in **Annexure 4**; CD-Rom Annex4_COST Simulation Benchmark model Results file.

APPENDIX F

MODEL CONTINUITY CHECK

A continuity check was performed on the model stoichiometry and mass balance.

Stoichiometry Continuity Check

The stoichiometry continuity check was performed in West and the result of the continuity check was successful.

Mass Balance Continuity Check

A mass balance continuity check was performed on the model to determine whether the model COD and nitrogen components balance..

The default parameters for ASM1 model where used in the COD and nitrogen mass balances simulations and is shown below in Table F-1.

Table F-13: Parameters used in COD and Nitrogen Mass Balance Continuity Check Simulations

Name	COD Sim Parameters	Nitrogen Sim Parameters	Unit
Autotrophic decay coefficient (b_A)	0.01	0.01	1/d
Heterotrophic decay coefficient (b_H)	0.4	0.4	1/d
Fraction of biomass converted to inert (f_P)	0.2	0.2	-
Fraction TSS to COD ($F_{TSS,COD}$)	0.75	0.75	-
Mass nitrogen per COD biomass (i_{XB})	0.086	0.086	gN/gCOD
Mass nitrogen per COD product (i_{XP})	0.02	0.02	gN/gCOD
Oxygen transfer coefficient (KLa)	500	500	1/d
Max. specific hydrolysis rate (k_h)	2	2	1/d
Ammonia half saturation coefficient for autotrophic biomass (K_{NH})	1	1	gNH_3/m^3
Oxygen half saturation coefficient for autotrophic biomass (K_{OA})	0.1	0.1	gO_2/m^3
Half saturation coefficient for heterotrophic biomass (K_S)	20	20	$gCOD/m^3$
Oxygen half saturation coefficient for heterotrophic biomass (K_{OH})	0.1	0.1	gO_2/m^3
Half saturation coefficient for hydrolysis (K_X)	0.02	0.02	gCOD/gCOD
Max. specific growth rate of autotrophic growth rate (μ_A)	0	0.55	1/d
Max. specific growth rate of heterotrophic growth rate (μ_H)	4	0	1/d
Oxygen saturation coefficient ($S_{O,sat}$)	10	10	g/m^3
Yield for autotrophic biomass (Y_A)	0.24	0.24	gCOD/gN
Yield for autotrophic biomass (Y_H)	0.67	0.67	gCOD/gCOD

COD Mass Balance Continuity Check:

The COD mass balance parameters and components concentrations are presented in Table F-1 and Table F-2 respectively. The resultant output OUR profile is shown in Figure F-1.

The total COD concentration is the sum of all COD components, represented by Equation (F-1).

$$COD_{TOTAL} = S_I + S_S + X_{BA} + X_{BH} + X_I + X_P + X_S \quad \text{(F-1)}$$

By using the component concentrations presented in Table F-2 and Equation (F-1) the initial and final COD concentrations are 1.595 gCOD/L and 1.389 gCOD/L.

The error in COD mass balance of the model is calculated as the difference of initial total COD concentration, final total COD concentration and area under OUR profile plot. The resultant Equation (F-2) is presented below.

$$Error_{COD} = COD_{TOTAL}^{Initial} - COD_{TOTAL}^{Final} - \int r_{total} dt \quad \text{(F-2)}$$

The area under the OUR profile was obtained using the Trapezoidal method; a value of 0.206 gCOD/L was obtained. Therefore the $Error_{COD}$ is equal to 0 gCOD/L by using Equation (F-2). Hence the result of the COD mass balance continuity check performed on the model is successful.

Table F-14: Initial and Final Concentrations obtained from Batch Reactor COD Mass Balance Continuity Check Simulations

Name	Initial Concentration (gCOD/L)	Final Concentration (gCOD/L)
Soluble Inert (S_I)	0.040	0.040
Readily Biodegradable (S_S)	0.100	0.000
Autotrophic Biomass (X_{BA})	0.100	0.100
Heterotrophic Biomass (X_{BH})	1.000	1.120
Particulate Inert (X_I)	0.100	0.100
Particulate Product (X_P)	0.005	0.028
Slowly Biodegradable (X_S)	0.250	0.000

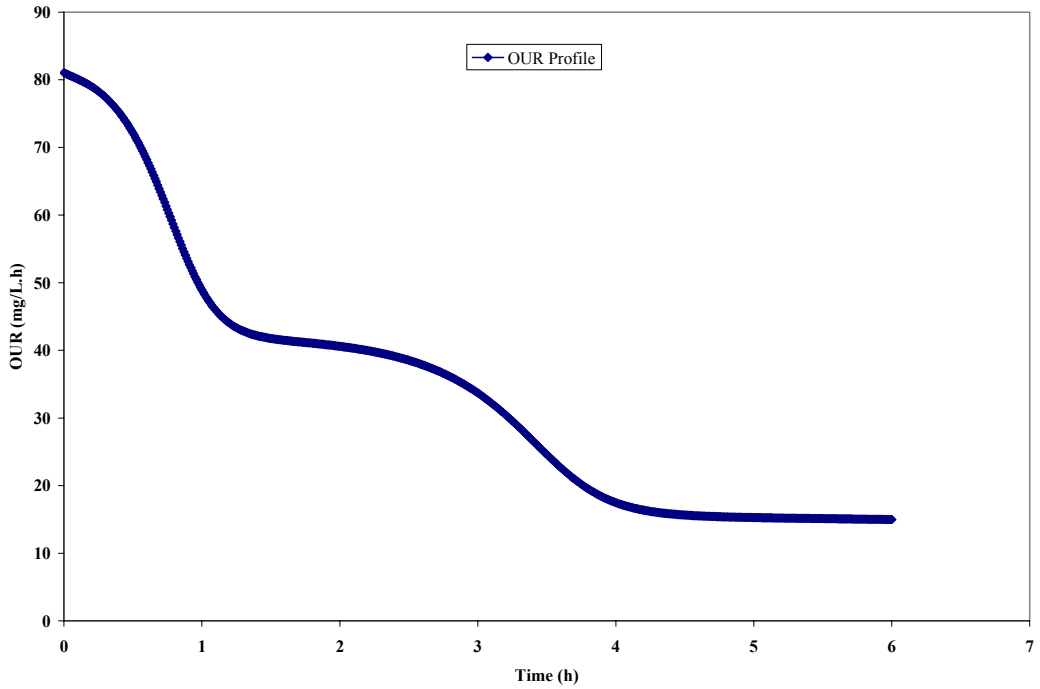

Figure F-10: Oxygen Uptake Rate (OUR) Profile the Area of the Plot is used in COD Mass Balance Continuity Check Simulations

Nitrogen Mass Balance Continuity Check:

The Nitrogen mass balance was performed in a similar method to the COD balance, the parameters and components concentrations used are presented in Table F-1 and Table F-3 respectively.

The total Nitrogen concentration is the sum of all Nitrogen concentration, represented by Equation (F-3).

$$N_{TOTAL} = S_{NH} + S_{NO} + \left(i_{XP} \cdot X_P\right) + \left(i_{XB} \cdot X_{BH}\right) + \left(i_{XB} \cdot X_{BA}\right) \quad \text{(F-3)}$$

The error in Nitrogen mass balance of the model is calculated as the difference of initial and final total Nitrogen concentration, represented by Equation (F-4) below.

$$Error_N = N_{TOTAL}^{Initial} - N_{TOTAL}^{Final} \quad \text{(F-4)}$$

The resultant $Error_N$ is 0 gN/L; hence Nitrogen mass balance continuity check performed on the model is successful.

Table F-15: Initial and Final Concentrations obtained from Batch Reactor Nitrogen Mass Balance Continuity Check Simulations

Name	Initial Concentration (g/L)	Final Concentration (g/L)
Ammonia and Ammonium (S_{NH})	0.013	0.000
Nitrate and Nitrite (S_{NO})	0.001	0.020
Heterotrophic Biomass (X_{BH})	0.086	0.078
Particulate Product (X_P)	0.000	0.000
Autotrophic Biomass (X_{BA})	0.008	0.009